Notes on tokamak equilibrium

by Youjun Hu

Institute of Plasma Physics, Chinese Academy of Sciences
Email: yjhu@ipp.cas.cn

Abstract

Axisymmetric plasma equilibrium is the basis for the analysis of stability and transport in tokamak plasmas. These are my notes when learning the tokamak equilibrium theory. To test what I have learned, I have developed two numerical codes, one of which constructs a flux coordinate system with a desired form of Jacobian by using discrete numerical equilibrium data $\Psi(R, Z)$ output by the EFIT code, another of which solves the fixed boundary Grad-Shafranov equation in a general coordinate system. These notes serve as a document for the codes. These notes are evolving. The latest version can be found at: http://theory.ipp.ac.cn/~yj/research_notes/tokamak_equilibrium.pdf.

1 Axisymmetric magnetic field

Due to the divergence-free nature of magnetic field, i.e., $\nabla \cdot \mathbf{B} = 0$, magnetic field can be generally expressed as the curl of a vector potential,

$$\mathbf{B} = \nabla \times \mathbf{A}. \tag{1}$$

We consider axisymmetric magnetic field. The axial symmetry means that, when expressed in the cylindrical coordinate system (R, ϕ, Z), the components of $\mathbf{B}$, namely B_R, B_Z, and B_ϕ, are all independent of ϕ. For this case, it can be proved that an axisymmetric vector potential $\mathbf{A}$ suffices for expressing the magnetic field, i.e., all the components of the vector potential $\mathbf{A}$ can also be taken independent of ϕ. Using this, Eq. (1) is written

$$\mathbf{B} = -\frac{\partial A_\phi}{\partial Z}\hat{\mathbf{R}} + \frac{1}{R}\frac{\partial(R A_\phi)}{\partial R}\hat{\mathbf{Z}} + \left(\frac{\partial A_R}{\partial Z} - \frac{\partial A_Z}{\partial R}\right)\hat{\boldsymbol{\phi}}. \tag{2}$$

In tokamak literature, $\hat{\boldsymbol{\phi}}$ direction is called the toroidal direction and (R, Z) plane is called the poloidal plane. Equation (2) indicates that two poloidal components of $\mathbf{B}$, namely B_R and B_Z, are determined by a single component of $\mathbf{A}$, namely A_ϕ. This motivates us to define a function $\Psi(R, Z)$ by

$$\Psi(R, Z) \equiv R A_\phi(R, Z). \tag{3}$$

Then Eq. (2) implies the poloidal components, B_R and B_Z, can be written as

$$B_R = -\frac{1}{R}\frac{\partial \Psi}{\partial Z} \tag{4}$$

and

$$B_Z = \frac{1}{R}\frac{\partial \Psi}{\partial R}. \tag{5}$$

It is obvious that it is the property of being axisymmetric and divergence-free that enables the two components of $\mathbf{B}$, B_R and B_Z, to be expressed in terms of a single function $\Psi(R, Z)$. (The function Ψ is usually called the "poloidal flux function" in tokamak literature. The reason for this nomenclature will become clear when we discuss the physical meaning of Ψ in Sec. 1.4.) Furthermore, it is ready to verify Ψ is constant along a magnetic field line, i.e. $\mathbf{B} \cdot \nabla \Psi = 0$. [Proof:

$$
\begin{aligned}
\mathbf{B} \cdot \nabla \Psi &= \mathbf{B} \cdot \left(\frac{\partial \Psi}{\partial R}\hat{\mathbf{R}} + \frac{\partial \Psi}{\partial Z}\hat{\mathbf{Z}}\right) \\
&= -\frac{1}{R}\frac{\partial \Psi}{\partial Z}\frac{\partial \Psi}{\partial R} + \frac{1}{R}\frac{\partial \Psi}{\partial R}\frac{\partial \Psi}{\partial Z} \\
&= 0.
\end{aligned}
\tag{6}
$$

] For later use, define $g \equiv R B_\phi(R, Z)$, then the toroidal component of the magnetic field is written

$$\mathbf{B}_\phi = B_\phi \hat{\boldsymbol{\phi}} = \frac{g}{R} \hat{\boldsymbol{\phi}} = g \nabla \phi. \tag{7}$$

Using Eqs. (4), (5), and (7), a general axisymmetric magnetic field can be written as

$$\begin{aligned}
\mathbf{B} &= B_R \hat{\mathbf{R}} + B_Z \hat{\mathbf{Z}} + B_\phi \hat{\boldsymbol{\phi}} \\
&= -\frac{1}{R} \frac{\partial \Psi}{\partial Z} \hat{\mathbf{R}} + \frac{1}{R} \frac{\partial \Psi}{\partial R} \hat{\mathbf{Z}} + g \nabla \phi \\
&= \frac{1}{R} \nabla \Psi \times \hat{\boldsymbol{\phi}} + g \nabla \phi \\
&= \nabla \Psi \times \nabla \phi + g \nabla \phi.
\end{aligned} \tag{8}$$

1.1 Gauge transformation of Ψ

Next, we discuss the gauge transformation of the vector potential $\mathbf{A}$ in the axisymmetric case. It is well-known that magnetic field remains the same under the following gauge transformation:

$$\mathbf{A}^{\text{new}} = \mathbf{A} + \nabla f, \tag{9}$$

where f is an arbitrary scalar field. Here we require that ∇f be axisymmetric because, as mentioned above, an axisymmetric vector potential suffices for describing an axisymmetric magnetic field. In cylindrical coordinates, ∇f is given by

$$\nabla f = \frac{\partial f}{\partial R} \hat{\mathbf{R}} + \frac{\partial f}{\partial Z} \hat{\mathbf{Z}} + \frac{1}{R} \frac{\partial f}{\partial \phi} \hat{\boldsymbol{\phi}}. \tag{10}$$

Since ∇f is axisymmetric, it follows that $\partial^2 f / \partial R \partial \phi = 0$, $\partial^2 f / \partial Z \partial \phi = 0$, and $\partial^2 f / \partial \phi^2 = 0$, which implies that $\partial f / \partial \phi$ is independent of R, Z, and ϕ, i.e., $\partial f / \partial \phi$ is actually a constant. Using this, the ϕ component of the gauge transformation (9) is written

$$\begin{aligned}
A_\phi^{\text{new}} &= A_\phi + \frac{1}{R} \frac{\partial f}{\partial \phi} \\
&= A_\phi + \frac{C}{R},
\end{aligned} \tag{11}$$

where C is a constant. Note that the requirement of axial symmetry greatly reduces the degree of freedom of the gauge transformation for A_ϕ (and thus for $R A_\phi$, i..e, Ψ). Multiplying Eq. (11) with R, we obtain the corresponding gauge transformation for Ψ,

$$\Psi^{\text{new}} = \Psi + C, \tag{12}$$

which indicates Ψ has the same gauge transformation as the familiar electric potential, i.e., adding a constant. (Note that the definition $\Psi(R, Z) \equiv R A_\phi$ does not mean $\Psi(R = 0, Z) = 0$ because A_ϕ can have a $1/R$ dependence under the gauge transformation (11)).

1.2 Magnetic surfaces

For axial symmetry system, we can define magnetic surfaces in a trivial way (for non-axisymmetric system, the definition may be a little harder, I will consider this later). The axial symmetry of tokamak magnetic field allows us to introduce a surface of revolution that is generated by rotating the projection of a magnetic field line on (R, Z) plane around the axis of symmetry, Z axis. The unique property of this revolution surface is that no field line point-intersects it and a field line

with one point on it will have the whole field line on it. This revolution surface is usually called magnetic surface or flux surface. For instance, consider an arbitrary magnetic field line, whose projection on (R, Z) plane is shown in Fig. 1. A magnetic surface is generated by rotating the projection line around the Z axis.
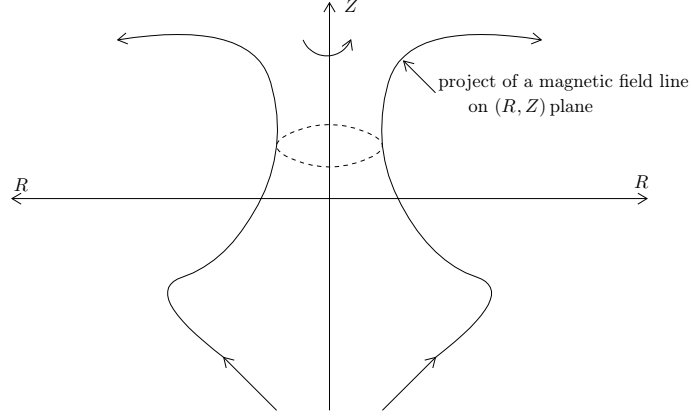

Figure 1. A magnetic surface in tokamak is a revolution surface generated by rotating the projection of a magnetic field line on the (R, Z) plane around the Z axis.

Because Ψ is constant along a magnetic field line and Ψ is independent of ϕ, it follows that the value of Ψ is constant on a magnetic surface. Therefore Ψ can be used as labels of magnetic surfaces.

1.3 Contours of Ψ on (R, Z) plane are magnetic surfaces

Because Ψ is constant along a magnetic field line and Ψ is independent of ϕ, it follows that the projection of a magnetic field line onto (R, Z) plane is a contour of Ψ. On the other hand, it is ready to prove that the contour of Ψ on (R, Z) plane is also the projection of a magnetic field line onto the plane, i.e., a magnetic surface. [Proof. The contour of Ψ on (R, Z) plane is written

$$d\Psi = 0, \tag{13}$$

i.e.,

$$\frac{\partial \Psi}{\partial R}dR + \frac{\partial \Psi}{\partial Z}dZ = 0. \tag{14}$$

$$\Rightarrow \frac{1}{R}\frac{\partial \Psi}{\partial R}dR + \frac{1}{R}\frac{\partial \Psi}{\partial Z}dZ = 0. \tag{15}$$

Using Eqs. (4) and (5), the above equation is written

$$B_Z dR - B_R dZ = 0, \tag{16}$$

i.e.,

$$\frac{dZ}{dR} = \frac{B_Z}{B_R}, \tag{17}$$

which is the equation of the projection of a magnetic field line on (R, Z) plane. Thus, we prove that the contour of Ψ is also the projection of a magnetic field line on (R, Z) plane.]

1.4 Relation of Ψ with the poloidal magnetic flux

Note that Ψ is defined by $\Psi = RA_\phi$, which is just a component of the vector potential $\mathbf{A}$, thereby not having an obvious physical meaning. Next, we try to find the physical meaning of Ψ, i.e., try to find some simple algebraic relation of Ψ with some quantity that can be measured in experiments.
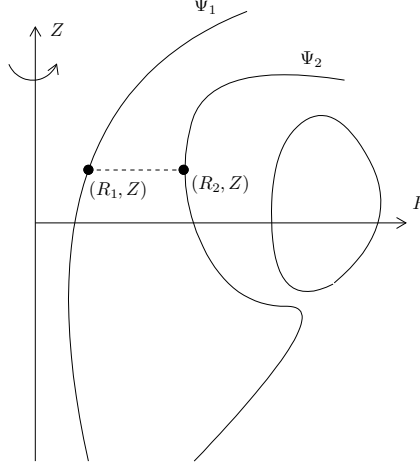

Figure 2. The poloidal magnetic flux Ψ_p between the two magnetic surfaces Ψ_1 and Ψ_2 is given by $\Psi_p = 2\pi(\Psi_2 - \Psi_1)$.

In Fig. 2, there are two magnetic surfaces labeled, respectively, by $\Psi = \Psi_1$ and $\Psi = \Psi_2$. Using Gauss's theorem in the toroidal volume between the two magnetic surface, we know that the poloidal magnetic flux through any toroidal ribbons between the two magnetic surfaces is equal to each other. Next, we calculate this poloidal magnetic flux. To make the calculation easy, we select a plane perpendicular to the Z axis, as is shown by the dash line in Fig. 1. In this case, only B_Z contribute to the poloidal magnetic flux, which is written (the positive direction of the plane is chosen in the direction of $\hat{\mathbf{Z}}$)

$$
\begin{aligned}
\Psi_p &= \int_{R_1}^{R_2} B_z(R, Z) 2\pi R \, dR \\
&= \int_{R_1}^{R_2} \frac{1}{R} \frac{\partial \Psi}{\partial R} 2\pi R \, dR \\
&= 2\pi \int_{R_1}^{R_2} \frac{\partial \Psi}{\partial R} \, dR \\
&= 2\pi [\Psi_2 - \Psi_1].
\end{aligned}
\tag{18}
$$

Equation (18) provides a simple physical meaning for Ψ, i.e., the difference of $2\pi\Psi$ between two magnetic surfaces is equal to the poloidal magnetic flux enclosed by the two magnetic surfaces. Noting that we are considering the axisymmetric case, the physical meaning of Ψ can also be stated as: the difference of Ψ between two magnetic surfaces is equal to the poloidal magnetic flux per radian. Due to this relation of Ψ with the poloidal flux Ψ_p, Ψ is usually called the "poloidal magnetic flux function" in tokamak literature. Note that it is the difference of Ψ between two locations that determines the the physical quantities Ψ_p, which is consistent with the fact that gauge transformation (12) dose not change the values of physical quantities.

1.5 Closed magnetic surfaces in tokamak

In most part of a tokamak plasma, the contours of Ψ on (R, Z) plane are closed curves. As discussed above, the contours of Ψ are the projection of magnetic lines on the poloidal plane. Closed contours of Ψ implies closed magnetic surfaces, as shown in Fig 3.
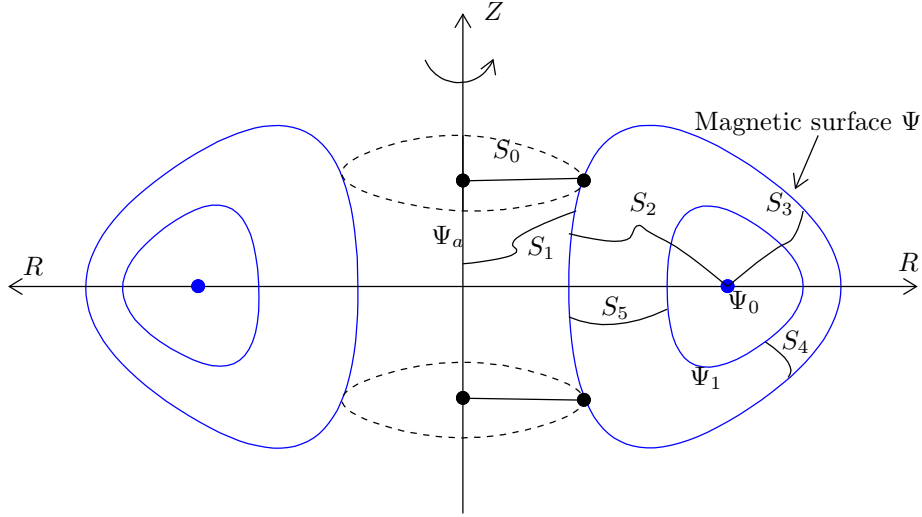
Figure 3. Closed magnetic surfaces (blue) and various toroidal surfaces used to define the poloidal magnetic flux. The magnetic flux through the toroidal surface S_2 and S_3 is equal to each other. Also the magnetic flux through S_4 and S_5 is equal to each other; the magnetic flux through S_0 and S_1 is equal to each other.

The innermost magnetic surface is actually a line, which is usually called the magnetic axis (in Fig. 3, Ψ_0 labels the magnetic axis). Because the magnetic axis is the point of maximum/minimum of $\Psi(R, Z)$, the value of $\nabla\Psi$ is zero at the magnetic axis. As a result, the poloidal component of the equilibrium magnetic field is zero on magnetic axis (refer to Eq. (8)), i.e., the magnetic field has only toroidal component there.

As discussed in Sec. 1.4, the poloidal magnetic flux enclosed by a magnetic surface Ψ (the poloidal magnetic flux through the toroidal surfaces S_2) is given by

$$\Psi_p = 2\pi \left(\Psi_0 - \Psi \right), \tag{19}$$

where Ψ_0 is the value of Ψ at the magnetic axis. Here the positive direction of the surface S_2 is defined to be in the clockwise direction when an observer looks along the direction of $\hat{\phi}$. In practice, we need to pay attention to the positive direction of the toroidal surface used to define the poloidal flux (there can be a sign difference when choosing different positive directions). Also note, in tokamak literature, the poloidal magnetic flux enclosed by a closed magnetic surface can have two different definitions, one of which is the the poloidal magnetic flux through the surface S_2 in Fig. 3, the other one is the poloidal magnetic flux through the central hole of the magnetic surface, i.e., the poloidal flux through S_1 in Fig. 3. The former definition is adopted in this article, except explicitly specified otherwise. In the latter case, the poloidal magnetic flux is written

$$\Psi_p = 2\pi(\Psi - \Psi_a), \tag{20}$$

where the positive direction of the surface S_1 is defined to be in the clockwise direction.

Also note that, since the poloidal magnetic field can be written as $\mathbf{B}_p = \nabla\Psi \times \nabla\phi$, the condition $\Psi_{\text{LCFS}} - \Psi_{\text{axis}} > 0$ means $\mathbf{B}_p$ points in the anticlockwise direction (viewed along ϕ direction), and $\Psi_{\text{LCFS}} - \Psi_{\text{axis}} < 0$ means $\mathbf{B}_p$ points in the clockwise direction.

1.6 Shape parameters of a closed magnetic surface

This section introduces parameters that characteristic the shape of the projection of a magnetic surface on the poloidal plane. The "midplane" is defined as the plane that passes through the magnetic axis and is perpendicular to the symmetric axis (Z axis). For a up-down symmetric (about the midplane) magnetic surface, its shape can be roughly characterized by four parameters, namely, the R coordinate of the innermost and outermost points on the midplane, R_{in} and R_{out}; the (R, Z) coordinators of the highest point of the magnetic surface, $(R_{\text{top}}, Z_{\text{top}})$. These four parameters are indicated in Fig. 4.
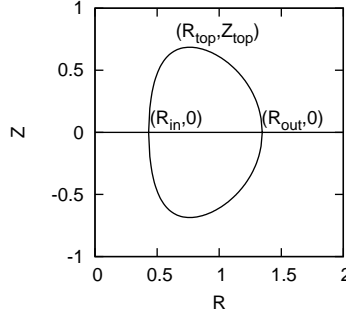
Figure 4. Four parameters characterizing the shape of a flux surface: the R coordinate of the innermost and outermost points in the middle-plane, R_{in} and R_{out}; the (R, Z) coordinators of the highest point of the flux surface, $(R_{\text{top}}, Z_{\text{top}})$.

In terms of these four parameters, we can define the major radius of a magnetic surface

$$R_0 = \frac{R_{\text{in}} + R_{\text{out}}}{2}, \tag{21}$$

(which is the R coordinate of the geometric center of the magnetic surface), the minor radius of a magnetic surface

$$a = \frac{R_{\text{out}} - R_{\text{in}}}{2}, \tag{22}$$

the triangularity of a magnetic surface

$$\delta = \frac{R_0 - R_{\text{top}}}{a}, \tag{23}$$

and, the ellipticity of a magnetic surface

$$\kappa = \frac{Z_{\text{top}}}{a}. \tag{24}$$

Strictly speaking, the ellipticity κ defined above is different from the elongation, which should be define by $(\kappa - 1)$ and thus is zero for a circular magnetic surface. However, many authors simply consider the ellipticity to be the elongation. Usually, we specify the value of R_0, a, δ, and κ, instead of $(R_{\text{in}}, R_{\text{out}}, R_{\text{top}}, Z_{\text{top}})$, to characterize the shape of a magnetic surface. Besides, using a and R_0, we can define another useful parameter $\varepsilon \equiv a / R_0$, which is called the inverse aspect ratio.

The four shape parameters for the typical Last-Closed-Flux-Surface (LCFS) of EAST tokamak are: major radius $R_0 = 1.85m$ (can reach $1.9m$), minor radius $a = 0.45m$, ellipticity $\kappa = 1.8$ (can be in the range from 1.7 to 1.9), triangularity $\delta = 0.6$ (can be in the range from 0.5 to 0.7). Note that the major radius R_0 of the LCFS is usually different from R_{axis} (the R coordinate of the magnetic axis). Usually we have $R_{\text{axis}} > R_0$ due to the Shafranov shift.

1.7 Safety factor

1.7.1 Definition of safety factor

Magnetic field lines on closed magnetic surfaces travel closed curves on the poloidal plane. Safety factor q is defined as the number of toroidal loops a magnetic field line goes when it makes one poloidal loop, i.e.

$$q \equiv \frac{\triangle \phi}{2\pi}, \tag{25}$$

where $\triangle \phi$ as the change of the toroidal angle when a magnetic field line travels a full poloidal loop.

1.7.2 Expression of safety factor in terms of magnetic field

The equation of magnetic field lines is given by

$$\frac{R d\phi}{d\ell_p} = \frac{B_\phi}{B_p}, \tag{26}$$

where $d\ell_p$ is the line element along the direction of $\mathbf{B}_p$ on the poloidal plane. Equation (26) can be arranged in the form

$$d\phi = \frac{1}{R}\frac{B_\phi}{B_p}d\ell_p, \tag{27}$$

which can be integrated over $d\ell_p$ to give

$$\triangle\phi = \oint \frac{1}{R}\frac{B_\phi}{B_p}d\ell_p, \tag{28}$$

where the line integration is along the poloidal magnetic field (the contour of Ψ on the poloidal plane). Using this, Eq. (25) is written

$$q = \frac{1}{2\pi}\oint \frac{1}{R}\frac{B_\phi}{B_p}d\ell_p. \tag{29}$$

The safety factor characterizes the average pitch angle of magnetic field lines on closed magnetic surfaces.

1.7.3 Expression of safety factor in terms of magnetic flux

The safety factor given by Eq. (29) is expressed in terms of the components of the magnetic field. The safety factor can also be expressed in terms of the magnetic flux. Define $d\Psi_p$ as the poloidal magnetic flux enclosed by two neighboring closed magnetic surface, then $d\Psi_p$ can be written

$$d\Psi_p = 2\pi R\, dx\, B_p \tag{30}$$

where dx is perpendicular to the first magnetic surface (so perpendicular to the $\mathbf{B}_p$) and its length is equal to the length from the point on this magnetic surface to the point on the neighbour magnetic surface. Using Eq. (30), the poloidal magnetic field is written as

$$B_p = \frac{1}{2\pi R}\frac{d\Psi_p}{dx}. \tag{31}$$

Substituting Eq. (31) into Eq. (29), we obtain

$$q = \frac{1}{2\pi}\oint \frac{1}{R}\frac{B_\phi}{B_p}d\ell_p = \frac{1}{2\pi}\oint \frac{1}{R}\frac{2\pi R\, dx\, B_\phi}{d\Psi_p}d\ell_p = \oint \frac{dx\, B_\phi}{d\Psi_p}d\ell_p. \tag{32}$$

We know $d\Psi_p$ is a constant independent of the poloidal location, so $d\Psi_p$ can be taken outside the integration to give

$$q = \frac{1}{d\Psi_p}\oint dx\, B_\phi d\ell_p \tag{33}$$

On the other hand, the toroidal magnetic flux enclosed by the two magnetic surfaces, $d\Psi_t$, is given by

$$d\Psi_t = \oint (B_\phi dx)d\ell_p \tag{34}$$

Using this, Eq. (33) is written as

$$q = \frac{d\Psi_t}{d\Psi_p} \tag{35}$$

Equation (35) indicates that the safety factor of a magnetic surface is equal to the differential of the toroidal magnetic flux with respect to the poloidal magnetic flux enclosed by the magnetic surface.

1.7.4 Rational surfaces vs. irrational surfaces

If the safety factor of a magnetic surface is a rational number, i.e., $q = n/m$, where m and n are integers, then this magnetic surface is called a rational surface, otherwise an irrational surface. It is obvious that a field line on a rational surface with $q = n/m$ closes itself after traveling n toroidal turns and m poloidal turns. An example of a magnetic field line on a rational surface is shown in Fig. 5.
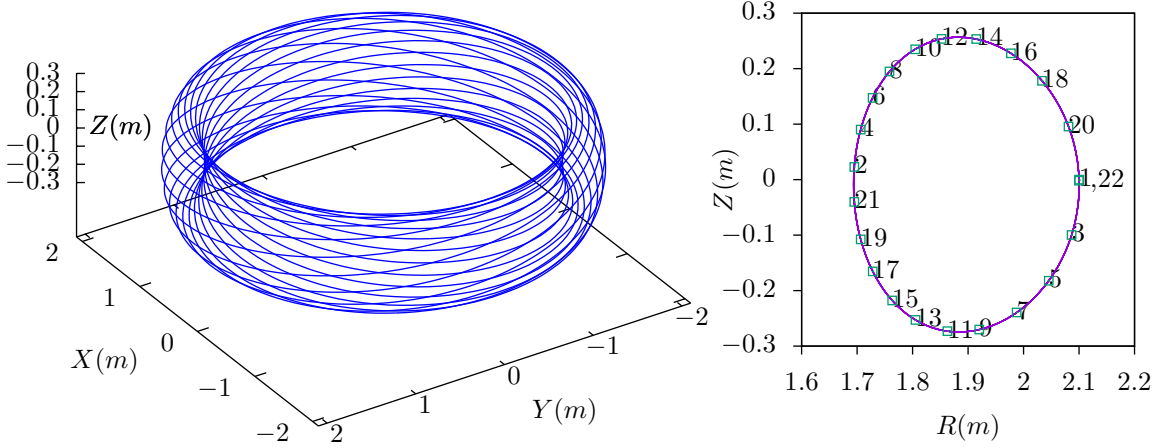
Figure 5. Left: A magnetic field line (blue) on a rational surface with $q = 2.1 = 21/10$ (magnetic field is from EAST discharge #59954@3.1s). This field line closes itself after traveling 21 toroidal loops and 10 poloidal loops. Right: The intersecting points of the magnetic field line with the $\phi = 0$ plane when it is traveling toroidally. The sequence of the intersecting points is indicated by the number labels. The 22nd intersecting point coincides with the 1st point and then the intersecting points repeat themselves.

2 Plasma current density in terms of Ψ and g

Using Ampère's law (neglecting the displacement current), the current density can be written in terms of the magnetic field as

$$\mu_0 \mathbf{J} = \nabla \times \mathbf{B} = -\frac{\partial B_\phi}{\partial Z}\hat{\mathbf{R}} + \frac{1}{R}\frac{\partial(RB_\phi)}{\partial R}\hat{\mathbf{Z}} + \left(\frac{\partial B_R}{\partial Z} - \frac{\partial B_Z}{\partial R}\right)\hat{\phi}. \tag{36}$$

2.1 Poloidal current density

Use Eq. (36) and the definition $g \equiv RB_\phi$, the poloidal components of the current density, J_Z and J_R, can be written as

$$\mu_0 J_R = -\frac{1}{R}\frac{\partial g}{\partial Z}, \tag{37}$$

and

$$\mu_0 J_Z = \frac{1}{R}\frac{\partial g}{\partial R}, \tag{38}$$

respectively. The poloidal plasma current density is usually small and can be safely neglected in most cases of interest (to be checked***).

2.2 Toroidal current density

Ampere's law (36) indicates the toroidal current density J_ϕ is given by

$$\begin{aligned}
\mu_0 J_\phi &= \frac{\partial B_R}{\partial Z} - \frac{\partial B_Z}{\partial R} \\
&= -\frac{1}{R}\frac{\partial^2 \Psi}{\partial Z^2} - \frac{\partial}{\partial R}\left(\frac{1}{R}\frac{\partial \Psi}{\partial R}\right).
\end{aligned} \tag{39}$$

Define a differential operator $\triangle^\star$ by

$$\triangle^* \equiv \frac{\partial^2}{\partial Z^2} + R\frac{\partial}{\partial R}\left(\frac{1}{R}\frac{\partial}{\partial R}\right), \tag{40}$$

which is very similar to the 2D Laplacian operator $\triangle = \nabla^2 = \partial^2/\partial Z^2 + \partial^2/\partial R^2$, then Eq. (39) is written

$$\mu_0 J_\phi = -\frac{1}{R}\triangle^*\Psi. \tag{41}$$

3 Constraint of force-balance on axisymmetric magnetic field

Next, we consider what constraint the force balance imposes on the axisymmetric magnetic field discussed above.

3.1 MHD momentum equation

The MHD momentum equation of plasmas is given by

$$\rho\left(\frac{\partial \mathbf{u}}{\partial t} + \mathbf{u}\cdot\nabla\mathbf{u}\right) = \rho_q\mathbf{E} + \mathbf{J}\times\mathbf{B} - \nabla\cdot\mathbb{P} \tag{42}$$

where ρ, ρ_q, $\mathbb{P}$, $\mathbf{J}$, $\mathbf{E}$, and $\mathbf{B}$ are mass density, charge density, thermal pressure tensor, current density, electric field, and magnetic field, respectively. The electric field force $\rho_q\mathbf{E}$ is usually ignored due to either $\rho_q = 0$ or $\mathbf{E} = 0$. Further assume that there is no plasma flow ($\mathbf{u} = 0$) and the plasma pressure is isotropic, then the steady state momentum equation (force balance equation) is written

$$\mathbf{J}\times\mathbf{B} = \nabla P, \tag{43}$$

where P is the scalar plasma pressure.

3.2 Force balance equation in tokamak plasmas: Grad-Shafranov equation

3.2.1 Parallel force balance

Consider the force balance in the direction of $\mathbf{B}$. Dotting the equilibrium equation (43) by $\mathbf{B}$, we obtain

$$0 = \mathbf{B}\cdot\nabla P, \tag{44}$$

which implies that P is constant along a magnetic field line. Since Ψ is also constant along a magnetic field line, P can be expressed in terms of only Ψ on a single magnetic line. Note that this does not necessarily mean P is a single-valued function of Ψ, i.e. $P = P(\Psi)$. For instance, P can take different value on different magnetic field lines with the same value of Ψ while still satisfying $\mathbf{B}\cdot\nabla P = 0$. However, for an asymmetric pressure, it is ready to prove that P is indeed a single-valued function of Ψ on a flux surface since Ψ is a constant on a magnetic surface (however, on different magnetic surfaces with the same value of Ψ, P can be different, refer to Sec. 17.8). On the other hand, if $P = P(\Psi)$, then we obtain

$$\mathbf{B}\cdot\nabla P = \frac{dP}{d\Psi}\mathbf{B}\cdot\nabla\Psi = 0,$$

i.e., Eq. (44) is satisfied. Therefore $P = P(\Psi)$ is equivalent to the force balance equation in the parallel (to the magnetic field) direction.

3.2.2 Toroidal force balance

Next, consider the ϕ component of Eq. (43), which is written

$$J_Z B_R - J_R B_Z = \frac{1}{R}\frac{\partial P}{\partial \phi}. \tag{45}$$

Since $P = P(\Psi)$, which implies $\partial P / \partial \phi = 0$, equation (45) reduces to

$$J_Z B_R - J_R B_Z = 0 \tag{46}$$

Using the expressions of the poloidal current density (37) and (38) in the force balance equation (46) yields

$$\frac{\partial g}{\partial R} B_R + \frac{\partial g}{\partial Z} B_Z = 0, \tag{47}$$

which can be further written

$$\mathbf{B} \cdot \nabla g = 0. \tag{48}$$

According to the same reasoning for the pressure, we conclude that Eq. (48) is equivalent to $g = g(\Psi)$. (The function g defined here is usually called the "poloidal current function" in tokamak literature. The reason for this name is discussed in Sec. 3.4.)

3.2.3 Force balance along the major radius

Next, consider the force balance in $\hat{\mathbf{R}}$ direction. The $\hat{\mathbf{R}}$ component of the force balance equation (43) is written

$$J_\phi B_Z - J_Z B_\phi = \frac{\partial P}{\partial R} \tag{49}$$

Using the expressions of the current density and magnetic field [Eqs. (5), (38), and (41)], equation (49) is written

$$-\frac{1}{R} \triangle^* \Psi \frac{1}{R} \frac{\partial \Psi}{\partial R} - \frac{1}{R} \frac{\partial g}{\partial R} \frac{g}{R} = \mu_0 \frac{\partial P}{\partial R}. \tag{50}$$

Using the fact that P and g are a function of only Ψ, i.e., $P = P(\Psi)$ and $g = g(\Psi)$, Eq. (50) is written

$$-\frac{1}{R} \triangle^* \Psi \frac{1}{R} \frac{\partial \Psi}{\partial R} - \frac{1}{R} \frac{dg}{d\Psi} \frac{\partial \Psi}{\partial R} \frac{g}{R} = \mu_0 \frac{dP}{d\Psi} \frac{\partial \Psi}{\partial R}, \tag{51}$$

which can be simplified to

$$\triangle^* \Psi = -\mu_0 R^2 \frac{dP}{d\Psi} - \frac{dg}{d\Psi} g, \tag{52}$$

i.e.,

$$\frac{\partial^2 \Psi}{\partial Z^2} + R \frac{\partial}{\partial R} \left(\frac{1}{R} \frac{\partial \Psi}{\partial R} \right) = -\mu_0 R^2 \frac{dP}{d\Psi} - \frac{dg}{d\Psi} g. \tag{53}$$

Equation (53) is known as Grad-Shafranov (GS) equation.

[Note that the Z component of the force balance equation is written

$$J_R B_\phi - J_\phi B_R = \frac{\partial P}{\partial Z}$$
$$\Rightarrow -\frac{\partial g}{\partial Z} \frac{1}{R} \frac{g}{R} - \frac{1}{R} \triangle^* \psi \frac{1}{R} \frac{\partial \Psi}{\partial Z} = \mu_0 \frac{dP}{d\Psi} \frac{\partial \Psi}{\partial Z}$$
$$\Rightarrow -\frac{dg}{d\Psi} \frac{\partial \Psi}{\partial Z} \frac{1}{R} \frac{g}{R} - \frac{1}{R} \triangle^* \Psi \frac{1}{R} \frac{\partial \Psi}{\partial Z} = \mu_0 \frac{dP}{d\Psi} \frac{\partial \Psi}{\partial Z}$$
$$\Rightarrow -\frac{dg}{d\Psi} \frac{1}{R} \frac{g}{R} - \frac{1}{R} \triangle^* \Psi \frac{1}{R} = \mu_0 \frac{dP}{d\Psi}$$
$$\Rightarrow \triangle^* \Psi = -\mu_0 R^2 \frac{dP}{d\Psi} - \frac{dg}{d\Psi} g$$

which turns out to be identical with the Grad-Shafranov equation. This is not a coincidence. The reason is that the force balance equation has been satisfied in three different directions, namely, in the $\hat{\phi}$, $\hat{\mathbf{R}}$, and $\mathbf{B}$ direction, and thus it must be satisfied in all directions.]

3.3 Expression of axisymmetric equilibrium magnetic field

A general axisymmetric magnetic field, which is not necessarily an equilibrium magnetic field, is given by Eq. (8), i.e.,

$$\mathbf{B} = \nabla \Psi \times \nabla \phi + g \nabla \phi, \tag{54}$$

For the above axisymmetric magnetic field to be consistent with the force balance equation (43), additional requirements for Ψ and g are needed. Specifically, Ψ is restricted by the GS equation and g must be a function of only Ψ. Therefore an axisymmetric equilibrium magnetic field is fully determined by specifying two functions, $\Psi = \Psi(R, Z)$ and $g = g(\Psi)$. The function Ψ is determined by solving the GS equation with specified boundary condition. Note that the GS equation contains two free functions, $P(\Psi)$ and $g(\Psi)$, both of which must be specified before the GS equation can be solved. (The way to specify the function $g(\Psi)$ to obtain desired global properties, such as total toroidal current and safety factor, will be discussed later.) This feature makes the process of solving GS equation different from solving usual partial differential equations where only boundary conditions are needed to be specified. For most cases, the terms on the right-hand side of the GS equation are nonlinear about Ψ and thus the GS equation is a two-dimensional (about the cylindrical coordinates R and Z) nonlinear partial differential equation for Ψ.

Equation (54) indicates that the poloidal and toroidal equilibrium magnetic field can be written as

$$\mathbf{B}_p = \nabla\Psi \times \nabla\phi, \tag{55}$$

and

$$\mathbf{B}_\phi = g\nabla\phi, \tag{56}$$

respectively.

It seems that many physical processes in tokamak are sensitive to the magnetic configuration. Therefore any serious numerical simulation should use magnetic field that satisfies the Grad-Shafranov equation and if possible use realistic magnetic field reconstructed from experimental data.

3.4 Relation of g with the poloidal plasma current

As is discussed in Sec. 3.2, to satisfy the force balance in the toroidal direction, $g \equiv RB_\phi$ must be a magnetic surface function, i.e., $g = g(\Psi)$. Using this, equations (37) and (38) are written

$$\mu_0 J_R = -\frac{1}{R}\frac{\partial g}{\partial \Psi}\frac{\partial \Psi}{\partial Z} = \frac{\partial g}{\partial \Psi}B_R, \tag{57}$$

and

$$\mu_0 J_Z = \frac{1}{R}\frac{\partial g}{\partial \Psi}\frac{\partial \Psi}{\partial R} = \frac{\partial g}{\partial \Psi}B_z, \tag{58}$$

respectively. The above two equations imply that

$$\frac{J_R}{J_Z} = \frac{B_R}{B_Z}, \tag{59}$$

which implies that the projections of $\mathbf{B}$ lines and $\mathbf{J}$ lines in the poloidal plane are identical to each other. This indicates that the $\mathbf{J}$ surfaces coincide with the magnetic surfaces. Using this and $\nabla \cdot \mathbf{J} = 0$, and following the same steps in Sec. 1.4, we obtain

$$I_{\mathrm{pol}} = \frac{1}{\mu_0}2\pi[g(\Psi_2) - g(\Psi_1)], \tag{60}$$

where I_{pol} is the poloidal current enclosed by the two magnetic surfaces, the positive direction of I_{pol} is chosen to be in the clockwise direction when observers look along $\hat{\phi}$. Equation (60) indicates that the difference of g between two magnetic surface is proportional to the poloidal current. For this reason, g is usually call the "poloidal current function".

In the above, we see that the relation of g with the poloidal electric current is similar to that of Ψ with the poloidal magnetic flux. This similarity is due to the following differential relations:

$$\begin{cases} \mathbf{B} = \nabla \times \mathbf{A} \\ \Psi = RA_\phi \end{cases}$$

$$\begin{cases} \mu_0\mathbf{J} = \nabla \times \mathbf{B} \\ g = RB_\phi \end{cases}$$

The poloidal plasma current density $\mathbf{J}_p$ can be further written as

$$
\begin{aligned}
\mathbf{J}_p &\equiv J_R\hat{\mathbf{R}} + J_Z\hat{\mathbf{Z}} \\
&= \frac{1}{\mu_0}\left(-\frac{1}{R}\frac{\partial g}{\partial Z}\hat{\mathbf{R}} + \frac{1}{R}\frac{\partial g}{\partial R}\hat{\mathbf{Z}}\right). \\
&= \frac{1}{\mu_0}\nabla g \times \nabla \phi
\end{aligned}
\tag{61}
$$

Using $g = g(\Psi)$, Eq. (61) is written

$$
\begin{aligned}
\mathbf{J}_p &= \frac{1}{\mu_0}\frac{dg}{d\Psi}\nabla\Psi \times \nabla\phi \\
&= \frac{1}{\mu_0}\frac{dg}{d\Psi}\mathbf{B}_p.
\end{aligned}
$$

3.5 Relation of plasma current density to pressure gradient

Due to the force balance condition, the plasma current is related to the plasma pressure. Using the equilibrium constraint in the $\mathbf{R}$ direction, J_ϕ given by Eq. (41) is written

$$
J_\phi = -\frac{1}{\mu_0 R}\triangle^*\Psi
\tag{62}
$$

$$
= R\frac{dP}{d\Psi} + \frac{1}{\mu_0 R}\frac{dg}{d\Psi}g.
\tag{63}
$$

The parallel (to the magnetic field) current density is written as

$$
\begin{aligned}
J_\parallel &\equiv \frac{\mathbf{J}\cdot\mathbf{B}}{B} \\
&= \frac{J_\phi B_\phi + \mathbf{J}_p\cdot\mathbf{B}_p}{B} \\
&= \frac{\left(R\frac{dP}{d\Psi} + \frac{1}{\mu_0 R}\frac{dg}{d\Psi}g\right)\frac{g}{R} + \frac{1}{\mu_0}\frac{dg}{d\Psi}\left(\frac{\nabla\Psi}{R}\right)^2}{B} \\
&= \frac{g\frac{dP}{d\Psi} + \frac{1}{\mu_0}\frac{dg}{d\Psi}\left[\left(\frac{g}{R}\right)^2 + \left(\frac{\nabla\Psi}{R}\right)^2\right]}{B} \\
&= \frac{g\frac{dP}{d\Psi} + \frac{1}{\mu_0}\frac{dg}{d\Psi}B^2}{B}.
\end{aligned}
\tag{64}
$$

For later use, define

$$
\begin{aligned}
\sigma &\equiv \frac{J_\parallel}{B} \\
&= g\frac{dP}{d\Psi}\frac{1}{B^2} + \frac{1}{\mu_0}\frac{dg}{d\Psi}.
\end{aligned}
\tag{65}
$$

Equation (65) is used in GTAW code to calculate $J_\parallel/B$ (actually calculated is $\mu_0 J_\parallel/B$)[11]. Note that the expression for $J_\parallel/B$ in Eq. (65) is not a magnetic surface function. Define σ_{ps} as

$$
\begin{aligned}
\sigma_{\text{ps}} &\equiv \sigma - \langle\sigma\rangle \\
&= g\frac{dP}{d\Psi}\left[\frac{1}{B^2} - \left\langle\frac{1}{B^2}\right\rangle\right] \\
&\equiv \frac{J_\parallel^{\text{ps}}}{B},
\end{aligned}
\tag{66}
\tag{67}
$$

where $J_\parallel^{\text{ps}}$ is called Pfirsch-Schluter (PS) current. In cylindrical geometry, due to the poloidal symmetry, the Pfiersch-Schluter current is obviously zero. In toroidal geometry, due to the poloidal asymmetry, the PS current is generally nonzero. Thus, this quantity characterizes a toroidal effect.

Another useful quantity is $\mu_0\langle\mathbf{J}\cdot\mathbf{B}\rangle$, which is written as

$$
\mu_0\langle\mathbf{J}\cdot\mathbf{B}\rangle = \mu_0 g\frac{dP}{d\Psi} + \frac{dg}{d\Psi}\langle B^2\rangle,
\tag{68}
$$

where $\langle...\rangle$ is flux surface averaging operator, which will be defined later in this note.

3.6 Solovév equilibrium

For most choices of $P(\Psi)$ and $g(\Psi)$, the GS equation has to be solved numerically. For the particular choice of P and g profiles given by

$$\frac{dP}{d\Psi} = -\frac{c_1}{\mu_0}, \tag{69}$$

$$g\frac{dg}{d\Psi} = -c_2 R_0^2, \tag{70}$$

analytical solution to the GS equation can be found, which is given by[12]

$$\Psi = \frac{1}{2}(c_2 R_0^2 + c_0 R^2)Z^2 + \frac{1}{8}(c_1 - c_0)(R^2 - R_0^2)^2, \tag{71}$$

where c_0, c_1, c_2, and R_0 are arbitrary constants. [Proof: By direct substitution, we can verify Ψ of this form is indeed a solution to the GS equation (53).] A useful choice for tokamak application is to set $c_0 = B_0/(R_0^2\kappa_0 q_0)$, $c_1 = B_0(\kappa_0^2 + 1)/(R_0^2\kappa_0 q_0)$, and $c_2 = 0$. Then Eq. (71) is written

$$\Psi = \frac{B_0}{2R_0^2\kappa_0 q_0}\left[R^2 Z^2 + \frac{\kappa_0^2}{4}(R^2 - R_0^2)^2\right], \tag{72}$$

which can be solved analytically to give the explicit form of the contour of Ψ on (R, Z) plane:

$$Z = \pm\frac{1}{R}\sqrt{\frac{2R_0^2\kappa_0 q_0}{B_0}\Psi - \frac{\kappa_0^2}{4}(R^2 - R_0^2)^2}, \tag{73}$$

which indicates the magnetic surfaces are up-down symmetrical. Using Eq. (69), i.e.,

$$\frac{dP}{d\Psi} = -\frac{c_1}{\mu_0} = -\frac{B_0(\kappa_0^2 + 1)}{\mu_0 R_0^2\kappa_0 q_0}, \tag{74}$$

the pressure is written

$$P = P_0 - \frac{B_0(\kappa_0^2 + 1)}{\mu_0 R_0^2\kappa_0 q_0}\Psi, \tag{75}$$

where P_0 is a constant of integration. Note Eq. (72) indicates that that $\Psi = 0$ at the magnetic axis ($R = R_0, Z = 0$). Therefore, Eq. (75) indicates that P_0 is the pressure at the magnetic axis. The toroidal field function g is a constant in this case, which implies there is no poloidal current in this equilibrium. (For the Solovev equilibrium (72), I found numerically that the value of the safety factor at the magnetic axis ($R = R_0, Z = 0$) is equal to $q_0 g/(R_0 B_0)$. This result should be able to be proved analytically. I will do this later. In calculating the safety factor, we also need the expression of $|\nabla\Psi|$, which is given analytically by

$$\begin{aligned}|\nabla\Psi| &= \sqrt{\left(\frac{\partial\Psi}{\partial R}\right)^2 + \left(\frac{\partial\Psi}{\partial Z}\right)^2}\\ &= \frac{B_0}{2R_0^2\kappa_0 q_0}\sqrt{[2RZ^2 + \kappa_0^2(R^2 - R_0^2)R]^2 + (2R^2 Z)^2}.\end{aligned} \tag{76}$$

)

Define $\Psi_0 = B_0 R_0^2$, and $\overline{\Psi} = \Psi/\Psi_0$, then Eq. (72) is written as

$$\overline{\Psi} = \frac{1}{2\kappa_0 q_0}\left[\overline{R}^2\overline{Z}^2 + \frac{\kappa_0^2}{4}(\overline{R}^2 - 1)^2\right], \tag{77}$$

where $\overline{R} = R/R_0$, $\overline{Z} = Z/R_0$. From Eq. (77), we obtain

$$\overline{Z} = \pm\frac{1}{\overline{R}}\sqrt{2\kappa_0 q_0\overline{\Psi} - \frac{\kappa_0^2}{4}(\overline{R}^2 - 1)^2}. \tag{78}$$

Given the value of κ_0, q_0, for each value of $\overline{\Psi}$, we can plot a magnetic surface on $(\overline{R}, \overline{Z})$ plane. An example of the nested magnetic surfaces is shown in Fig. 6.
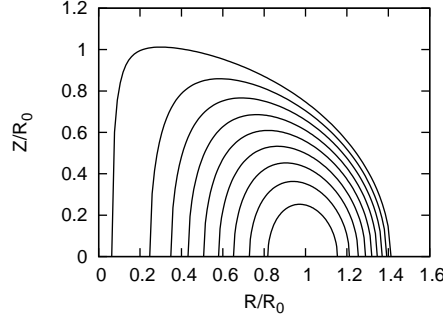
Figure 6. Flux surfaces of Solovév equilibrium for $\kappa_0 = 1.5$ and $q_0 = 1.5$, with $\overline{\Psi}$ varying from zero (center) to 0.123 (edge). The value of $\overline{\Psi}$ on the edge is determined by the requirement that the minimum of $\overline{R}$ is equal to zero. (To prevent "divided by zero" that appears in Eq. (78) when $R = 0$, the value of $\overline{\Psi}$ on the edge is shifted to $0.123 - \varepsilon$ when plotting the above figure, where ε is a small number, $\varepsilon = 10^{-3}$ in this case.)

The minor radius of a magnetic surface of the Solovev equilibrium can be calculated by using Eq. (73), which gives

$$R_{\text{in}} = \sqrt{R_0^2 - \sqrt{A\Psi}},\tag{79}$$

$$R_{\text{out}} = \sqrt{R_0^2 + \sqrt{A\Psi}},\tag{80}$$

and thus

$$a = \frac{R_{\text{out}} - R_{\text{in}}}{2} = \frac{\sqrt{R_0^2 + \sqrt{A\Psi}} - \sqrt{R_0^2 - \sqrt{A\Psi}}}{2}.\tag{81}$$

where $A = 8R_0^2 q_0 / (B_0 \kappa_0)$. In my code of constructing Solovev magnetic surface, the value of a is specified by users, and then Eq. (81) is solved numerically to obtain the value of Ψ of the flux surface. Note that the case $\Psi = 0$ corresponds to $R_{\text{in}} = R_{\text{out}} = R_0$, i.e., the magnetic axis, while the case $\Psi = R_0^2 B_0 \kappa_0 / (8q_0)$ corresponds to $R_{\text{in}} = 0$. Therefore, the reasonable value of Ψ of a magnetic surface should be in the range $0 \leqslant \Psi < R_0^2 B_0 \kappa_0 / (8q_0)$. This range is used as the interval bracketing a root in the bisection root finder.

Using Eq. (81), the inverse aspect ratio of a magnetic surface labeled by Ψ can be approximated as[12]

$$\varepsilon \approx \sqrt{\frac{2q_0 \Psi}{\kappa_0 R_0^2 B_0}}.\tag{82}$$

Therefore, the value of Ψ of a magnetic surface with the inverse aspect ratio ε is approximately given by

$$\Psi = \frac{\varepsilon^2 \kappa_0 R_0^2 B_0}{2q_0}.\tag{83}$$

3.7 Equilibrium scaling

The GS equation is given by Eq. (53), i.e.,

$$\frac{\partial^2 \Psi}{\partial Z^2} + R\frac{\partial}{\partial R}\left(\frac{1}{R}\frac{\partial \Psi}{\partial R}\right) = -\mu_0 R^2 \frac{dP}{d\Psi} - \frac{dg}{d\Psi}g.\tag{84}$$

If a solution to the GS equation is obtained, the solution can be scaled to obtain a family of solutions. Given an equilibrium with $\Psi(R, Z)$, $P(\Psi)$, $g(\Psi)$, then it is ready to prove that $\Psi_2 = s\Psi$, $P_2 = s^2 P(\Psi)$, and $g_2 = \pm s g(\Psi)$ is also a solution to the GS equation, where s is a constant. In this case, both the poloidal and toroidal magnetic fields are increased by a factor of s, and thus the safety factor remains unchanged. Also note that the pressure is increased by s^2 factor and thus the value of β (the ratio of the therm pressure to magnetic pressure) remains unchanged. Note that $g_2 = \pm s g(\Psi)$, which indicates that the direction of the toroidal magnetic field can be reversed without breaking the force balance. Also note that $\Psi_2 = s\Psi$ and s can be negative, which indicates that the direction of the toroidal current can also be reversed without breaking the force balance.

The second kind of scaling is to set $\Psi_2 = \Psi$, $P_2 = P(\Psi)$, and $g_2^2 = g^2(\Psi) + c$. It is ready to prove that the scaled expression is still a solution to the GS equation because $g_2 g_2' = g g'$. This scaling keep the pressure and the poloidal field unchanged and thus the poloidal beta β_p remains unchanged. This scaling scales the toroidal field and thus can be used to generate a series of equilibria with different profile of safety factor.

Another scaling, which is trivial, is to set $\Psi_2 = \Psi$, $P_2 = P(\Psi) + c$, and $g_2 = g(\Psi)$. This scaling can be used to test the effects of the pressure (not the pressure gradient) on various physical processes.

When a numerical equilibrium is obtained, one can use these scaling methods together to generate new equilibria that satisfy particular global conditions. Note that the shape of magnetic surfaces of the scaled equilibrium remains the same as the original one.

3.8 Plasma rotation

In deriving the Grad-Shafranov equation, we have assumed that there is no plasma flow. Next, let us examine whether this assumption is justified for plasmas in EAST tokamak.

The complete momentum equation is given by

$$\rho_m \left[\frac{\partial \mathbf{U}}{\partial t} + \mathbf{U} \cdot \nabla \mathbf{U} \right] = \rho_q \mathbf{E} + \mathbf{J} \times \mathbf{B} - \nabla \cdot \mathbb{P}, \tag{85}$$

where $\rho_q \mathbf{E}$ term can be usually neglected due to either $\rho_q \approx 0$ or $\mathbf{E} \approx 0$, $\mathbb{P}$ is a pressure tensor, which is different from the scalar pressure considered in this note. The equilibrium with pressure tensor can be important for neutral beam heating plasma, where pressure contributed by fast ions can be a tensor. With plasma flow and scalar pressure and neglecting electric force term, the steady state momentum equation is written

$$\rho_m \mathbf{U} \cdot \nabla \mathbf{U} = \mathbf{J} \times \mathbf{B} - \nabla P, \tag{86}$$

where the term on the left-hand side is the contribution of plasma flow to the force balance. Let us estimate the magnitude of this term. Macroscopic flows in tokamak are usually along the toroidal direction (the poloidal flow is usually heavily damped). The toroidal flow usually has the same toroidal angular frequency on a magnetic surface, i.e., the flow can be written as

$$\mathbf{U} = R \omega_T(\psi) \mathbf{e}_\phi, \tag{87}$$

where $\omega_T = \omega_T(\psi)$ is the toroidal angular frequency of the flow, which can have radial variation. Using this expression, the left-hand side of Eq. (86) is written as

$$\begin{aligned}
\rho_m \mathbf{U} \cdot \nabla \mathbf{U} &= \rho_m R \omega_T \mathbf{e}_\phi \cdot \nabla (R \omega_T \mathbf{e}_\phi) \\
&= \rho_m R \omega_T \frac{1}{R} \frac{\partial}{\partial \phi} (R \omega_T \mathbf{e}_\phi) \\
&= -\rho_m R \omega_T^2 \mathbf{e}_R,
\end{aligned} \tag{88}$$

which is just the centripetal force. For typical EAST plasma, the rotation frequency $f_T = \omega_T / 2\pi$ is less than 10kHz. For $f_T = 10$kHz, $R = 1.8m$ and $\rho_m = 1.3 \times 10^{-7}kg/m^3$ [Mass density of EAST#38300@3.9s, $\rho_m = n_D m_D = 4 \times 10^{19} m^{-3} \times 2 \times 1.6726 \times 10^{-27}$kg $= 1.3 \times 10^{-7}$kg$/m^3$], the above fore is about 9.23×10^2 newton. On the other hand, the pressure gradient force in Eq. (86) is about 4×10^4 newton, which is one order larger than the force contributed by the rotation. [Pressure gradient force is estimated by using $\nabla P \approx P_0 / a$, where P_0 is the thermal pressure at the magnetic axis and a is the minor radius of plasma. For typical EAST plasmas (EAST#38300@3.9s), $P_0 \approx 2 \times 10^4$Pa, $a = 0.45m$. Then $\nabla P \approx P_0 / a = 4 \times 10^4 N / m^3$.] This indicates the rotation has little influence on the force balance. In other words, the EAST tokamak equilibrium can be well described by the static equilibrium without rotation.

3.9 Efficiency of tokamak magnetic field in confining plasma: Plasma beta

To characterize the efficiency of the magnetic field of tokamaks in confining plasmas, introduce the plasma β, which is defined as the ratio of the thermal pressure to the magnetic pressure, i.e.,

$$\beta = \frac{p}{B^2 / 2\mu_0}. \tag{89}$$

Since the pressure in tokamak plasmas is inhomogeneous, the volume averaged pressure is usually used to define the beta. In tokamak plasmas, the toroidal beta β_t and the poloidal beta β_p are defined, respectively, by

$$\beta_t = \frac{\langle p \rangle}{B_{t0}^2/2\mu_0}, \tag{90}$$

$$\beta_p = \frac{\langle p \rangle}{B_{pa}^2/2\mu_0}, \tag{91}$$

where $\langle ... \rangle$ is the volume averaging, B_{t0} is the vacuum toroidal magnetic field at the magnetic axis (or geometrical center of the plasma), B_{pa} is the averaged poloidal magnetic field on the plasma surface. In tokamaks, the toroidal magnetic field is dominant and thus the the toroidal beta β_t (not β_p) is the usual way to characterize the the efficiency of the magnetic field in confining plasmas. Why do we need β_p? The short answer is that β_p characterizes the efficiency of the plasma current in confining the plasma. This can be seen by using Ampere's law to approximately write the poloidal magnetic field B_{pa} as $B_{pa} \approx \mu_0 I_p/(2\pi a)$. Then β_p is written

$$\beta_p \approx \frac{\langle p \rangle}{I_p^2/(8\pi^2 a^2)}, \tag{92}$$

which is the ratio of the pressure to the plasma current, and thus characterizes the efficiency of the plasma current in confining the plasma. Furthermore β_p is closely related to the normalized beta β_N introduced in the next subsection (refer to Eq. (94)). In addition, β_p is proportional to an important current, the so-called bootstrap current, in tokamak plasmas. I will discuss this later.

3.10 Beta limit

Beta limit means there is a limit for the value of beta beyond which the plasma will encounter a serious disruption. Early calculation of the beta limit on JET shows that the maximal β_t obtained is proportional to $I_p/(a B_{t0})$ for $I_p[\mathrm{MA}]/a B_{t0} \leqslant 3$, where $I_p[\mathrm{MA}]$ is the plasma current in mega Ampere, a is the plasma minor radius in meter, B_{t0} is the toroidal magnetic field in Tesla. This scaling relation $\beta_{t\,\max} \propto I_p/(a B_{t0})$ is often called Troyon scaling. This scaling relation motivates the definition a normalized beta, β_N, which is defined by

$$\beta_N = 10^8 \frac{a B_{t0}}{I_p} \beta_t, \tag{93}$$

where all quantities are in SI units. Equation (93) can also be written as

$$\beta_N = 10^8 \frac{\langle p \rangle}{I_p/a}, \tag{94}$$

which indicates that β_N can be considered as the efficiency of the plasma current in confining the plasma. The normalized beta β_N is an operational parameter indicating how close the plasma is to reach destabilizing major MHD activities. Its typical value is of order unit. The maximum value of β_N before the onset of deleterious instability is typically 3.5, although significantly higher values, e.g., $\beta_N = 7.2$, have been achieved in the low aspect ratio tokamak NSTX[15]. The ability to increase the value of β_N can be considered to be the ability of controlling the major MHD instabilities, and thus can be used to characterize how well a tokamak device is operated. One goal of EAST tokamak during 2015-2016 is to sustain a plasma with $\beta_N \geqslant 2$ for at least 10 seconds.

(check** The tearing mode, specifically the neoclassical tearing mode (NTM) is expected to set the beta limit in a reactor.)

(**check: Tokamak experiments have found that it is easier to achieve high β_N in large I_p plasmas than in small I_p plasmas. However, experiments found it is easier to achieve high β_p in small I_p plasmas than in large I_p plasmas. Examining the expression of β_N and β_p given by Eqs. (92) and Eq. (94), respectively, we recognize that pressure limit should have a scaling of $\langle p \rangle \propto I_p^\alpha$ with $1 < \alpha < 2$.)

Tokamak experiments have also found that it is easier to achieve higher β_t in low B_t plasmas than in higher B_t plasmas, which indicates that the efficiency of the magnetic field in confining plasma is a decreasing function of the magnitude of the magnetic field.

3.11 Why bigger tokamaks with larger plasma current are desired

As is mentioned in Sec. 3.9, the beta limit study on JET tokamak shows that the maximal β_t obtained is proportional to $I_p / a B_{t0}$. This means the maximal plasmas pressure obtained is proportional to I_p/a, i.e.,

$$\langle p \rangle \propto \frac{I_p}{a} \tag{95}$$

The total plasma energy is given by $E \approx \langle p \rangle \, 2\pi R a^2$, where R is the major radius of the device. Using Eq. (95), we obtain

$$E \propto I_p a R. \tag{96}$$

Since fusion power is proportional to the plasma energy, the above relation indicates, to obtain larger fusion power, we desire bigger tokamaks with larger plasma current.

The reason why larger plasma current is disired can also be appreciated by examining an empirical scaling of the the energy confinement time τ_E given by

$$\tau_E \propto \frac{I^2}{T}, \tag{97}$$

which is proportional to I^2.

Another fundamental reason for building larger tokamaks is that the energy confinement time $\tau_E \sim a^2/\chi$ increases with the machine size, where χ is the heat diffusitivity. In addition, the heat diffusitivity χ decreases with increasing machine size if the diffusitivity satisfies the gyro-Bohm scaling, which is given by

$$\chi_{GB} = \frac{\sqrt{m_i} \, T_i^{3/2}}{a B^2 q_i^2}, \tag{98}$$

which is inverse proportional to the machine size a. However, if the diffusitivity satisfies the Bohm scaling, which is given by

$$\chi_B = \frac{T}{|q|B}, \tag{99}$$

then, the diffusitivity is independent of the machine size. The Bohm diffusitivity χ_B is a/ρ_s times larger than the gyro-Bohm diffusitivity χ_{GB}, where ρ_s is the gyro-radius. Heat diffusitivity scaling in the low confinemet operation (L mode) in presnt-day tokamaks is obvserved to be Bohm or worse than Bohm.

3.12 Density limit

The maximum density that can be obtained in stable plasma operations (without disruption) is empirically given by

$$n_e \approx 1.5 n_G, \tag{100}$$

where n_G is the Greenwalt density, which is given by

$$n_G = 10^{20} \frac{I_p}{\pi a^2} \times 10^{-6} \tag{101}$$

where I_p is the plasma current, a is the minor radius, all physical quantities are in SI units. The $1.5 n_G$ gives the density limit that can be achieved for a tokamak operation scenario with plasma current I_p and plasma minor radius a. The Greenwalt density limit is an empirical one, which, like other empirical limits, can be exceeded in practice (for example, the density actually achieved in an experiment can be $n_e = 1.6 n_G$). Equation (101) indicates that the Greenwalt density is proportional to the current density. Therefore the ability to operate in large plasma current density means the ability to operate with high plasma density.

Note that neither the pressure limit nor the density limit is determined by the force-balance constraints. They are determined by the stability of the equilibrium. On the other hand, since the stability of the equilibrium is determined by the equilibrium itself, the pressure and density limit involves equilibrium quantities. For this reason, I decide to mention these contents (pressure and density limits) in these notes on equilibrium. Next, I will return to the discussions of equilibrium.

4 Free boundary equilibrium problem

Free boundary equilibrium problem refers to the case where the value of Ψ on the boundary of the computational box is unknown and must be determined from the current from both the plasma and external coils. Suppose the computational box is a rectangle in (R, Z) plane. If all the current perpendicular to (R, Z) plane is known, the value of Ψ at any point can be uniquely determined by using the Green function method, which gives

$$\Psi(R', Z') = \int_P G(R, Z; R', Z') J_\phi \, dR \, dZ + \sum_{i=1}^{N_c} G(R_i^c, Z_i^c; R', Z') I_\phi. \tag{102}$$

In solving the equilibrium problem, the current in external coils is given and known while the current carried by the plasma is unknown, which need to be derived from the information of Ψ via Eq. (62), i.e.,

$$J_\phi = -\frac{1}{\mu_0 R} \triangle^* \Psi. \tag{103}$$

To numerically solve GS equation within the computational box, we need the value of Ψ on the boundary of the box as a boundary condition. Thus we need to adopt some initial guess of the value of Ψ on the boundary, then solve the GS equation to get the value of Ψ within the computational box. Using the computed Ψ, we can calculate the value of the plasma current perpendicular to the (R, Z) plane through Eq. (103). After this, all the current (current in the plasma and in the external coils) perpendicular to the poloidal plane is known, we can calculate the value of Ψ on the boundary of the box, Ψ_b, by using the Green function formulation Eq. (102). Note that Ψ_b calculated this way usually differs from the initial guess of the value of Ψ on the boundary. Thus, we need to use the Ψ_b calculated this way as a new guess value of Ψ on the computational boundary and repeat the above procedures. The process is repeated until Ψ_b obtained in two successive iterations agrees with each other to a prescribed tolerance.

5 Fixed boundary equilibrium problem

Before considering the free boundary equilibrium problem, it is instructive to consider the fixed boundary equilibrium problem, where the shape of the last closed flux surface is given. This kind of problem provides basic knowledge for dealing with the more complicated free boundary problem. In dealing with the fixed boundary problem, the curvilinear coordinate system is useful. Specifically, the convenience provided by a curvilinear coordinate system in solving the fixed boundary tokamak equilibrium problem is that the curvilinear coordinates can be properly chosen to make one of the coordinate surfaces coincide with the given boundary flux surface, so that the boundary condition becomes trivial in this curvilinear coordinate system.

Next section discusses the basic theory of curvilinear coordinates system. (I learned the theory of general coordinates from the appendix of Ref. [3], which is concise and easy to understand.) Many analytical theories and numerical codes use the curvilinear coordinate systems that are constructed with one coordinate surface coinciding with the magnetic surface. These kinds of curvilinear coordinates are usually called the magnetic surface coordinates. In these coordinate systems, we need to choose a poloidal coordinate θ and a toroidal coordinate ζ. A particular choice for θ and ζ is one that makes the magnetic field lines be straight lines on (θ, ζ) plane. This kind of coordinate system is usually called a flux coordinate system. A further tuned magnetic coordinate system is the so-called field-line aligned coordinate system, in which chaning one of the three coordinates with the other two fixed would correspond to following a magnetic field line.

6 Curvilinear coordinate system

6.1 Coordinates transformation and Jacobian

In the Cartesian coordinates, a point is described by its coordinates (x, y, z), which, in vector form, is written as

$$\mathbf{r} = x\hat{\mathbf{x}} + y\hat{\mathbf{y}} + z\hat{\mathbf{z}}, \tag{104}$$

where $\mathbf{r}$ is the location vector of the point. The transformation between the Cartesian coordinates system, (x, y, z), and a general coordinates system, (x_1, x_2, x_3), can be written as

$$\mathbf{r} = x(x_1, x_2, x_3)\hat{\mathbf{x}} + y(x_1, x_2, x_3)\hat{\mathbf{y}} + z(x_1, x_2, x_3)\hat{\mathbf{z}}. \tag{105}$$

(For example, cylindrical coordinates (R, ϕ, Z) can be considered as a general coordinate systems, which are defined by $\mathbf{r} = R\cos\phi\hat{\mathbf{x}} + R\sin\phi\hat{\mathbf{y}} + Z\hat{\mathbf{z}}$.) The transformation function in Eq. (105) can be written as

$$\begin{aligned} x &= x(x_1, x_2, x_3) \\ y &= y(x_1, x_2, x_3) \\ z &= z(x_1, x_2, x_3) \end{aligned} \tag{106}$$

The Jacobian determinant (or simply called Jacobian) of the transformation in Eq. (106) is defined by

$$\mathcal{J} = \begin{vmatrix} \frac{\partial x}{\partial x_1} & \frac{\partial x}{\partial x_2} & \frac{\partial x}{\partial x_3} \\ \frac{\partial y}{\partial x_1} & \frac{\partial y}{\partial x_2} & \frac{\partial y}{\partial x_3} \\ \frac{\partial z}{\partial x_1} & \frac{\partial z}{\partial x_2} & \frac{\partial z}{\partial x_3} \end{vmatrix}, \tag{107}$$

which can also be written as

$$\mathcal{J} = \frac{\partial \mathbf{r}}{\partial x_1} \times \frac{\partial \mathbf{r}}{\partial x_2} \cdot \frac{\partial \mathbf{r}}{\partial x_3}. \tag{108}$$

It is easy to prove that the Jacobian $\mathcal{J}$ in Eq. (108) can also be written (the derivation is given in my notes on Jacobian)

$$\mathcal{J} = (\nabla x_1 \times \nabla x_2 \cdot \nabla x_3)^{-1}. \tag{109}$$

In most cases, the Jacobian of the transformation from the Cartesian coordinates to a particular coordinate system are simply called the Jacobian of that particular coordinate system without mentioning that this transformation is with respect to the Cartesian coordinates. Using this nomenclature, the Jacobian $\mathcal{J}$ of the Cartesian coordinates is obviously equal to one since the transformation is defined with respect to the Cartesian coordinates. If the Jacobian of a coordinate system is greater than zero, it is called a right-hand coordinate system. Otherwise it is called a left-hand system.

6.2 Orthogonality relation between two sets of basis vectors

In a curvilinear coordinate system (x_1, x_2, x_3), we will encounter two kinds of basis vectors: ∇x_i and $\partial \mathbf{r}/\partial x_i$, with $i = 1, 2, 3$. These two kinds of basis vectors satisfy the following orthogonality relation:

$$\nabla x_i \cdot \frac{\partial \mathbf{r}}{\partial x_j} = \delta_{ij}, \tag{110}$$

where δ_{ij} is the Kronical delta function. [Proof: Working in a Cartesian coordinate system (x, y, z) with the corresponding basis vectors denoted by $(\hat{\mathbf{x}}, \hat{\mathbf{y}}, \hat{\mathbf{z}})$, then the left-hand side of Eq. (110) can be written as

$$\begin{aligned} \nabla x_i \cdot \frac{\partial \mathbf{r}}{\partial x_j} &= \left[\left(\frac{\partial x_i}{\partial x}\right)\hat{\mathbf{x}} + \left(\frac{\partial x_i}{\partial y}\right)\hat{\mathbf{y}} + \left(\frac{\partial x_i}{\partial z}\right)\hat{\mathbf{z}}\right] \cdot \left[\frac{\partial x}{\partial x_j}\hat{\mathbf{x}} + x\frac{\partial \hat{\mathbf{x}}}{\partial x_j} + \frac{\partial y}{\partial x_j}\hat{\mathbf{y}} + y\frac{\partial \hat{\mathbf{y}}}{\partial x_j} + \frac{\partial z}{\partial x_j}\hat{\mathbf{z}} + z\frac{\partial \hat{\mathbf{z}}}{\partial x_j}\right] \\ &= \left[\left(\frac{\partial x_i}{\partial x}\right)\hat{\mathbf{x}} + \left(\frac{\partial x_i}{\partial y}\right)\hat{\mathbf{y}} + \left(\frac{\partial x_i}{\partial z}\right)\hat{\mathbf{z}}\right] \cdot \left[\frac{\partial x}{\partial x_j}\hat{\mathbf{x}} + 0 + \frac{\partial y}{\partial x_j}\hat{\mathbf{y}} + 0 + \frac{\partial z}{\partial x_j}\hat{\mathbf{z}} + 0\right] \tag{111} \\ &= \frac{\partial x_i}{\partial x}\frac{\partial x}{\partial x_j} + \frac{\partial x_i}{\partial y}\frac{\partial y}{\partial x_j} + \frac{\partial x_i}{\partial z}\frac{\partial z}{\partial x_j} \\ &= \frac{\partial x_i}{\partial x_j} \tag{112} \\ &= \delta_{ij}, \end{aligned}$$

where the second equality is due to $\partial\hat{\mathbf{x}}/\partial x^j = 0$, $\partial\hat{\mathbf{y}}/\partial x^j = 0$, $\partial\hat{\mathbf{z}}/\partial x^j = 0$ since $\hat{\mathbf{x}}, \hat{\mathbf{y}}, \hat{\mathbf{z}}$ are constant vectors independent of spatial location; the chain rule has been used in obtaining Eq. (112)]

It can be proved that ∇x^i is a contravariant vector while $\partial \mathbf{r} / \partial x^i$ is a covariant vector (I do not prove this and do not bother with the meaning of these names). The orthogonality relation in Eq. (110) is fundamental to the theory of general coordinates. (The cylindrical coordinate system (R, ϕ, Z) is an example of general coordinates. As an exercise, we can verify that the cylindrical coordinates have the above property. In this case, $x = x_1 \cos x_2$, $y = x_1 \sin x_2$, $z = x_3$, where $x_1 \equiv R$, $x_2 \equiv \phi$, $x_3 \equiv Z$.) The orthogonality relation allows one to write the covariant basis vectors in terms of contravariant basis vectors and vice versa. For example, the orthogonality relation tells that $\partial \mathbf{r} / \partial x_1$ is orthogonal to ∇x_2 and ∇x_3, thus, $\partial \mathbf{r} / \partial x_1$ can be written as

$$\frac{\partial \mathbf{r}}{\partial x_1} = A \nabla x_2 \times \nabla x_3, \tag{113}$$

where A is a unknown variable to be determined. To determine A, dotting Eq. (113) by ∇x_1, and using the orthogonality relation again, we obtain

$$1 = A(\nabla x_2 \times \nabla x_3) \cdot \nabla x_1, \tag{114}$$

which gives

$$\begin{aligned} A &= \frac{1}{(\nabla x_2 \times \nabla x_3) \cdot \nabla x_1} \\ &= \mathcal{J} \end{aligned} \tag{115}$$

Thus $\partial \mathbf{r} / \partial x_1$ is written, in terms of ∇x_1, ∇x_2, and ∇x_3, as

$$\frac{\partial \mathbf{r}}{\partial x_1} = \mathcal{J} \nabla x_2 \times \nabla x_3. \tag{116}$$

Similarly, we obtain

$$\frac{\partial \mathbf{r}}{\partial x_2} = \mathcal{J} \nabla x_3 \times \nabla x_1 \tag{117}$$

and

$$\frac{\partial \mathbf{r}}{\partial x_3} = \mathcal{J} \nabla x_1 \times \nabla x_2. \tag{118}$$

Equations (116)-(118) can be generally written

$$\frac{\partial \mathbf{r}}{\partial x_i} = \mathcal{J} \nabla x_j \times \nabla x_k, \tag{119}$$

where (i, j, k) represents the cyclic order in the variables (x_1, x_2, x_3). Equation (119) expresses the covariant basis vectors in terms of the contravariant basis vectors. On the other hand, from Eq. (116)-(118), we obtain

$$\nabla x_i = \mathcal{J}^{-1} \frac{\partial \mathbf{r}}{\partial x_j} \times \frac{\partial \mathbf{r}}{\partial x_k}, \tag{120}$$

which expresses the contravariant basis vectors in terms of the covariant basis vectors.

6.3 An example: (ψ, θ, ζ) coordinates

Suppose (ψ, θ, ζ) is an arbitrary general coordinate system. Then the covariant basis vectors are $\nabla \psi$, $\nabla \theta$, and $\nabla \zeta$, and the corresponding contravariant basis vectors are written as

$$\frac{\partial \mathbf{r}}{\partial \psi} = \mathcal{J} \nabla \theta \times \nabla \zeta, \tag{121}$$

$$\frac{\partial \mathbf{r}}{\partial \theta} = \mathcal{J} \nabla \zeta \times \nabla \psi, \tag{122}$$

$$\frac{\partial \mathbf{r}}{\partial \zeta} = \mathcal{J} \nabla \psi \times \nabla \theta, \tag{123}$$

where $\mathcal{J} = [(\nabla \psi \times \nabla \theta) \cdot \nabla \zeta]^{-1}$. In Einstein's notation, contravariant basis vectors are denoted with upper indices as

$$\mathbf{e}^\psi \equiv \nabla \psi; \ \ \mathbf{e}^\theta \equiv \nabla \theta; \ \ \mathbf{e}^\zeta \equiv \nabla \zeta. \tag{124}$$

and the covariant basis vectors are denoted with low indices as

$$\mathbf{e}_\psi \equiv \frac{\partial \mathbf{r}}{\partial \psi}; \;\; \mathbf{e}_\theta \equiv \frac{\partial \mathbf{r}}{\partial \theta}; \;\; \mathbf{e}_\zeta \equiv \frac{\partial \mathbf{r}}{\partial \zeta}.$$

Then the orthogonality relation, Eq. (110), is written as

$$\mathbf{e}^\alpha \cdot \mathbf{e}_\beta = \delta_{\alpha\beta}. \tag{125}$$

Then, in term of the contravairant basis vectors, $\mathbf{A}$ is written

$$\mathbf{A} = A_\psi \mathbf{e}^\psi + A_\theta \mathbf{e}^\theta + A_\zeta \mathbf{e}^\zeta, \tag{126}$$

where $A_\psi = \mathbf{A} \cdot \mathbf{e}_\psi$, $A_\theta = \mathbf{A} \cdot \mathbf{e}_\theta$, and $A_\zeta = \mathbf{A} \cdot \mathbf{e}_\zeta$. Similarly, in term of the covariant basis vectors, $\mathbf{A}$ is written

$$\mathbf{A} = A^\psi \mathbf{e}_\psi + A^\theta \mathbf{e}_\theta + A^\zeta \mathbf{e}_\zeta, \tag{127}$$

where $A^\psi = \mathbf{A} \cdot \mathbf{e}^\psi$, $A^\theta = \mathbf{A} \cdot \mathbf{e}^\theta$, and $A^\zeta = \mathbf{A} \cdot \mathbf{e}^\zeta$.

[In passing, we note that $\Psi \equiv A_\phi R$ is the covariant toroidal component of $\mathbf{A}$ in cylindrical coordinates (R, ϕ, Z). The proof is as follows. Note that the covariant form of $\mathbf{A}$ should be expressed in terms of the contravariant basis vector (∇R, $\nabla \phi$, and ∇Z), i.e.,

$$\mathbf{A} = A_1 \nabla R + A_2 \nabla \phi + A_3 \nabla Z. \tag{128}$$

where A_2 is the covariant toroidal component of $\mathbf{A}$. To obtain A_2, we take scalar product of Eq. (128) with $\partial \mathbf{r} / \partial \phi$ and use the orthogonality relation (110), which gives

$$\mathbf{A} \cdot \frac{\partial \mathbf{r}}{\partial \phi} = A_2. \tag{129}$$

In cylindrical coordinates (R, ϕ, Z), the location vector is written as

$$\mathbf{r}(R, Z, \phi) = R\hat{\mathbf{e}}_R(\phi) + Z\hat{\mathbf{e}}_Z. \tag{130}$$

Using this, we obtain

$$\frac{\partial \mathbf{r}}{\partial \phi} = R\hat{\mathbf{e}}_\phi, \tag{131}$$

Use Eq. (131) in Eq. (129) giving

$$A_2 = A_\phi R, \tag{132}$$

which indicates that $\Psi = A_\phi R$ is the covariant toroidal component of the vector potential.]

6.4 Gradient and directional derivative in general coordinates (ψ, θ, ζ)

The gradient of a scalar function $f(\psi, \theta, \zeta)$ is readily calculated from the chain rule,

$$\nabla f = \frac{\partial f}{\partial \psi} \nabla \psi + \frac{\partial f}{\partial \theta} \nabla \theta + \frac{\partial f}{\partial \zeta} \nabla \zeta. \tag{133}$$

Note that the gradient of a scalar function is in the covariant representation. The inverse form of this expression is obtained by dotting the above equation respectively by the three contravariant basis vectors, yielding

$$\frac{\partial f}{\partial \psi} = (\mathcal{J} \nabla \theta \times \nabla \zeta) \cdot \nabla f = \frac{\partial \mathbf{r}}{\partial \psi} \cdot \nabla f \tag{134}$$

$$\frac{\partial f}{\partial \theta} = (\mathcal{J} \nabla \zeta \times \nabla \psi) \cdot \nabla f = \frac{\partial \mathbf{r}}{\partial \theta} \cdot \nabla f \tag{135}$$

$$\frac{\partial f}{\partial \zeta} = (\mathcal{J} \nabla \psi \times \nabla \theta) \cdot \nabla f = \frac{\partial \mathbf{r}}{\partial \zeta} \cdot \nabla f \tag{136}$$

Using Eq. (133), the directional derivative in the direction of $\nabla \psi$ is written as

$$\nabla \psi \cdot \nabla f = |\nabla \psi|^2 \frac{\partial f}{\partial \psi} + (\nabla \theta \cdot \nabla \psi) \frac{\partial f}{\partial \theta} + (\nabla \zeta \cdot \nabla \psi) \frac{\partial f}{\partial \zeta}. \tag{137}$$

6.5   Divergence operator in general coordinates (ψ, θ, ζ)

To calculate the divergence of a vector, it is desired that the vector should be in the contravariant form we can make use of the fact that

$$\nabla \cdot (\nabla \alpha \times \nabla \beta) = 0, \tag{138}$$

for any scalar quantities α and β. Therefore we write vector $\mathbf{A}$ as

$$\mathbf{A} = A^1 \mathcal{J} \nabla \theta \times \nabla \zeta + A^2 \mathcal{J} \nabla \zeta \times \nabla \psi + A^3 \mathcal{J} \nabla \psi \times \nabla \theta, \tag{139}$$

where $A^1 = \mathbf{A} \cdot \nabla \psi$, etc.. Then the divergence of $\mathbf{A}$ is readily calculated as

$$
\begin{aligned}
\nabla \cdot \mathbf{A} &= \nabla(A^1 \mathcal{J}) \cdot (\nabla \theta \times \nabla \zeta) + \nabla(A^2 \mathcal{J}) \cdot (\nabla \zeta \times \nabla \psi) + \nabla(A^3 \mathcal{J}) \cdot (\nabla \psi \times \nabla \theta) \tag{140} \\
&= \frac{1}{\mathcal{J}} \left(\frac{\partial A^1 \mathcal{J}}{\partial \psi} + \frac{\partial A^2 \mathcal{J}}{\partial \theta} + \frac{\partial A^3 \mathcal{J}}{\partial \zeta} \right), \tag{141}
\end{aligned}
$$

where the second equality is obtained by using Eqs. (134), (135), and (136).

6.6   Laplacian operator in general coordinates (ψ, θ, ζ)

The Laplacian operator is defined by $\nabla^2 \equiv \nabla \cdot \nabla$. Then $\nabla^2 f$ is written as (f is an arbitrary function)

$$
\begin{aligned}
\nabla^2 f &= \nabla \cdot \nabla f \\
&= \nabla \cdot \left(\frac{\partial f}{\partial \psi} \nabla \psi + \frac{\partial f}{\partial \theta} \nabla \theta + \frac{\partial f}{\partial \zeta} \nabla \zeta \right). \tag{142}
\end{aligned}
$$

To proceed, we can use the divergence formula (141) to exress the divergence in the above expression. However, the vector in the above (blue term) is not in the covariant form desired by the divergence formula (141). If we want to directly use the formula (141), we need to transform the vector (blue term in expression (142)) to the covariant form. This process seems to be a little complicated. Therefore, I choose not to use this method. Instead, I try to simplify expression (142) by using basic vector identities:

$$
\begin{aligned}
\nabla^2 f &= \nabla\left(\frac{\partial f}{\partial \psi} \right) \cdot \nabla \psi + \nabla\left(\frac{\partial f}{\partial \theta} \right) \cdot \nabla \theta + \nabla\left(\frac{\partial f}{\partial \zeta} \right) \cdot \nabla \zeta \\
&\quad + \frac{\partial f}{\partial \psi} \nabla^2 \psi + \frac{\partial f}{\partial \theta} \nabla^2 \theta + \frac{\partial f}{\partial \zeta} \nabla^2 \zeta. \tag{143}
\end{aligned}
$$

Using the gradient formula, the above expression is further written as

$$
\begin{aligned}
\nabla^2 f &= \frac{\partial^2 f}{\partial \psi^2} |\nabla \psi|^2 + \frac{\partial^2 f}{\partial \psi \partial \theta} \nabla \psi \cdot \nabla \theta + \frac{\partial^2 f}{\partial \psi \partial \zeta} \nabla \psi \cdot \nabla \zeta \\
&\quad + \frac{\partial^2 f}{\partial \theta \partial \psi} \nabla \theta \cdot \nabla \psi + \frac{\partial^2 f}{\partial \theta^2} |\nabla \theta|^2 + \frac{\partial^2 f}{\partial \theta \partial \zeta} \nabla \theta \cdot \nabla \zeta \\
&\quad + \frac{\partial^2 f}{\partial \zeta \partial \psi} \nabla \zeta \cdot \nabla \psi + \frac{\partial^2 f}{\partial \zeta \partial \theta} \nabla \zeta \cdot \nabla \theta + \frac{\partial^2 f}{\partial \zeta^2} |\nabla \zeta|^2 \\
&\quad + \frac{\partial f}{\partial \psi} \nabla^2 \psi + \frac{\partial f}{\partial \theta} \nabla^2 \theta + \frac{\partial f}{\partial \zeta} \nabla^2 \zeta, \tag{144}
\end{aligned}
$$

and can be simplified as

$$
\begin{aligned}
\nabla^2 f &= \frac{\partial^2 f}{\partial \psi^2} |\nabla \psi|^2 + 2\frac{\partial^2 f}{\partial \psi \partial \theta} \nabla \psi \cdot \nabla \theta + 2\frac{\partial^2 f}{\partial \psi \partial \zeta} \nabla \psi \cdot \nabla \zeta \\
&\quad + \frac{\partial^2 f}{\partial \theta^2} |\nabla \theta|^2 + 2\frac{\partial^2 f}{\partial \theta \partial \zeta} \nabla \theta \cdot \nabla \zeta \\
&\quad + \frac{\partial^2 f}{\partial \zeta^2} |\nabla \zeta|^2 \\
&\quad + \frac{\partial f}{\partial \psi} \nabla^2 \psi + \frac{\partial f}{\partial \theta} \nabla^2 \theta + \frac{\partial f}{\partial \zeta} \nabla^2 \zeta. \tag{145}
\end{aligned}
$$

Assume (ψ, θ, ζ) are field-line following coordinates with $\partial \mathbf{r} / \partial \theta$ along the field line direction, then neglect all the parallel derivatives, i.e., derivative over θ, then the above expression is reduced to

$$
\begin{aligned}
\nabla^2 f &= \frac{\partial^2 f}{\partial \psi^2} |\nabla \psi|^2 + 2\frac{\partial^2 f}{\partial \psi \partial \zeta} \nabla \psi \cdot \nabla \zeta + \frac{\partial^2 f}{\partial \zeta^2} |\nabla \zeta|^2 \\
&\quad + \frac{\partial f}{\partial \psi} \nabla^2 \psi + \frac{\partial f}{\partial \zeta} \nabla^2 \zeta. \tag{146}
\end{aligned}
$$

This approximation reduces the Laplacian operator from being three-dimensional to being two-dimensional. This approximation is often called the high-n approximation, where n is the toroidal mode number (mode number along ζ direction).

6.7 Curl operator in general coordinates (ψ, θ, ζ)

To take the curl of a vector, it should be in the covariant representation since we can make use of the fact that $\nabla \times \nabla \alpha = 0$. Thus the curl of $\mathbf{A}$ is written as

$$
\begin{aligned}
\nabla \times \mathbf{A} &= \nabla \times (A_1 \nabla\psi + A_2 \nabla\theta + A_3 \nabla\zeta) \\
&= \nabla A_1 \times \nabla\psi + \nabla A_2 \times \nabla\theta + \nabla A_3 \times \nabla\zeta \\
&= \left(\frac{\partial A_1}{\partial \theta}\nabla\theta + \frac{\partial A_1}{\partial \zeta}\nabla\zeta\right) \times \nabla\psi + \left(\frac{\partial A_2}{\partial \psi}\nabla\psi + \frac{\partial A_2}{\partial \zeta}\nabla\zeta\right) \times \nabla\theta + \left(\frac{\partial A_3}{\partial \psi}\nabla\psi + \frac{\partial A_3}{\partial \theta}\nabla\theta\right) \times \nabla\zeta \\
&= \frac{1}{\mathcal{J}}\left(\frac{\partial A_2}{\partial \psi} - \frac{\partial A_1}{\partial \theta}\right)\mathcal{J}\nabla\psi \times \nabla\theta + \frac{1}{\mathcal{J}}\left(\frac{\partial A_1}{\partial \zeta} - \frac{\partial A_3}{\partial \psi}\right)\mathcal{J}\nabla\zeta \times \nabla\psi + \frac{1}{\mathcal{J}}\left(\frac{\partial A_3}{\partial \theta} - \frac{\partial A_2}{\partial \zeta}\right)\mathcal{J}\nabla\theta \times \\
&\quad \nabla\zeta.
\end{aligned}
\tag{147}
$$

Note that taking the curl of a vector in the covariant form leaves the vector in the contravariant form.

6.8 Metric tensor for general coordinate system

Consider a general coordinate system (ψ, θ, ζ). The metric tensor is the transformation matrix between the covariant basis vectors and the contravariant ones. To obtain the metric matrix, we write the contrariant basis vectors in terms of the covariant ones, such as

$$
\nabla\psi = a^1 \mathcal{J}\nabla\theta \times \nabla\zeta + a^2 \mathcal{J}\nabla\zeta \times \nabla\psi + a^3 \mathcal{J}\nabla\psi \times \nabla\theta.
\tag{148}
$$

Taking the scalar product respectively with $\nabla\psi$, $\nabla\theta$, and $\nabla\zeta$, Eq. (148) is written as

$$
a^1 = |\nabla\psi|^2,
\tag{149}
$$

$$
a^2 = \nabla\psi \cdot \nabla\theta,
\tag{150}
$$

$$
a^3 = \nabla\psi \cdot \nabla\zeta.
\tag{151}
$$

Similarly, we write

$$
\nabla\theta = b^1 \mathcal{J}\nabla\theta \times \nabla\zeta + b^2 \mathcal{J}\nabla\zeta \times \nabla\psi + b^3 \mathcal{J}\nabla\psi \times \nabla\theta,
\tag{152}
$$

Taking the scalar product with $\nabla\psi$, $\nabla\theta$, and $\nabla\zeta$, respectively, the above becomes

$$
b^1 = \nabla\theta \cdot \nabla\psi
\tag{153}
$$

$$
b^2 = |\nabla\theta|^2,
\tag{154}
$$

$$
b^3 = \nabla\theta \cdot \nabla\zeta.
\tag{155}
$$

The same situation applies for the $\nabla\zeta$ basis vector,

$$
\nabla\zeta = c^1 \nabla\theta \times \nabla\zeta \mathcal{J} + c^2 \nabla\zeta \times \nabla\psi \mathcal{J} + c^3 \nabla\psi \times \nabla\theta \mathcal{J},
\tag{156}
$$

Taking the scalar product with $\nabla\psi$, $\nabla\theta$, and $\nabla\zeta$, respectively, the above equation becomes

$$
c^1 = \nabla\zeta \cdot \nabla\psi
\tag{157}
$$

$$
c^2 = \nabla\zeta \cdot \nabla\theta
\tag{158}
$$

$$
c^3 = |\nabla\zeta|^2
\tag{159}
$$

Summarizing the above results in matrix form, we obtain

$$
\begin{pmatrix} \nabla\psi \\ \nabla\theta \\ \nabla\zeta \end{pmatrix} = \begin{pmatrix} |\nabla\psi|^2 & \nabla\psi \cdot \nabla\theta & \nabla\psi \cdot \nabla\zeta \\ \nabla\theta \cdot \nabla\psi & |\nabla\theta|^2 & \nabla\theta \cdot \nabla\zeta \\ \nabla\zeta \cdot \nabla\psi & \nabla\zeta \cdot \nabla\theta & |\nabla\zeta|^2 \end{pmatrix} \begin{pmatrix} \nabla\theta \times \nabla\zeta \mathcal{J} \\ \nabla\zeta \times \nabla\psi \mathcal{J} \\ \nabla\psi \times \nabla\theta \mathcal{J} \end{pmatrix}
\tag{160}
$$

Similarly, to convert contravariant basis vector to covariant one, we write

$$
\nabla\theta \times \nabla\zeta \mathcal{J} = d_1 \nabla\psi + d_2 \nabla\theta + d_3 \nabla\zeta
\tag{161}
$$

Taking the scalar product respectively with $\nabla\theta \times \nabla\zeta \mathcal{J}$, $\nabla\zeta \times \nabla\psi \mathcal{J}$, and $\nabla\psi \times \nabla\theta \mathcal{J}$, the above equation becomes

$$d_1 = |\nabla\theta \times \nabla\zeta|^2 \mathcal{J}^2 \tag{162}$$

$$d_2 = (\nabla\theta \times \nabla\zeta \mathcal{J}) \cdot (\nabla\zeta \times \nabla\psi \mathcal{J}) \tag{163}$$

$$d_3 = (\nabla\theta \times \nabla\zeta \mathcal{J}) \cdot (\nabla\psi \times \nabla\theta \mathcal{J}) \tag{164}$$

For the second contravariant basis vector

$$\nabla\phi \times \nabla\psi \mathcal{J} = e_1 \nabla\psi + e_2 \nabla\theta + e_3 \nabla\zeta \tag{165}$$

$$e_1 = (\nabla\zeta \times \nabla\psi) \cdot (\nabla\theta \times \nabla\zeta) \mathcal{J}^2 \tag{166}$$

$$e_2 = (\nabla\zeta \times \nabla\psi) \cdot (\nabla\zeta \times \nabla\psi) \mathcal{J}^2 \tag{167}$$

$$e_3 = (\nabla\zeta \times \nabla\psi) \cdot (\nabla\psi \times \nabla\theta) \mathcal{J}^2 \tag{168}$$

For the third contravariant basis vector

$$\nabla\psi \times \nabla\theta \mathcal{J} = f_1 \nabla\psi + f_2 \nabla\theta + f_3 \nabla\zeta \tag{169}$$

$$f_1 = (\nabla\psi \times \nabla\theta) \cdot (\nabla\theta \times \nabla\zeta) \mathcal{J}^2 \tag{170}$$

$$f_2 = (\nabla\psi \times \nabla\theta) \cdot (\nabla\zeta \times \nabla\psi) \mathcal{J}^2 \tag{171}$$

$$f_3 = (\nabla\psi \times \nabla\theta) \cdot (\nabla\psi \times \nabla\theta) \mathcal{J}^2 \tag{172}$$

Summarizing these results, we obtain

$$\begin{pmatrix} \nabla\theta \times \nabla\zeta \mathcal{J} \\ \nabla\zeta \times \nabla\psi \mathcal{J} \\ \nabla\psi \times \nabla\theta \mathcal{J} \end{pmatrix} = \begin{pmatrix} |\nabla\theta \times \nabla\zeta|^2 \mathcal{J}^2 & (\nabla\theta \times \nabla\zeta) \cdot (\nabla\zeta \times \nabla\psi) \mathcal{J}^2 & (\nabla\theta \times \nabla\zeta) \cdot (\nabla\psi \times \nabla\theta) \mathcal{J}^2 \\ (\nabla\zeta \times \nabla\psi) \cdot (\nabla\theta \times \nabla\zeta) \mathcal{J}^2 & (\nabla\zeta \times \nabla\psi) \cdot (\nabla\zeta \times \nabla\psi) \mathcal{J}^2 & (\nabla\zeta \times \nabla\psi) \cdot (\nabla\psi \times \nabla\theta) \mathcal{J}^2 \\ (\nabla\psi \times \nabla\theta) \cdot (\nabla\theta \times \nabla\zeta) \mathcal{J}^2 & (\nabla\psi \times \nabla\theta) \cdot (\nabla\zeta \times \nabla\psi) \mathcal{J}^2 & (\nabla\psi \times \nabla\theta) \cdot (\nabla\psi \times \nabla\theta) \mathcal{J}^2 \end{pmatrix} \begin{pmatrix} \nabla\psi \\ \nabla\theta \\ \nabla\zeta \end{pmatrix}$$

Note that the matrix in Eqs. (160) and (173) should be the inverse of each other. It is ready to prove this by directly calculating the product of the two matrix.

6.8.1 Special case: metric tensor for (ψ, θ, ϕ) coordinate system

Suppose that (ψ, θ, ϕ) are arbitrary general coordinates except that ϕ is the usual toroidal angle in cylindrical coordinates. Then $\nabla\phi = 1/R\hat{\phi}$ is perpendicular to both $\nabla\psi$ and $\nabla\theta$. Using this, Eq. (160) is simplified to

$$\begin{pmatrix} \nabla\psi \\ \nabla\theta \\ \nabla\phi \end{pmatrix} = \begin{pmatrix} |\nabla\psi|^2 & \nabla\psi \cdot \nabla\theta & 0 \\ \nabla\psi \cdot \nabla\theta & |\nabla\theta|^2 & 0 \\ 0 & 0 & 1/R^2 \end{pmatrix} \begin{pmatrix} \nabla\theta \times \nabla\phi \mathcal{J} \\ \nabla\phi \times \nabla\psi \mathcal{J} \\ \nabla\psi \times \nabla\theta \mathcal{J} \end{pmatrix} \tag{174}$$

Similarly, Eq. (173) is simplified to

$$\begin{pmatrix} \nabla\theta \times \nabla\phi \mathcal{J} \\ \nabla\phi \times \nabla\psi \mathcal{J} \\ \nabla\psi \times \nabla\theta \mathcal{J} \end{pmatrix} = \begin{pmatrix} |\nabla\theta|^2 \mathcal{J}^2/R^2 & -\nabla\theta \cdot \nabla\psi \mathcal{J}^2/R^2 & 0 \\ -\nabla\psi \cdot \nabla\theta \mathcal{J}^2/R^2 & |\nabla\psi|^2 \mathcal{J}^2/R^2 & 0 \\ 0 & 0 & R^2 \end{pmatrix} \begin{pmatrix} \nabla\psi \\ \nabla\theta \\ \nabla\phi \end{pmatrix} \tag{175}$$

[Note that the matrix in Eqs. (174) and (175) should be the inverse of each other. The product of the two matrix,

$$\begin{pmatrix} |\nabla\theta|^2 \mathcal{J}^2/R^2 & -\nabla\theta \cdot \nabla\psi \mathcal{J}^2/R^2 & 0 \\ -\nabla\psi \cdot \nabla\theta \mathcal{J}^2/R^2 & \frac{\mathcal{J}^2}{R^2}|\nabla\psi|^2 & 0 \\ 0 & 0 & R^2 \end{pmatrix} \begin{pmatrix} |\nabla\psi|^2 & \nabla\psi \cdot \nabla\theta & 0 \\ \nabla\psi \cdot \nabla\theta & |\nabla\theta|^2 & 0 \\ 0 & 0 & 1/R^2 \end{pmatrix}, \tag{176}$$

can be calculated to give

$$\begin{pmatrix} A & 0 & 0 \\ 0 & A & 0 \\ 0 & 0 & 1 \end{pmatrix},$$

where

$$A = |\nabla\theta|^2 |\nabla\psi|^2 \mathcal{J}^2/R^2 - (\nabla\theta \cdot \nabla\psi)^2 \mathcal{J}^2.$$

By using the definition of the Jacobian in Eq. (109), it is easy to verify that $A = 1$, i.e.,

$$|\nabla \theta|^2 |\nabla \psi|^2 - (\nabla \theta \cdot \nabla \psi)^2 = \frac{R^2}{\mathcal{J}^2}, \tag{177}$$

]

6.9 Covariant and contravariant representation of equilibrium magnetic field

The axisymmetric equilibrium magnetic field is given by Eq. (54), i.e.,

$$\mathbf{B} = \nabla \Psi \times \nabla \phi + g(\Psi) \nabla \phi. \tag{178}$$

In (ψ, θ, ϕ) coordinate system, the above expression can be written as

$$\mathbf{B} = -\Psi_\psi \nabla \phi \times \nabla \psi - \Psi_\theta \nabla \phi \times \nabla \theta + g(\Psi) \nabla \phi, \tag{179}$$

where the subscripts denote the partial derivatives with the corresponding subscripts. Note that Eq. (179) is a mixed representation, which involves both covariant and contravariant basis vectors. Equation (179) can be converted to contravariant form by using the metric tensor, giving

$$\mathbf{B} = -\Psi_\psi \nabla \phi \times \nabla \psi - \Psi_\theta \nabla \phi \times \nabla \theta + g(\Psi) \frac{1}{R^2} \mathcal{J} \nabla \psi \times \nabla \theta. \tag{180}$$

Similarly, Eq. (179) can also be transformed to covariant form, giving

$$\mathbf{B} = \left(\Psi_\psi \frac{\mathcal{J}}{R^2} \nabla \psi \cdot \nabla \theta + \Psi_\theta \frac{\mathcal{J}}{R^2} |\nabla \theta|^2 \right) \nabla \psi + \left(-\Psi_\psi \frac{\mathcal{J}}{R^2} |\nabla \psi|^2 - \Psi_\theta \frac{\mathcal{J}}{R^2} \nabla \theta \cdot \nabla \psi \right) \nabla \theta + g(\Psi) \nabla \phi. \tag{181}$$

For the convenience of notation, define

$$h^{\alpha \beta} = \frac{\mathcal{J}}{R^2} \nabla \alpha \cdot \nabla \beta, \tag{182}$$

then Eq. (181) is written as

$$\mathbf{B} = (\Psi_\psi h^{\psi \theta} + \Psi_\theta h^{\theta \theta}) \nabla \psi + (-\Psi_\psi h^{\psi \psi} - \Psi_\theta h^{\psi \theta}) \nabla \theta + g(\Psi) \nabla \phi. \tag{183}$$

7 Magnetic surface coordinate system (ψ, θ, ϕ)

A coordinate system (ψ, θ, ϕ), where ϕ is the usual cylindrical toroidal angle, is called a magnetic surface coordinate system if Ψ is a function of only ψ, i.e., $\partial \Psi / \partial \theta = 0$ (we also have $\partial \Psi / \partial \phi = 0$ since we are considering axially symmetrical case). In terms of (ψ, θ, ϕ) coordinates, the contravariant form of the magnetic field, Eq. (180), is written as

$$\mathbf{B} = -\Psi' \nabla \phi \times \nabla \psi + g(\Psi) \frac{\mathcal{J}}{R^2} \nabla \psi \times \nabla \theta, \tag{184}$$

where $\Psi' \equiv d\Psi / d\psi$. The covariant form of the magnetic field, Eq. (181), is written as

$$\mathbf{B} = \left(\Psi' \frac{\mathcal{J}}{R^2} \nabla \psi \cdot \nabla \theta \right) \nabla \psi + \left(-\Psi' \frac{\mathcal{J}}{R^2} |\nabla \psi|^2 \right) \nabla \theta + g(\Psi) \nabla \phi. \tag{185}$$

7.1 Local and global safety factors

The local safety factor $\hat{q}$ is defined by

$$\hat{q} = \frac{\mathbf{B} \cdot \nabla \phi}{\mathbf{B} \cdot \nabla \theta}, \tag{186}$$

which characterizes the local pitch angle of a magnetic field line on a magnetic surface (i.e. in (θ, ϕ) plane). Substituting the contravariant representation of the magnetic field, Eq. (184), into the above equation, the local safety factor is written

$$\hat{q}(\psi, \theta) = -\frac{g}{R^2} \frac{\mathcal{J}}{\Psi'}. \tag{187}$$

Note that the expression $\hat{q}$ in Eq. (187) depends on the Jacobian $\mathcal{J}$. This is because the definition of $\hat{q}$ depends on the definition of θ, which in turn depends on the the Jacobian $\mathcal{J}$. [In passing, note that in terms of $\hat{q}$, the contravariant form of the magnetic field, Eq. (184), is written

$$\mathbf{B} = -\Psi'(\nabla\phi \times \nabla\psi + \hat{q}\nabla\psi \times \nabla\theta). \tag{188}$$

and the parallel differential operator $\mathbf{B}_0 \cdot \nabla$ is written as

$$\mathbf{B}_0 \cdot \nabla = -\Psi'(\nabla\phi \times \nabla\psi + \hat{q}\nabla\psi \times \nabla\theta) \cdot \nabla = -\Psi'\mathcal{J}^{-1}\left(\frac{\partial}{\partial\theta} + \hat{q}\frac{\partial}{\partial\phi}\right). \tag{189}$$

]

   The global safety factor defined in Eq. (29) is actually the poloidal average of the local safety factor, i.e.,

$$q(\psi) \;\equiv\; \frac{1}{2\pi}\int_0^{2\pi}\hat{q}d\theta \tag{190}$$

$$=\; -\frac{1}{2\pi}\frac{g}{\Psi'}\int_0^{2\pi}\frac{\mathcal{J}}{R^2}d\theta. \tag{191}$$

The physical meaning of q is obvious: it represents the number of toroidal circles a magnetic field line travels when the line travels a complete poloidal loop. Note that q and $\hat{q}$ defined this way can be negative, which depends on the choice of the positive direction of ϕ and θ coordinates (note that the safety factor given in G-eqdsk file is always positive, i.e. it is the absolute value of the safety factor defined here).

   (In passing, let us consider the numerical calculation of q. Using the relation $d\ell_p$ and $d\theta$ [Eq. (197)], equation (191) is further written

$$q(\psi) \;=\; -\frac{1}{2\pi}\frac{g}{\Psi'}\oint \text{sign}(\mathcal{J})\frac{d\ell_p}{R|\nabla\psi|}$$

$$=\; -\frac{1}{2\pi}g\frac{\text{sign}(\mathcal{J})}{\text{sign}(\Psi')}\oint\frac{d\ell_p}{R|\nabla\Psi|}. \tag{192}$$

Equation (192) is used in the GTAW code to numerically calculate the value of q on magnetic surfaces, which agrees with the value specified in the G-eqdsk file. Using $B_p = |\nabla\Psi|\,/\,R$ and $B_\phi = g\,/\,R$, the absolute value of q is written

$$|q| = \frac{1}{2\pi}\oint\frac{1}{R}\frac{|B_\phi|}{B_p}d\ell_p, \tag{193}$$

which is the familiar formula we see in textbooks.)

7.2 Relation between Jacobian and poloidal angle θ

Given the definition of a magnetic surface coordinate system (ψ, θ, ϕ), the Jacobian of this system is fully determied. On the other hand, given the definition of ψ, ϕ, and the Jacobian, the definition of θ is fully determined (can have some trivial shifting freedoms). Next, let us discuss how to calculate θ in this case. In (ψ, θ, ϕ) coordinates, a line element is written

$$d\mathbf{l} = \frac{\partial\mathbf{r}}{\partial\psi}d\psi + \frac{\partial\mathbf{r}}{\partial\theta}d\theta + \frac{\partial\mathbf{r}}{\partial\phi}d\phi \tag{194}$$

The line element that lies on a magnetic surface (i.e., $d\psi = 0$) and in a poloidal plane (i.e., $d\phi = 0$) is then written

$$d\boldsymbol{\ell}_p \;=\; \frac{\partial\mathbf{r}}{\partial\theta}d\theta$$

$$=\; \mathcal{J}\nabla\phi \times \nabla\psi d\theta. \tag{195}$$

We use the convention that $d\ell_p$ and $d\theta$ take the same sign, i.e.,

$$d\ell_p = |\mathcal{J}\nabla\phi \times \nabla\psi|d\theta. \tag{196}$$

Using the fact that $\nabla\psi$ and $\nabla\phi$ is orthogonal and $\nabla\phi = \hat{\boldsymbol{\phi}}/R$, the above equation is written as

$$d\theta = \frac{R}{|\mathcal{J}\nabla\psi|}dl_p \tag{197}$$

Given $|\mathcal{J}\nabla\psi|$, Eq. (197) can be integrated to determine the θ coordinate of points on a magnetic surface.

7.3 Calculating poloidal angle

Once $|\mathcal{J}\nabla\psi|$ is known, the value of θ of a point can be obtained by integrating expression (197), yielding

$$\theta_{i,j} = \theta_{\mathrm{ref},j} + \int_{\mathbf{x}_{\mathrm{ref},j}}^{\mathbf{x}_{i,j}} \frac{R}{|\mathcal{J}\nabla\psi|} dl_p, \tag{198}$$

where the curve integration is along the contour $\Psi = \Psi_j$, $\mathbf{x}_{\mathrm{ref},j}$ is a reference point on the contour, where value of the poloidal angle is chosen as $\theta_{\mathrm{ref},j}$. It is here that the positive direction of θ can be selected. Depending on the positive direction chosen for the poloidal angle, the sign of the Jacobian of the constructed coordinates can have a sign difference from the $\mathcal{J}$ appearing in Eq. (198). Denote the Jacobian of the constructed coordinates by $\mathcal{J}'$, then

$$\mathcal{J}' = \pm\mathcal{J} \tag{199}$$

This sign can be determined after the radial coordinate and the positive direction of the poloidal angle are chosen. In `GTAW` code, I choose the positive direction of θ to be in anticlockwise direction when observers look along the direction of $\hat{\boldsymbol{\phi}}$. To achieve this, the line integration in Eq. (198) should be along the anticlockwise direction. (I use the determination of the direction matrix, a well known method in graphic theory, to determine the direction from a given set of discrete points on a magnetic surface.)

7.3.1 Normalized poloidal angle

The span of θ defined by Eq. (198) is usually not 2π in one poloidal loop. This poloidal angle can be scaled by $s(\psi)$ to define a new poloidal coordinate $\bar{\theta}$, whose span is 2π in one poloidal loop, where $s(\psi)$ is a magnetic surface function given by

$$s(\psi) = \frac{2\pi}{\oint \frac{R}{|\mathcal{J}\nabla\psi|} dl_p}. \tag{200}$$

Then $\bar{\theta}$ is written as

$$\begin{aligned} \bar{\theta}_{i,j} &= s(\psi_j)\theta_{i,j} \\ &= s(\psi_j)\left(\theta_{\mathrm{ref},j} + \int_{\mathbf{x}_{\mathrm{ref},j}}^{\mathbf{x}_{i,j}} \frac{R}{|\mathcal{J}\nabla\psi|} dl_p\right) \\ &= \bar{\theta}_{\mathrm{ref},j} + s(\psi_j)\int_{\mathbf{x}_{\mathrm{ref},j}}^{\mathbf{x}_{i,j}} \frac{R}{|\mathcal{J}\nabla\psi|} dl_p, \end{aligned} \tag{201}$$

where $\bar{\theta}_{\mathrm{ref},j} = s(\psi_j)\theta_{\mathrm{ref},j}$. Sine we have modified the definition of the poloidal angle, the Jacobian of the new coordinates $(\psi, \bar{\theta}, \phi)$ is different from that of (ψ, θ, ϕ). The Jacobian $\mathcal{J}_{\mathrm{new}}$ of the new coordinates $(\psi, \bar{\theta}, \phi)$ is written as

$$\begin{aligned} \mathcal{J}_{\mathrm{new}} &\equiv \frac{1}{(\nabla\psi \times \nabla\bar{\theta})\cdot\nabla\phi} \\ &= \frac{1}{\{\nabla\psi \times \nabla[s(\psi)\theta]\}\cdot\nabla\phi} \\ &= \frac{1}{s(\psi)}\frac{1}{(\nabla\psi \times \nabla\theta)\cdot\nabla\phi} \\ &= \frac{1}{s(\psi)}\mathcal{J}' \\ &= \pm\frac{1}{s(\psi)}\mathcal{J} \end{aligned} \tag{202}$$

The Jacobian $\mathcal{J}$ can be set to various forms to achieve various poloidal coordinates, which will be discussed in the next section. After the Jacobian and the radial coordinate ψ is chosen, all the quantities on the right-hand side of Eq. (201) are known and the integration can be performed to obtain the value of $\bar{\theta}_{i,j}$ of each point on each flux surface.

[The reference points $\mathbf{x}_{\mathrm{ref},j}$ and the values of poloidal angle at these points can be chosen by us. One choice of the reference points $\mathbf{x}_{\mathrm{ref},j}$ are those points on the horizontal ray in the midplane that starts from the magnetic axis and points to the low filed side of the device and $\bar{\theta}_{\mathrm{ref},j}$ at these points is chosen as zero (this is my choice in the `GTAW` code). In the `GEM` code, the reference points are chosen at the high-field side of the midplane and $\bar{\theta}_{\mathrm{ref},j} = -\pi$ at the reference points.]

7.3.2 Jacobian for equal-arc-length poloidal angle

If the Jacobian $\mathcal{J}$ is chosen to be of the following form

$$\mathcal{J} = \frac{R}{|\nabla \psi|}. \tag{203}$$

Then $\bar{\theta}_{i,j}$ in Eq. (201) is written

$$\bar{\theta}_{i,j} = \bar{\theta}_{\mathrm{ref},j} + \frac{2\pi}{\oint dl_p} \int_{\mathbf{x}_{\mathrm{ref},j}}^{\mathbf{x}_{i,j}} dl_p. \tag{204}$$

and the Jacobian of new coordinates $(\psi, \bar{\theta}, \phi)$, $\mathcal{J}_{\mathrm{new}}$, which is given by Eq. (202), now takes the form

$$\mathcal{J}_{\mathrm{new}} = \pm \frac{\oint dl_p}{2\pi} \frac{R}{|\nabla \psi|} = \pm \frac{\oint dl_p}{2\pi} \frac{R}{|\nabla \Psi|} \frac{d\Psi}{d\psi}. \tag{205}$$

Equation (204) indicates a set of poloidal points with equal arc intervals corresponds to a set of uniform θ_i points. Therefore this choice of the Jacobian is called the equal-arc-length Jacobian. Note that Eq. (204) does not involve the radial coordinate ψ. Therefore the values of θ of points on any magnetic surface can be determined before the radial coordinate is chosen. By using Eq. (204) (to calculate θ) and the definition of ψ (to calculate ψ), we obtain a magnetic surface coordinate system $(\psi, \bar{\theta}, \phi)$.

7.3.3 Jacobian for equal-volume poloidal angle

The volume element in (ψ, θ, ϕ) coordinates is given by $dV = |\mathcal{J}| d\theta d\phi d\psi$. If we choose a Jacobian that is independent of θ, then uniform θ grids will correspond to grids with uniform volume interval. In this case, $\mathcal{J}$ is written as

$$\mathcal{J} = h(\psi), \tag{206}$$

where $h(\psi)$ is a function independent of θ. Then $\bar{\theta}_{i,j}$ in Eq. (201) is written

$$\bar{\theta}_{i,j} = \bar{\theta}_{\mathrm{ref},j} + \frac{2\pi}{\oint \frac{R}{|\nabla \psi|} dl_p} \int_{\mathbf{x}_{\mathrm{ref},j}}^{\mathbf{x}_{i,j}} \frac{R}{|\nabla \psi|} dl_p \tag{207}$$

and the Jacobian of the new coordinates $(\psi, \bar{\theta}, \phi)$, $\mathcal{J}_{\mathrm{new}}$, is given by Eq. (202), which now takes the following form:

$$\mathcal{J}_{\mathrm{new}} = \pm \frac{1}{2\pi} \oint \frac{R}{|\nabla \psi|} dl_p. \tag{208}$$

Note that both $\bar{\theta}_{i,j}$ and $\mathcal{J}_{\mathrm{new}}$ are independent of the function $h(\psi)$ introduced in Eq. (206). ($h(\psi)$ is eliminated by the normalization procedure specified in Sec. 7.3.1 due to the fact that $h(\psi)$ is constant on a magnetic surface.)

The equal-volume poloidal angle is useful in achieving loading balance for parallel particle simulations. Assume that markers are loaded uniform in space and the poloidal angle is domain decomposed and assigned to different MPI process. Then the equal-volume poloidal angle can make marker number in each MPI process be equal to each other and thus work loading to each process be equal. (**check**If the domain decomposition is also applied to the radial direction, to achieve loading balance, then the radial coordinate ψ should be chosen in a way that makes $\oint (R/\nabla \psi) dl_p$ be independent of ψ, so that $\mathcal{J}_{\mathrm{new}}$ in Eq. (208) is constant in space.**)

7.3.4 Jacobian for straight-field-line poloidal angle

If the Jacobian $\mathcal{J}$ is chosen to be of the following form

$$\mathcal{J}(\psi, \theta) = R^2,$$

then Eq. (187) implies that the local safety factor, $\hat{q}(\psi, \theta) = -g / \Psi'$, is a magnetic surface function, i.e., the magnetic field lines are straight in (ψ, θ) plane. In the case, the poloidal angle in Eq. (201) is written

$$\overline{\theta}_{i,j} = \overline{\theta}_{\text{ref},j} + \frac{2\pi}{\oint \frac{1}{R|\nabla\psi|}dl_p} \int_{\mathbf{x}_{\text{ref},j}}^{\mathbf{x}_{i,j}} \frac{1}{R|\nabla\psi|}dl_p, \tag{209}$$

The Jacobian $\mathcal{J}_{\text{new}}$ given by Eq. (202) now takes the form

$$\mathcal{J}_{\text{new}} = \pm R^2 \frac{\oint \frac{1}{R|\nabla\psi|}dl_p}{2\pi}. \tag{210}$$

Let us denote an arbitary poloidal angle by θ and the above straight-field-line poloidal angle by ϑ, then it is ready to find the following relation between θ and ϑ:

$$\vartheta = \vartheta_{\text{ref},j} + \frac{1}{q}\int_{\theta_{\text{ref},j}}^{\theta} \hat{q}d\theta, \tag{211}$$

where $\hat{q}$ is the local safety factor corresponding to the arbitary poloidal angle θ, i.e., $\hat{q} = \mathbf{B} \cdot \nabla\phi / (\mathbf{B} \cdot \nabla\theta)$. [Proof: Using $d\theta = \frac{R}{|\mathcal{J}\nabla\psi|}dl_p$, the poloidal angle ϑ given in Eq. (209) is written as

$$
\begin{aligned}
\vartheta &= \vartheta_{\text{ref},j} + \frac{2\pi}{\oint \frac{1}{R|\nabla\psi|}dl_p} \int_{\mathbf{x}_{\text{ref},j}}^{\mathbf{x}_{i,j}} \frac{1}{R|\nabla\psi|}dl_p \\
&= \vartheta_{\text{ref},j} + \frac{2\pi}{\oint \frac{1}{R|\nabla\psi|}\frac{|\mathcal{J}\nabla\psi|}{R}d\theta} \int_{\mathbf{x}_{\text{ref},j}}^{\mathbf{x}_{i,j}} \frac{1}{R|\nabla\psi|}\frac{|\mathcal{J}\nabla\psi|}{R}d\theta \\
&= \vartheta_{\text{ref},j} + \frac{2\pi}{\oint \frac{|\mathcal{J}|}{R^2}d\theta} \int_{\mathbf{x}_{\text{ref},j}}^{\mathbf{x}_{i,j}} \frac{|\mathcal{J}|}{R^2}d\theta.
\end{aligned} \tag{212}
$$

Using $\hat{q} = -\frac{g}{R^2}\frac{\mathcal{J}}{\Psi'}$, where $\mathcal{J}$ is the Jacobian of (ψ, θ, ϕ) coordinates, then the above ϑ is reduced to expression (211).]

7.3.5 Comparison between different types of poloidal angle

Figure 7 compares the equal-arc-poloidal angle and the straight-line poloidal angle, which shows that the resolution of the straight-line poloidal angle is not good near the low-field-side midplane.
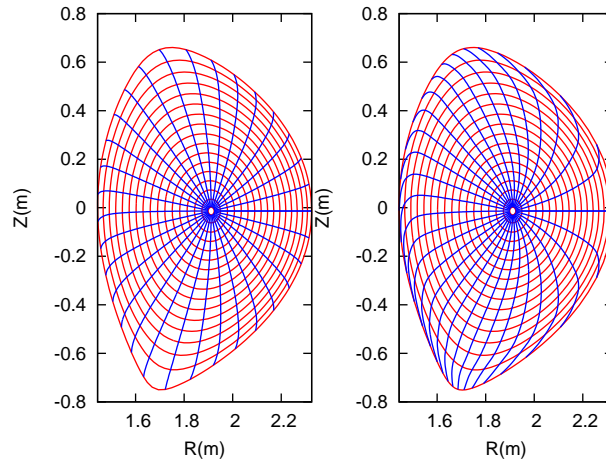

Figure 7. The equal-arc poloidal angle (left) and the straight-line poloidal angle (right) for EAST equilibrium #38300@3.9s. The blue lines correspond to the equal-θ lines, with uniform θ interval between neighbour lines. The red lines correspond to the magnetic surfaces, which start from $\sqrt{\overline{\Psi}_t} = 0.01714$ (the innermost magnetic surface) and end at $\sqrt{\overline{\Psi}_t} = 0.9851$ (the boundary magnetic surface), and are equally spaced in $\sqrt{\overline{\Psi}_t}$.

7.3.6 Verification of Jabobian

After the magnetic coordinates are constructed, we can evaluate the Jacobian $\mathcal{J}_{\text{new}}$ by using directly the definition of the Jacobian, i.e.,

$$\mathcal{J}_{\text{new}} = \frac{1}{(\nabla\psi \times \nabla\overline{\theta}) \cdot \nabla\phi},$$

which can be further written as

$$\mathcal{J}_{\text{new}} = R(R_{\overline{\theta}}Z_\psi - R_\psi Z_{\overline{\theta}}), \tag{213}$$

where the partial differential can be evaluated by using numerical differential schemes. The results obtained by this way should agree with results obtained from the analytical form of the Jacobian. This consistency check provide a verification for the correctness of the theory derivation and numerical implementation. In evaluating the Jacobian by using the analytical form, we may need to evaluate $\nabla\psi$, which finally reduces to evaluating $\nabla\Psi$. The value of $|\nabla\Psi|$ is obtained numerically based on the numerical data of Ψ given in cylindrical coordinate grids. Then the cubic spline interpolating formula is used to obtain the value of $|\nabla\Psi|$ at desired points. ($\mathcal{J}_{\text{new}}$ calculated by the second method (i.e. using analytic form) is used in the GTAW code; the first methods are also implemented in the code for the benchmark purpose.) In the following sections, for notation ease, the Jacobiban of the constructed coordinate system will be denoted by $\mathcal{J}$, instead of $\mathcal{J}_{\text{new}}$.

7.3.7 Radial coordinate

The radial coordinate ψ can be chosen to be various surface function, e.g., volume, poloidal or toroidal magnetic flux within a magnetic surface. The frequently used radial coordinates include $\overline{\Psi}$, and $\sqrt{\overline{\Psi}}$, where $\overline{\Psi}$ is defined by

$$\overline{\Psi} = \frac{\Psi - \Psi_0}{\Psi_a - \Psi_0}, \tag{214}$$

where Ψ_0 and Ψ_a are the values of Ψ at the magnetic axis and LCFS, respectively. Other choices of the radial coordinates include the toroidal magnetic flux and its square root, $\overline{\Psi}_t$, and $\sqrt{\overline{\Psi}_t}$, where Ψ_t and $\overline{\Psi}_t$ are defined by

$$\frac{d\Psi_t}{d\Psi} = 2\pi q, \, \Psi_t(0) = 0 \tag{215}$$

and

$$\overline{\Psi}_t = \frac{\Psi_t}{\Psi_t(1)}, \tag{216}$$

respectively, where $\Psi_t(0)$ and $\Psi_t(1)$ are the values of Ψ_t at the magnetic axis and LCFS, respectively.

If $\psi = \sqrt{\overline{\Psi}_t}$, then

$$\frac{d\Psi}{d\psi} = \frac{d\Psi}{d\Psi_t}\frac{d\Psi_t}{d\psi} = \frac{1}{2\pi q}\frac{d\Psi_t}{d\psi} = \frac{1}{2\pi q}\frac{d\Psi_t}{d\overline{\Psi}_t}\frac{d\overline{\Psi}_t}{d\psi} = \frac{1}{2\pi q}\Psi_t(1)\,2\psi \tag{217}$$

The cylindrical coordinates (R, ϕ, Z) is a right-hand system, with the positive direction of Z pointing vertically up. In GTAW code, the positive direction of θ is chosen in the anticlockwise direction when observers look along the direction of $\hat{\phi}$. Then the definition $\mathcal{J}^{-1} = \nabla\psi \times \nabla\theta \cdot \nabla\phi$ indicates that (1) $\mathcal{J}$ is negative if $\nabla\psi$ points from the magnetic axis to LCFS; (2) $\mathcal{J}$ is positive if $\nabla\psi$ points from the LCFS to the magnetic axis. This can be used to determine the sign of Jacobian after using the analytical formula to obtain the absolute value of Jacobian.

If $\psi = \overline{\Psi}$ or $\psi = \sqrt{\overline{\Psi}}$, $\nabla\psi$ points from the magnetic axis to LCFS.

8 Constructing magnetic surface coordinate system from discrete $\Psi(R, Z)$ data

Given an axisymmetric tokamak equilibrium in (R, ϕ, Z) coordinates (e.g., 2D data $\Psi(R, Z)$ on a rectangular grids (R, Z) in G-file), we can construct a magnetic surface coordinates (ψ, θ, ϕ) by the following two steps. (1) Find out a series of magnetic surfaces on (R, Z) plane and select

radial coordinates for each magnetic surface (e.g. the poloidal flux within each magnetic surface). (2) Specify the Jacobian or some property that we want the poloidal angle to have. Then calculate the poloidal angle of each point on each flux surface (on the $\phi = \mathrm{const}$ plane) by using Eq. (197) (if the Jacobian is specified) or some method specified by us to achieve some property we prefer for the poloidal angle (if a Jacobian is not direclty specifed). Then we obtain the magnetic surface coordinates system (ψ, θ, ϕ).

8.1 Finding magnetic surfaces

Two-dimensional data $\Psi(R, Z)$ on a rectangular grids (R, Z) is read from the G_EQDSK file (G-file) of EFIT code. Based on the 2D array data, I use 2D cubic spline interpolation to construct a interpolating function $\Psi = \Psi(R, Z)$. To construct a magnetic surface coordinate system, I need to find the contours of Ψ, i.e., magnetic surfaces. The values of Ψ on the magnetic axis, Ψ_0, and the value of Ψ on the last closed flux surface (LCFS), Ψ_b, are given in G-file. Using these two values, I construct a 1D array "psival" with value of elements changing uniform from Ψ_0 to Ψ_b. Then I try to find the contours of Ψ with contour level value ranging from Ψ_0 to Ψ_b. This is done in the following way: construct a series of straight line (in the poloidal plane) that starts from the location of the magnetic axis and ends at one of the points on the LCFS. Combine the straight line equation, $Z = Z(R)$, with the interpolating function $\Psi(R, Z)$, we obtain a one variable function $h = \Psi(R, Z(R))$. Then finding the location where Ψ is equal to a specified value Ψ_i, is reduced to finding the root of the equation $\Psi(R, Z(R)) - \Psi_i = 0$. Since this is a one variable equation, the root can be easily found by using simple root finding scheme, such as bisection method (bisection method is used in GTAW code). After finding the roots for each value in the array "psival" on each straight lines, the process of finding the contours of Ψ is finished. The contours of Ψ found this way are plotted in Fig. 8.
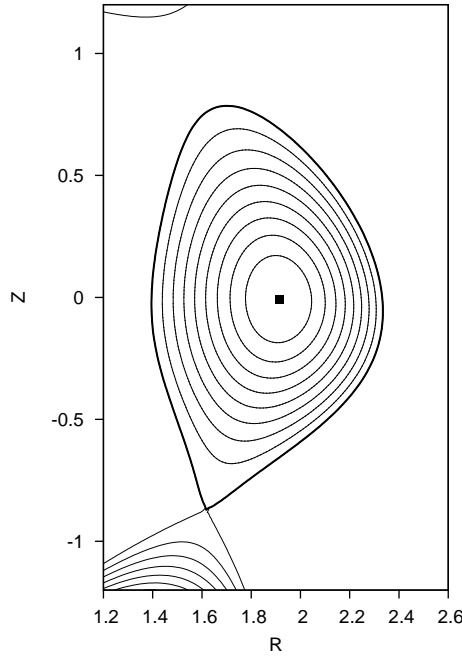

Figure 8. Verification of the numerical code that calculates the contours of the poloidal flux Ψ. The bold line in the figure indicates the LCFS. The contour lines (solid lines) given by the gnuplot program agrees well with the results I calculate by using interpolation and root-finding method (the two sets of contours are indistinguishable in this scale). My code only calculate the contour lines within the LCFS, while those given by gnuplot contains additional contour lines below the X point and on the left top in the figure. Eqdisk file of the equilibrium was provided by Dr. Guoqiang Li (filename: g013606.07104).

In the above, we mentioned that the point of magnetic axis and points on the LCFS are needed to construct the straight lines. In G-file, points on LCFS are given explicitly in an array. The location of magnetic axis is also explicitly given in G-file. It is obvious that some of the straight lines $Z = Z(R)$ that pass through the location of magnetic axis and points on the LCFS will have very large or even infinite slope. On these lines, finding the accurate root of the equation $\Psi(R, Z(R)) - \Psi_i = 0$ is difficult or even impossible. The way to avoid this situation is obvious: switch to use function $R = R(Z)$ instead of $Z = Z(R)$ when the slope of $Z = Z(R)$ is large (the switch condition I used is $|dZ/dR| > 1$).

In constructing the flux surface coordinate with desired Jacobian, we will need the absolute value of the gradient of Ψ, $|\nabla\Psi|$, on some specified spatial points. To achieve this, we need to construct a interpolating function for $|\nabla\Psi|$. The $|\nabla\Psi|$ can be written as

$$|\nabla\Psi| = \sqrt{\left(\frac{\partial\Psi}{\partial R}\right)^2 + \left(\frac{\partial\Psi}{\partial Z}\right)^2}, \tag{218}$$

By using the center difference scheme to evaluate the partial derivatives with respect to R and Z in the above equation (using one side difference scheme for the points on the rectangular boundary), we can obtain an 2D array for the value of $|\nabla\Psi|$ on the rectangular (R, Z) grids. Using this 2D array, we can construct an interpolating function for $\nabla\Psi$ by using the cubic spline interpolation scheme.
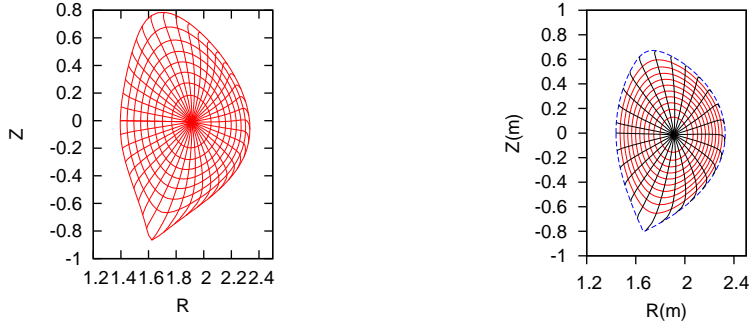

Figure 9. Grid points (the intersecting points of two curves in the figure) corresponding to uniform poloidal flux and uniform poloidal arc length for EAST equilibrium shot 13606 at 7.1s (left) (G-file name: g013606.07104) and shot 38300 at 3.9s (right) (G-file name: g038300.03900).
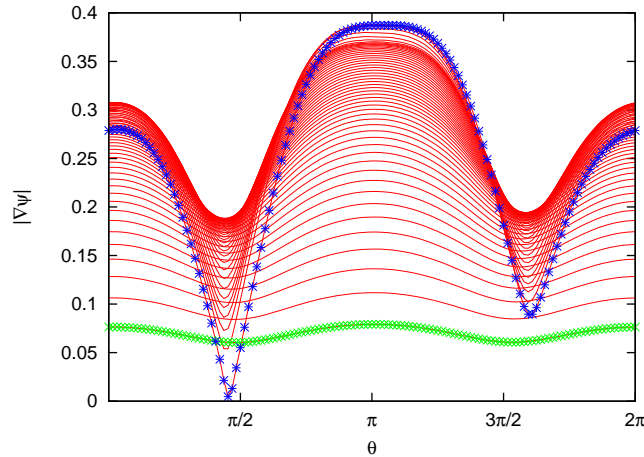

Figure 10. $|\nabla\Psi|$ as a function of the poloidal angle. The different lines corresponds to the values of $|\nabla\Psi|$ on different magnetic surfaces. The stars correspond to the values on the boundary magnetic surface while the plus signs correspond to the value on the innermost magnetic surface (the magnetic surface adjacent to the magnetic axis). The equilibrium is for EAST shot 38300 at 3.9s.
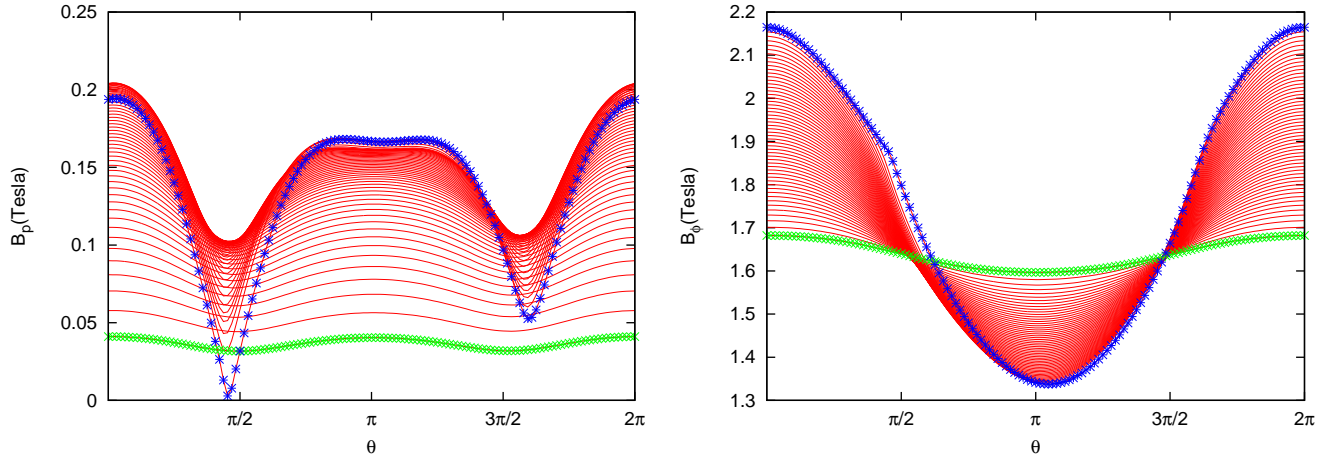
Figure 11. The Poloidal magnetic field $B_p = |\nabla \Psi| / R$ (left) and toroidal magnetic field $B_\phi = g / R$ (right) as a function of the poloidal angle. The different lines corresponds to the values on different magnetic surfaces. The stars correspond to the values on the boundary magnetic surface while the plus signs correspond to the value on the innermost magnetic surface (the magnetic surface adjacent to the magnetic axis). The equilibrium is for EAST shot 38300 at 3.9s.
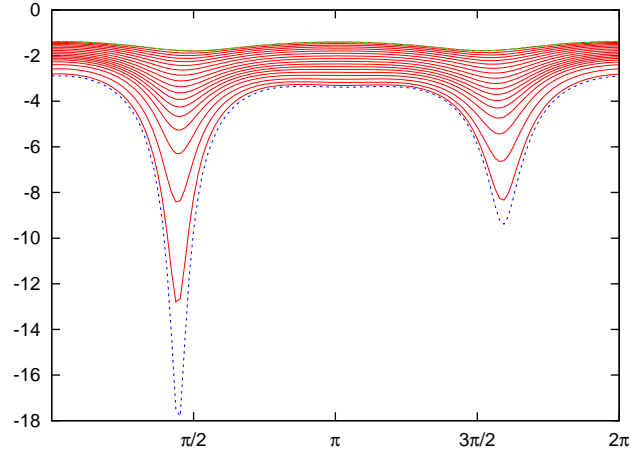
Figure 12. Equal-arc Jacobian as a function of the poloidal angle on different magnetic surfaces. The dotted line corresponds to the values of Jacobian on the boundary magnetic surface. The equilibrium is for EAST shot 38300 at 3.9s.
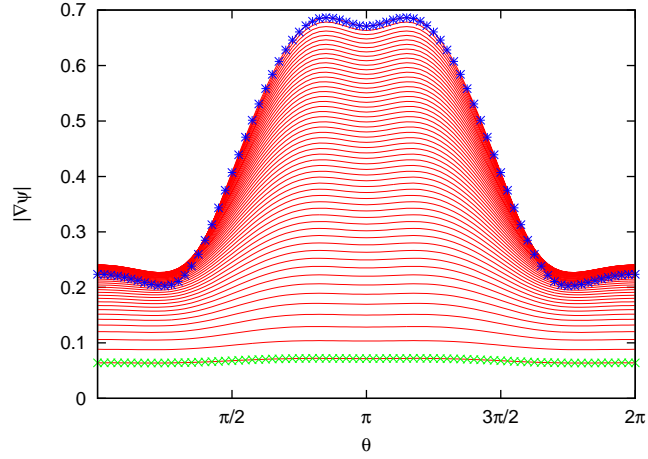
Figure 13. $|\nabla \Psi|$ as a function of the poloidal angle. The different lines corresponds to values of $|\nabla \Psi|$ on different magnetic surfaces. The stars correspond to the values of $|\nabla \Psi|$ on the boundary magnetic surface while the plus signs correspond to the value on the innermost magnetic surface (the magnetic surface adjacent to the magnetic axis). The equilibrium is a Solovev equilibrium.
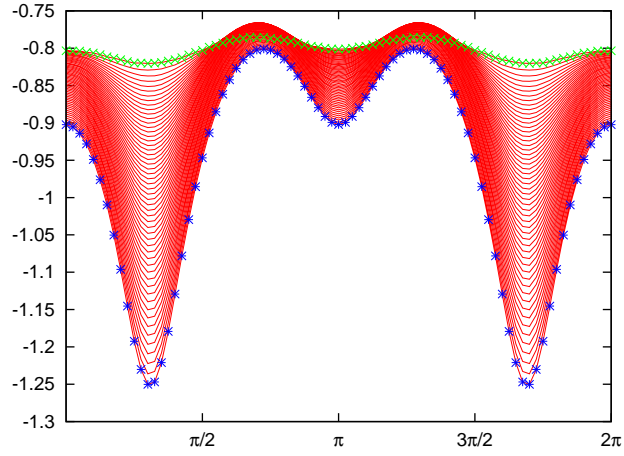

Figure 14. Jacobian on different magnetic surfaces as a function of the poloidal angle. The equilibrium is a Solovev equilibrium and the Jacobian is an equal-arc Jacobian. The stars correspond to the values of Jacobian on the boundary magnetic surface while the plus signs correspond to the value on the innermost magnetic surface (the magnetic surface adjacent to the magnetic axis).

8.2 Expression of metric elements of magnetic coordinates (ψ, θ, ϕ)

Metric elements of the (ψ, θ, ϕ) coordinates, e.g., $\nabla \psi \cdot \nabla \theta$, are often needed in practical calculations. Next, we express these metric elements in terms of the cylindrical coordinates (R, Z) and their partial derivatives with respect to ψ and θ. Note that, in this case, the coordinate system is $(\psi,$

θ, ϕ) while R and Z are functions of ψ and θ, i.e.,

$$R = R(\psi, \theta), \tag{219}$$

$$Z = R(\psi, \theta). \tag{220}$$

Then ∇R and ∇Z are written as

$$\nabla R = \hat{\mathbf{R}} = R_\psi \nabla \psi + R_\theta \nabla \theta, \tag{221}$$

$$\nabla Z = \hat{\mathbf{Z}} = Z_\psi \nabla \psi + Z_\theta \nabla \theta, \tag{222}$$

wehre $R_\psi \equiv \partial R / \partial \psi$, etc. Equations (221) and (222) can be solved to give

$$\nabla \psi = \frac{1}{R_\psi Z_\theta - Z_\psi R_\theta} (Z_\theta \hat{\mathbf{R}} - R_\theta \hat{\mathbf{Z}}), \tag{223}$$

$$\nabla \theta = \frac{1}{Z_\psi R_\theta - R_\psi Z_\theta} (Z_\psi \hat{\mathbf{R}} - R_\psi \hat{\mathbf{Z}}). \tag{224}$$

Using the above expressions, the Jacobian of (ψ, θ, ϕ) coordinates, $\mathcal{J}$, is written as

$$\begin{aligned}
\mathcal{J}^{-1} &= \nabla \psi \times \nabla \theta \cdot \nabla \phi \\
&= -\frac{1}{(R_\psi Z_\theta - Z_\psi R_\theta)^2} (Z_\theta R_\psi \hat{\phi} - R_\theta Z_\psi \hat{\phi}) \times \frac{\hat{\phi}}{R} \\
&= -\frac{1}{(Z_\theta R_\psi - R_\theta Z_\psi) R},
\end{aligned} \tag{225}$$

i.e.,

$$\mathcal{J} = R(R_\theta Z_\psi - R_\psi Z_\theta). \tag{226}$$

Using this, Expressions (223) and (224) are written as

$$\nabla \psi = -\frac{R}{\mathcal{J}} (Z_\theta \hat{\mathbf{R}} - R_\theta \hat{\mathbf{Z}}) \tag{227}$$

and

$$\nabla \theta = \frac{R}{\mathcal{J}} (Z_\psi \hat{\mathbf{R}} - R_\psi \hat{\mathbf{Z}}). \tag{228}$$

Then the elements of the metric matrix are written as

$$|\nabla \psi|^2 = \frac{R^2}{\mathcal{J}^2} (Z_\theta^2 + R_\theta^2), \tag{229}$$

$$|\nabla \theta|^2 = \frac{R^2}{\mathcal{J}^2} (Z_\psi^2 + R_\psi^2), \tag{230}$$

and

$$\nabla \psi \cdot \nabla \theta = -\frac{R^2}{\mathcal{J}^2} (Z_\theta Z_\psi + R_\theta R_\psi). \tag{231}$$

Equations (229), (230), and (231) are the expressions of the metric elements in terms of R, R_ψ,

R_θ, Z_ψ, and Z_θ. [Combining the above results, we obtain

$$\frac{\nabla\psi\cdot\nabla\theta}{|\nabla\psi|^2} = -\frac{Z_\theta Z_\psi + R_\theta R_\psi}{Z_\theta^2 + R_\theta^2}. \tag{232}$$

Equation (231) is used in GTAW code. Using the above results, $h^{\alpha\beta} = \frac{\mathcal{J}}{R^2}\nabla\alpha\cdot\nabla\beta$ are written as

$$h^{\psi\psi} = \frac{\mathcal{J}}{R^2}|\nabla\psi|^2 = \frac{1}{\mathcal{J}}(Z_\theta^2 + R_\theta^2) \tag{233}$$

$$h^{\theta\theta} = \frac{\mathcal{J}}{R^2}|\nabla\theta|^2 = \frac{1}{\mathcal{J}}(Z_\psi^2 + R_\psi^2), \tag{234}$$

$$h^{\psi\theta} = \frac{\mathcal{J}}{R^2}\nabla\psi\cdot\nabla\theta = -\frac{1}{\mathcal{J}}(Z_\theta Z_\psi + R_\theta R_\psi) \tag{235}$$

As a side product of the above results, we can calculate the arc length in the poloidal plane along a constant ψ surface, $d\ell$, which is expressed as

$$\begin{aligned}
d\ell &= \sqrt{(dR)^2 + (dZ)^2} \\
&= \sqrt{(R_\psi d\psi + R_\theta d\theta)^2 + (Z_\psi d\psi + Z_\theta d\theta)^2}.
\end{aligned}$$

Note that $d\psi = 0$ since we are considering the arc length along a constant ψ surface in (R, Z) plane. Then the above equation is reduced to

$$\begin{aligned}
d\ell &= \sqrt{(R_\theta d\theta)^2 + (Z_\theta d\theta)^2} \\
&= \sqrt{R_\theta^2 + Z_\theta^2}\, d\theta \\
&= \frac{|\mathcal{J}\nabla\psi|}{R}d\theta, \tag{236}
\end{aligned}$$

which agrees with Eq. (197).]

9 Constructing model tokamak magnetic field

In some cases (e.g., turbulence simulation), for simplicity, model tokamak magnetic field, which is not an exact solution to the GS equation, is often used. In the model, the safety factor profile $q(\psi)$, toroidal field function $g(\psi)$ and the magnetic surface shape $(R(\psi,\theta), Z(\psi,\theta))$ are given. To use this model in a simulation, we need to calculate its poloidal magnetic field, which is determined by the poloidal magnetic flux function Ψ. To determine Ψ, we need to use Eq. (191), i.e.,

$$q(\psi) = -\frac{1}{2\pi}\frac{g}{\Psi'}\int_0^{2\pi}\frac{\mathcal{J}}{R^2}d\theta, \tag{237}$$

and re-organize the formula as

$$\frac{d\Psi}{d\psi} = -\frac{1}{2\pi}\frac{g(\psi)}{q(\psi)}\int_0^{2\pi}\frac{\mathcal{J}}{R^2}d\theta, \tag{238}$$

which can be integrated to obtain Ψ and thus the poloidal magnetic field $\mathbf{B}_p = \nabla\Psi\times\nabla\phi$, where $\mathcal{J} = [(\nabla\psi\times\nabla\theta)\cdot\nabla\phi]^{-1}$.

In most papers using the model tokamak magnetic field, the toroidal field function $g(\psi)$ is always chosen to be a constant. The safety profile can be chosen to be any form that we prefer. A typical magnetic surface shape used in simulations is the Miller shape, which is given by

$$
\begin{aligned}
R(r,\theta) &= R_0(r) + r\cos[\theta + (\sin^{-1}\delta(r))\sin\theta] \\
Z(r,\theta) &= \kappa(r)\, r\sin\theta
\end{aligned}
\tag{239}
$$

where $r = \psi$ is the radial coordinate, $R_0(r)$, $\delta(r)$, and $\kappa_r(r)$ are the Shafronov shift, triangularity, and elongation profiles, which can be arbitrarily specified. For the special case of R_0 being a constant, $\delta(r) = 0$, and $\kappa(r) = 1$, this shape reduces to a concentric-circular magnetic field. An example of calculating the poloidal field of the model field is given in Sec. 13. This kind of model field can be called theoretical physicists' tokamak. Computational physicists also use this model, e.g. for code benchmarking. The famous DIII-D cyclone base case is an example, which was extensively used for benchmarking gyrokinetic simulation of ion temperature driven turbulence.

10 Magnetic surface averaging

10.1 Definition

The magnetic surface average of a physical quantiy G is defined by

$$
\langle G\rangle \equiv \lim_{\triangle\Psi\to 0}\left(\frac{\iiint_{\triangle\Psi}G\,d^3V}{\iiint_{\triangle\Psi}d^3V}\right),
\tag{240}
$$

where the volume integration is over a small volume between two adjacent flux surfaces with Ψ difference being $\triangle\Psi$. (This formula is used in my PIC code to calculate the radial heat flux.) The above 3D volume integration can also be written as a 2D surface integration. The differential volume element is given by $d^3V = |\mathcal{J}|d\psi d\theta d\phi$, where $\mathcal{J}$ is the Jacobian of (ψ, θ, ϕ) coordinates. Using this, equation (240) is written as

$$
\begin{aligned}
\langle G\rangle &= \lim_{\triangle\Psi\to 0}\left(\frac{\iiint_{\triangle\Psi}G|\mathcal{J}|d\psi d\theta d\phi}{\iiint_{\triangle\Psi}|\mathcal{J}|d\psi d\theta d\phi}\right) \\
&= \frac{d\psi\iint G|\mathcal{J}|d\theta d\phi}{d\psi\iint |\mathcal{J}|d\theta d\phi} \\
&= \frac{\iint G|\mathcal{J}|d\theta d\phi}{\iint |\mathcal{J}|d\theta d\phi},
\end{aligned}
\tag{241}
$$

which is a 2D averaging over a magnetic surface and thus is called magnetic surface average.

The magnetic surface average only contains the contribution from the $n = 0$ component (n is the toroidal mode number), i.e., axisymmetric component, since the surface averaging of any $n \neq 0$ harmonic is zero. On the other hand, all poloidal harmonics of G can contribute to the surface average since the Jacobian has a poloidal angle dependence. $\langle G\rangle$ is sometimes called the "zonal" component of G if the radial wavelength of $\langle G\rangle$ is much smaller than the equilibrium scale length. If the radial wavelength of $\langle G\rangle$ is comparable to the equilibrium scale length, $\langle G\rangle$ is usually just called "mean" component in tokamak literatures. For example, mean flows are of system space scale and thus are easy to be observed in experiments. On the other hand, the "zonal" flow, which

usually refers to the turbulence generated secondary flow, is of much smaller radial scale (the radial wavelength of zonal flow is of serval Larmor radius) and thus is difficult to observe in experiments.

Sometimes, we do not want the Jacobian explicitly to appear in the formula. This can be achived by writing the differential volume element as

$$d^3V = Rd\phi \frac{d\Psi}{|\nabla\Psi|} dl_p. \tag{242}$$

Using $B_p = |\nabla\Psi|/R$, the volume element is further written as

$$d^3V = d\phi \frac{d\Psi}{B_p} dl_p \tag{243}$$

Using this, the averaging defined in Eq. (240) is written as

$$
\begin{aligned}
\langle G \rangle &= \lim_{\Delta\Psi\to 0} \frac{\iiint_{\Delta\Psi} G d\phi \frac{d\Psi}{B_p} dl_p}{\iiint_{\Delta\Psi} d\phi \frac{d\Psi}{B_p} dl_p} \\
&= \frac{\iint G \frac{1}{B_p} d\phi dl_p}{\iint \frac{1}{B_p} d\phi dl_p}.
\end{aligned} \tag{244}
$$

If G is axisymmetric, then the above equation is written as

$$\langle G \rangle = \frac{\oint G \frac{1}{B_p} dl_p}{\oint \frac{1}{B_p} dl_p}. \tag{245}$$

(Equation (245) is used in the GTAW code to calculate the magnetic surface averaging.) Using Eq. (197) and $B_p = |\nabla\Psi|/R$, equation (245) can also be written as

$$\langle G \rangle = \frac{\int_0^{2\pi} G |\mathcal{J}| d\theta}{\int_0^{2\pi} |\mathcal{J}| d\theta}. \tag{246}$$

Noting that the Jacobian does not change sign, the above equation is written as

$$\langle G \rangle = \frac{\int_0^{2\pi} G \mathcal{J} d\theta}{\int_0^{2\pi} \mathcal{J} d\theta}. \tag{247}$$

Using the expression of the volume element $d\tau = |\mathcal{J}| d\theta d\phi d\psi$, the volume within a magnetic surface is written

$$V(\psi) = \int d\tau = \int |\mathcal{J}| d\theta d\phi d\psi = 2\pi \int_{\psi_0}^{\psi} \int_0^{2\pi} |\mathcal{J}| d\theta d\psi. \tag{248}$$

Using this, the differential of V with respect to ψ is written as

$$V' \equiv \frac{dV}{d\psi} = 2\pi \int_0^{2\pi} |\mathcal{J}| d\theta. \tag{249}$$

Using this, Eq. (246) is written as

$$\langle G \rangle = \frac{2\pi}{V'} \int_0^{2\pi} G |\mathcal{J}| d\theta \tag{250}$$

10.2 Flux Surface Functions

Next, examine the meaning of the following volume integral

$$D(\psi) \equiv \int_V \mathbf{B} \cdot \nabla\theta d\tau, \tag{251}$$

where the volume $V = V(\psi)$, which is the volume within the magnetic surface labeled by ψ. Using $\nabla \cdot \mathbf{B} = 0$, the quantity D can be further written as

$$D = \int_V \nabla \cdot (\theta \mathbf{B}) d\tau. \tag{252}$$

Note that θ is not a single-value function of the spacial points. In order to evaluate the integration in Eq. (252), we need to select one branch of θ, which can be chosen to be $0 \leqslant \theta < 2\pi$. Note that function $\theta = \theta(R, Z)$ is not continuous in the vicinity of the contour of $\theta = 0$. Next, we want to use the Gauss's theorem to convert the above volume integration to surface integration. Noting the discontinuity of the integrand $\theta \mathbf{B}$ in the vicinity of the contour of $\theta = 0$, the volume should be cut along the contour, thus, generating two surfaces. Denote these two surfaces by S_1 and S_2, then equation (252) is written as

$$D = \int_{S_1} \theta \mathbf{B} \cdot d\mathbf{S} + \int_{S_2} \theta \mathbf{B} \cdot d\mathbf{S} + \int_{S_3} \theta \mathbf{B} \cdot d\mathbf{S},$$

where the direction of surface S_1 is in the negative direction of θ, the direction of S_2 is in the positive direction of θ, and the surface S_3 is the toroidal magnetic surface $\psi = \psi_0$. The surface integration through S_3 is obviously zero since $\mathbf{B}$ lies in this surface. Therefore, we have

$$\begin{aligned} D &= \int_{S_1} \theta \mathbf{B} \cdot d\mathbf{S} + \int_{S_2} \theta \mathbf{B} \cdot d\mathbf{S} + 0 \\ &= \int_{S_1} 0 \mathbf{B} \cdot d\mathbf{S} + \int_{S_2} 2\pi \mathbf{B} \cdot d\mathbf{S} \\ &= 2\pi \int_{S_2} \mathbf{B} \cdot d\mathbf{S}. \end{aligned} \tag{253}$$

Eq. (253) indicates that D is 2π times the magnetic flux through the S_2 surface. Thus, the poloidal flux through S_2 is written as

$$\Psi_p = \frac{1}{2\pi} D = \frac{1}{2\pi} \int_V \mathbf{B} \cdot \nabla \theta d\tau. \tag{254}$$

Using the expression of the volume element $d\tau = |\mathcal{J}| d\theta d\phi d\psi$, Ψ_p can be further written in terms of flux surface averaged quantities.

$$\begin{aligned} \Psi_p &= \frac{1}{2\pi} \int_V \mathbf{B} \cdot \nabla \theta |\mathcal{J}| d\theta d\phi d\psi \\ &= \int_0^\psi d\psi \int_0^{2\pi} \mathbf{B} \cdot \nabla \theta |\mathcal{J}| d\theta \\ &= \int_0^\psi d\psi \int_0^{2\pi} \Psi' \nabla \psi \times \nabla \phi \cdot \nabla \theta |\mathcal{J}| d\theta \\ &= -\text{sign}(\mathcal{J}) \int_0^\psi d\psi \int_0^{2\pi} \Psi'(\psi) d\theta \\ &= -2\pi \, \text{sign}(\mathcal{J}) \int_0^\psi \Psi'(\psi) d\psi \\ &= -2\pi \, \text{sign}(\mathcal{J}) [\Psi(\psi) - \Psi(0)]. \end{aligned} \tag{255}$$

Note that the sign of the Jacobian appears in Eq. (255), which is due to the positive direction of surface S_2 is determined by the positive direction of θ, which in turn is determined by the sign of the Jacobian (In my code, however, the positive direction of θ is chosen by me and the sign of the Jacobian is determined by the positive direction of θ). We can verify the sign of Eq. (255) is

exactly consistent with that in Eq. (19).

Similarly, the toroidal flux within a flux surface is written as

$$\Psi_t = \frac{1}{2\pi}\int_V \mathbf{B}\cdot\nabla\phi d\tau, \tag{256}$$

the poloidal current within a flux surface is written as

$$K(\psi) = \frac{1}{2\pi}\int_V \mathbf{J}\cdot\nabla\theta d\tau, \tag{257}$$

and toroidal current within a flux surface is written as

$$I(\psi) = \frac{1}{2\pi}\int_V \mathbf{J}\cdot\nabla\phi d\tau. \tag{258}$$

(**check**)The toroidal magnetic flux is written as

$$
\begin{aligned}
\Psi_t &= \frac{1}{2\pi}\int \mathbf{B}\cdot\nabla\phi|\mathcal{J}|d\theta d\phi d\psi \\
&= \int_0^\psi d\psi \int_0^{2\pi} g\frac{1}{R^2}|\mathcal{J}|d\theta \\
&= \int_0^\psi \left[g\frac{V'}{2\pi}\left\langle \frac{1}{R^2}\right\rangle \right]d\psi.
\end{aligned} \tag{259}
$$

$$\Rightarrow \Psi_t' = g\frac{V'}{2\pi}\left\langle \frac{1}{R^2}\right\rangle$$

$$\Rightarrow \frac{d\Psi_t}{dV} = g\frac{1}{2\pi}\left\langle \frac{1}{R^2}\right\rangle$$

$$\Rightarrow \frac{d\Psi}{dV} = \frac{g}{2\pi q}\frac{1}{2\pi}\left\langle \frac{1}{R^2}\right\rangle. \tag{260}$$

Next, calculate the derivative of the toroidal flux with respect to the poloidal flux.

$$
\begin{aligned}
\frac{d\Psi_t}{d\Psi_p} &= \frac{\Psi_t'}{\Psi_p'} \\
&= -\frac{gV'}{(2\pi)^2\Psi'}\left\langle \frac{1}{R^2}\right\rangle,
\end{aligned} \tag{261}
$$

Comparing this result with Eq. (505) indicates that it is equal to the safety factor, i.e.,

$$\frac{d\Psi_t}{d\Psi_p} = q(\psi). \tag{262}$$

$$-\mathrm{sgn}(\mathcal{J})\frac{V'}{(2\pi)^2}\frac{g}{\Psi'}\langle R^{-2}\rangle$$

By using the contravariant representation of current density (360), the poloidal current within a magnetic surface is written as

$$K(\psi) = \frac{1}{2\pi}\int \mathbf{J}\cdot\nabla\theta \mathcal{J}d\theta d\phi d\psi$$

$$
\begin{aligned}
&= \frac{1}{\mu_0} \int (-g') \nabla\phi \times \nabla\psi \cdot \nabla\theta \mathcal{J} d\theta d\psi \\
&= -\frac{1}{\mu_0} \int g' d\theta d\psi \\
&= -\frac{2\pi}{\mu_0} \int_0^\psi g' d\psi \\
&= -\frac{2\pi}{\mu_0} [g(\psi) - g(0)].
\end{aligned}
\tag{263}
$$

Note that the poloidal current is proportional to g, which explains why g is sometimes called poloidal current function in tokamak literature.

$$
-\left[\left(\Psi' \frac{\mathcal{J}}{R^2} |\nabla\psi|^2 \right)_\psi + \left(\Psi' \frac{\mathcal{J}}{R^2} \nabla\psi \cdot \nabla\theta \right)_\theta \right] \nabla\psi \times \nabla\theta - g' \nabla\phi \times \nabla\psi,
$$

The toroidal current is written as

$$
\begin{aligned}
I_\phi(\psi) &= \frac{1}{2\pi} \int \mathbf{J} \cdot \nabla\phi \mathcal{J} d\theta d\phi d\psi \\
&= -\frac{1}{2\pi\mu_0} \int \left[\left(\Psi' \frac{\mathcal{J}}{R^2} |\nabla\psi|^2 \right)_\psi + \left(\Psi' \frac{\mathcal{J}}{R^2} \nabla\psi \cdot \nabla\theta \right)_\theta \right] \nabla\psi \times \nabla\theta \cdot \nabla\phi \mathcal{J} d\theta d\phi d\psi \\
&= -\frac{1}{\mu_0} \int \left[\left(\Psi' \frac{\mathcal{J}}{R^2} |\nabla\psi|^2 \right)_\psi + \left(\Psi' \frac{\mathcal{J}}{R^2} \nabla\psi \cdot \nabla\theta \right)_\theta \right] d\theta d\psi \\
&= -\frac{1}{\mu_0} \int \left[\left(\Psi' \frac{\mathcal{J}}{R^2} |\nabla\psi|^2 \right)_\psi \right] d\theta d\psi \\
&= -\frac{1}{\mu_0} \int_0^{2\pi} d\theta \int_0^\psi d\psi \left(\Psi' \frac{\mathcal{J}}{R^2} |\nabla\psi|^2 \right)_\psi \\
&= -\frac{1}{\mu_0} \int_0^{2\pi} d\theta \left(\Psi' \frac{\mathcal{J}}{R^2} |\nabla\psi|^2 - 0 \right).
\end{aligned}
\tag{264}
$$

The last equality is due to $\nabla\psi = 0$ at $\psi = 0$. By using the flux surface average operator, Eq. (264) is written

$$
I_\phi(\psi) = -\frac{V'\Psi'}{2\pi\mu_0} \left\langle \frac{|\nabla\psi|^2}{R^2} \right\rangle.
\tag{265}
$$

Next, calculate another useful surface-averaged quantity,

$$
\begin{aligned}
\frac{\langle \mathbf{J} \cdot \mathbf{B} \rangle}{\langle \mathbf{B} \cdot \nabla\phi \rangle} &= \frac{\left\langle \frac{g^2}{\mathcal{J}} \left[\left(\frac{1}{g} \Psi' \frac{\mathcal{J}}{R^2} |\nabla\psi|^2 \right)_\psi + \left(\frac{1}{g} \Psi' \nabla\psi \cdot \nabla\theta \frac{\mathcal{J}}{R^2} \right)_\theta \right] \right\rangle}{\mu_0 \langle g/R^2 \rangle} \\
&= \frac{\frac{2\pi}{V'} \int_0^{2\pi} d\theta g^2 \left[\left(\frac{1}{g} \Psi' \frac{\mathcal{J}}{R^2} |\nabla\psi|^2 \right)_\psi + \left(\frac{1}{g} \Psi' \nabla\psi \cdot \nabla\theta \frac{\mathcal{J}}{R^2} \right)_\theta \right]}{\mu_0 g \langle R^{-2} \rangle} \\
&= \frac{\frac{2\pi}{V'} g^2 \int_0^{2\pi} d\theta \left[\left(\frac{1}{g} \Psi' \frac{\mathcal{J}}{R^2} |\nabla\psi|^2 \right)_\psi + \left(\frac{1}{g} \Psi' \nabla\psi \cdot \nabla\theta \frac{\mathcal{J}}{R^2} \right)_\theta \right]}{\mu_0 g \langle R^{-2} \rangle} \\
&= \frac{\frac{2\pi}{V'} g \int_0^{2\pi} d\theta \left[\left(\frac{1}{g} \Psi' \frac{\mathcal{J}}{R^2} |\nabla\psi|^2 \right)_\psi \right]}{\mu_0 \langle R^{-2} \rangle} \\
&= \frac{\frac{2\pi}{V'} g \int_0^{2\pi} d\theta \left[\left(\frac{1}{g} \Psi' \frac{\mathcal{J}}{R^2} |\nabla\psi|^2 \right)_\psi \right]}{\mu_0 \langle R^{-2} \rangle}
\end{aligned}
\tag{266}
$$

The differential with respect to ψ and the integration with respect to θ can be interchanged, yielding

$$
\begin{aligned}
\frac{\langle \mathbf{J} \cdot \mathbf{B} \rangle}{\langle \mathbf{B} \cdot \nabla \phi \rangle} &= \frac{\frac{2\pi}{V'} g \left[\frac{1}{g} \Psi' \left(\int_0^{2\pi} d\theta \frac{\mathcal{J}}{R^2} |\nabla \psi|^2 \right) \right]_\psi}{\mu_0 \langle R^{-2} \rangle} \\
&= \frac{\frac{1}{V'} g \left[\frac{1}{g} \Psi' V' \left\langle \frac{|\nabla \psi|^2}{R^2} \right\rangle \right]_\psi}{\mu_0 \langle R^{-2} \rangle} \\
&= \frac{g}{\mu_0 V' \langle R^{-2} \rangle} \left[\frac{\Psi' V'}{g} \left\langle \frac{|\nabla \psi|^2}{R^2} \right\rangle \right]_\psi
\end{aligned}
\tag{267}
$$

11 Magnetic surface coordinates $(\psi,\ \theta,\ \zeta)$ with general toroidal angle ζ

11.1 Definition of general toroidal angle ζ

In Sec. 7.1, we introduced the local safety factor $\hat{q}(\psi, \theta)$. Equation (187) indicates that if the Jacobian is chosen to be of the particular form $\mathcal{J} = h(\psi) R^2$, where $h(\psi)$ is an arbitrary function of ψ, then the local safety factor is independent of θ, i.e., magnetic line is straight in (θ, ϕ) plane. On the other hand, if we want to make field line straight in (θ, ϕ) plane, the Jacobian must be chosen to be of the specific form $\mathcal{J} = h(\psi) R^2$. We note that, as mentioned in Sec. 7.2, the poloidal angle is fully determined by the choice of the Jacobian. The specific choice of $\mathcal{J} = \alpha(\psi) R^2$ is usually too restrictive for choosing a desired poloidal angle (for example, the equal-arc poloidal angle can not be achieved by this choice of Jacobian). Is there any way that we can make the field line straight in a coordinate system at the same time ensure that the Jacobian can be freely adjusted to obtain desired poloidal angle? The answer is yes. The obvious way to achieve this is to define a new toroidal angle ζ that generalizes the usual toroidal angle ϕ. Define a new toroidal angle ζ by[7]

$$
\zeta = \phi - q(\psi)\delta(\psi, \theta),
\tag{268}
$$

where $\delta = \delta(\psi, \theta)$ is a unknown function to be determined by the constraint of field line being straight in (θ, ζ) plane. The new local safety factor in (ψ, θ, ζ) coordinates, $\hat{q}_{\text{new}} = \mathbf{B} \cdot \nabla \zeta / \mathbf{B} \cdot \nabla \theta$, is written as

$$
\begin{aligned}
\hat{q}_{\text{new}} &= \frac{\mathbf{B} \cdot \nabla \zeta}{\mathbf{B} \cdot \nabla \theta} \\
&= \frac{(\nabla \Psi \times \nabla \phi + g \nabla \phi) \cdot \nabla(\phi - q\delta)}{(\nabla \Psi \times \nabla \phi + g \nabla \phi) \cdot \nabla \theta} \\
&= \frac{(\nabla \Psi \times \nabla \phi + g \nabla \phi) \cdot [\nabla \phi - \nabla(q\delta)]}{(\nabla \Psi \times \nabla \phi) \cdot \nabla \theta} \\
&= \frac{g |\nabla \phi|^2 + (\nabla \Psi \times \nabla \phi) \cdot [-\nabla(q\delta)]}{(\nabla \Psi \times \nabla \phi) \cdot \nabla \theta}.
\end{aligned}
\tag{269}
$$

In (ψ, θ, ϕ) coordinates, the above equation is written as

$$
\begin{aligned}
\hat{q}_{\text{new}} &= \frac{g |\nabla \phi|^2 - \Psi'(\nabla \psi \times \nabla \phi) \cdot \left[\frac{\partial(q\delta)}{\partial \theta} \nabla \theta + \frac{\partial(q\delta)}{\partial \psi} \nabla \psi \right]}{-\Psi' \mathcal{J}^{-1}} \\
&= -\frac{g}{\Psi'} \frac{\mathcal{J}}{R^2} - q \frac{\partial \delta}{\partial \theta},
\end{aligned}
\tag{270}
$$

where $\mathcal{J}$ is the Jacobian of (ψ, θ, ϕ) coordinates. Using the expression of the local safety factor given in Eq. (187), the above equation is written

$$\hat{q}_{\text{new}} = \hat{q} - q\frac{\partial\delta}{\partial\theta}, \tag{271}$$

To make the new local safety factor be independent of θ, the right-hand side of Eq. (270) should be independent of θ, i.e.,

$$\hat{q} - q\frac{\partial\delta}{\partial\theta} = c(\psi), \tag{272}$$

where $c(\psi)$ can be an arbitrary function of ψ. The most convenient choice for $c(\psi)$ is $c(\psi) = q$, i.e., making the new local safety factor be equal to the original global safety factor. In this case, equation (272) is written as

$$\frac{\partial\delta}{\partial\theta} = \frac{\hat{q}}{q} - 1, \tag{273}$$

which can be integrated over θ to give

$$\delta(\psi, \theta) = c(\psi, \theta_{\text{ref}}) + \frac{1}{q}\int_{\theta_{\text{ref}}}^{\theta} \hat{q}d\theta - \theta, \tag{274}$$

where θ_{ref} is an arbitrarily chosen starting poloidal angle for the integration, $c(\psi, \theta_{\text{ref}})$ is the constant of integration. Since there is no other requirements for the ψ dependence of δ, the constant of integration, $c(\psi, \theta_{\text{ref}})$, can be chosen to be zero. Then the above equations is written

$$\delta = \frac{1}{q}\int_{\theta_{\text{ref}}}^{\theta} \hat{q}d\theta - \theta, \tag{275}$$

i.e.,

$$\delta = \frac{1}{q}\int_{\theta_{\text{ref}}}^{\theta} \frac{\mathbf{B}\cdot\nabla\phi}{\mathbf{B}\cdot\nabla\theta}d\theta - \theta \tag{276}$$

Substituting the above equation into the definition of ζ (Eq. 268), we obtain

$$\zeta = \phi - \int_{\theta_{\text{ref}}}^{\theta} \frac{\mathbf{B}\cdot\nabla\phi}{\mathbf{B}\cdot\nabla\theta}d\theta + q\theta, \tag{277}$$

which is the formula for calculating the general toroidal angle. In summary, magneitc field line is straight in (θ, ζ) plane if ζ is defined by Eq. (277) and the slope of the field line is q. In this method, we make the field line straight by defining a new toroidal angle, instead of requiring the Jacobian to take particular forms. Thus, the freedom of choosing the form of the Jacobian is still available to be used later to define a good poloidal angle coordinate. Note that the Jacobian of the new coordinaes (ψ, θ, ζ) is equal to that of (ψ, θ, ϕ). [Proof:

$$\begin{aligned} \mathcal{J}_{\text{new}}^{-1} &= \nabla\psi \times \nabla\theta \cdot \nabla\zeta \\ &= \nabla\psi \times \nabla\theta \cdot \nabla(\phi - q\delta) \\ &= \nabla\psi \times \nabla\theta \cdot \nabla\phi - \nabla\psi \times \nabla\theta \cdot \nabla(q\delta) \\ &= \nabla\psi \times \nabla\theta \cdot \nabla\phi - 0 \\ &= \mathcal{J}^{-1}. \end{aligned}$$

] Also note that $\delta(\psi, \theta)$ defined by Eq. (275) is a periodic funtion of θ. [Proof: Equation (275) implies that

$$\begin{aligned} \delta(\psi, \theta + 2\pi) &= \frac{1}{q}\int_{\theta_{\text{ref}}}^{\theta+2\pi} \hat{q}d\theta - \theta - 2\pi \\ &= \frac{1}{q}\int_{\theta_{\text{ref}}}^{\theta} \hat{q}d\theta - \theta - 2\pi + \frac{1}{q}\int_{\theta}^{\theta+2\pi} \hat{q}d\theta \\ &= \delta(\psi, \theta) - 2\pi + \frac{1}{q}\int_{\theta}^{\theta+2\pi} \hat{q}d\theta \\ &= \delta(\psi, \theta). \end{aligned} \tag{278}$$

]

[In numerical implementation, the term $\int_{\theta_{\mathrm{ref}}}^{\theta} \frac{\mathbf{B} \cdot \nabla \phi}{\mathbf{B} \cdot \nabla \theta} d\theta$ appearing in δ is computed by using

$$
-\int_{\theta_{\mathrm{ref}}}^{\theta} \frac{\mathbf{B} \cdot \nabla \phi}{\mathbf{B} \cdot \nabla \theta} d\theta \;=\; -\int_{\theta_{\mathrm{ref}}}^{\theta} \frac{g}{R^2} \; \frac{\mathcal{J}}{\Psi'} d\,\theta \;=\; -\int_{\theta_{\mathrm{ref}}}^{\theta} \frac{g}{R^2} \; \frac{1}{\Psi'} \frac{R}{|\nabla \psi|} d\,l_p \;=\; -\int_{\theta_{\mathrm{ref}}}^{\theta} \frac{g}{R} \; \frac{1}{|\nabla \Psi|} d\,l_p \;=\; -
$$

$$
\int_{\theta_{\mathrm{ref}}}^{\theta} \frac{1}{R} \frac{B_\phi}{B_p} d\ell_p. \tag{279}
$$

For later use, from Eq. (240), we obtain

$$
\frac{\partial(\delta q)}{\partial \psi} \;=\; -\frac{d}{d\psi}\Big(\frac{g}{\Psi'}\Big) \int_{\theta_{\mathrm{ref}}}^{\theta} \frac{\mathcal{J}}{R^2} d\theta - \frac{g}{\Psi'} \frac{\partial}{\partial \psi} \int_{\theta_{\mathrm{ref}}}^{\theta} \frac{\mathcal{J}}{R^2} d\theta - \frac{dq}{d\psi} \theta. \tag{280}
$$

This formula is used in GTAW code to calculate $\partial(\delta q)/\partial \psi$, where the derivative $\partial(g/\Psi')/\partial \psi$ is calculated numerically by using the central difference scheme.]

11.2   Contravariant form of magnetic field in (ψ, θ, ζ) coordinates

Recall that the contravariant form of the magnetic field in (ψ, θ, ϕ) coordinates is given by Eq. (188), i.e.,

$$
\mathbf{B} = -\Psi'(\nabla \phi \times \nabla \psi + \hat{q} \nabla \psi \times \nabla \theta). \tag{281}
$$

Next, let us derive the corresponding form in (ψ, θ, ζ) coordinates. Using the definition of ζ, equation (281) is written as

$$
\begin{aligned}
\mathbf{B} &= -\Psi' \nabla(\zeta + q\delta) \times \nabla \psi - \Psi' \hat{q} \nabla \psi \times \nabla \theta \\
&= -\Psi' \nabla \zeta \times \nabla \psi - \Psi' \nabla(q\delta) \times \nabla \psi - \Psi' \hat{q} \nabla \psi \times \nabla \theta \\
&= -\Psi' \nabla \zeta \times \nabla \psi - \Psi' q \frac{\partial \delta}{\partial \theta} \nabla \theta \times \nabla \psi - \Psi' \hat{q} \nabla \psi \times \nabla \theta
\end{aligned} \tag{282}
$$

Using Eq. (273), the above equation is simplified as

$$
\mathbf{B} \;=\; -\Psi'(\nabla \zeta \times \nabla \psi + q \nabla \psi \times \nabla \theta). \tag{283}
$$

Equation (283) is the contravariant form of the magnetic field in (ψ, θ, ζ) coordinates.

11.3   Relation between the partial derivatives in (ψ, θ, ϕ) and (ψ, θ, ζ) coordinates

Noting the simple fact that

$$
\frac{d}{dx} = \frac{d}{d(x+c)}, \tag{284}
$$

where c is a constant, we conclude that

$$
\left(\frac{\partial f}{\partial \zeta}\right)_{\psi, \theta} = \left(\frac{\partial f}{\partial \phi}\right)_{\psi, \theta}, \tag{285}
$$

(since $\phi = \zeta + q(\psi)\delta(\psi, \theta)$, where the part $q(\psi)\delta(\psi, \theta)$ acts as a constant when we hold ψ and θ constant), i.e., the symmetry property with respect to the new toroidal angle ζ is identical with the one with respect to the old toroidal angle ϕ. On the other hand, generally we have

$$\left(\frac{\partial f}{\partial \psi}\right)_{\theta, \zeta} \neq \left(\frac{\partial f}{\partial \psi}\right)_{\theta, \phi} \tag{286}$$

and

$$\left(\frac{\partial f}{\partial \theta}\right)_{\psi, \zeta} \neq \left(\frac{\partial f}{\partial \theta}\right)_{\psi, \phi}. \tag{287}$$

In the special case that f is axisymmetric (i.e., f is independent of ϕ in (ψ, θ, ϕ) coordinates), then two sides of Eqs. (286) and (287) are equal to each other. Note that the partial derivatives $\partial/\partial\psi$ and $\partial/\partial\theta$ in Sec. 11.1 and 11.2 are taken in (ψ, θ, ϕ) coordinates. Because the quantities involved in Sec. 11.1 and 11.2 are axisymmetric, these partial derivatives are equal to their counterparts in (ψ, θ, ζ) coordinates.

11.4 Steps to construct a straight-line flux coordinate system

In Sec. 8, we have provided the steps to construct the magnetic surface coordinate system (ψ, θ, ϕ). Only one additional step is needed to construct the straight-line flux coordinate system (ψ, θ, ζ). The additional step is to calculate the generalized toroidal angle ζ according to Eq. (268), where δ is obtained from Eq. (240). This step introduces the new toroidal angle ζ and thus introduces a new magnetic surfaces coordinate system (ψ, θ, ζ), which is a straight-line flux coordinate system. Also note that the Jacobian of (ψ, θ, ζ) coordinates happens to be equal to that of (ψ, θ, ϕ) coordinates.

11.5 Form of operator $\boldsymbol{B} \cdot \boldsymbol{\nabla}$ in $(\boldsymbol{\psi}, \boldsymbol{\theta}, \boldsymbol{\zeta})$ coordinates

The usefulness of the contravariant form [Eq. (283)] of the magnetic field lies in that it allows a simple form of $\mathbf{B} \cdot \nabla$ operator in a coordinate system. (The operator $\mathbf{B}_0 \cdot \nabla$ is usually called magnetic differential operator.) In (ψ, θ, ζ) coordinate system, by using the contravariant form Eq. (283), the operator is written as

$$
\begin{aligned}
\mathbf{B} \cdot \nabla f &= -\Psi'(\nabla\zeta \times \nabla\psi) \cdot \nabla f(\psi, \theta, \zeta) - \Psi' q(\nabla\psi \times \nabla\theta) \cdot \nabla f(\psi, \theta, \zeta) \\
&= -\Psi' \mathcal{J}^{-1}\left(\frac{\partial}{\partial \theta} + q\frac{\partial}{\partial \zeta}\right)f.
\end{aligned} \tag{288}
$$

Next, consider the solution of the magnetic differential equation, which is given by

$$\mathbf{B} \cdot \nabla f = h. \tag{289}$$

where $h = h(\psi, \theta, \zeta)$ is some known function. Using Eq. (288), the magnetic differential equation is written as

$$\left(\frac{\partial}{\partial \theta} + q(\psi)\frac{\partial}{\partial \zeta}\right)f = -\frac{1}{\Psi'}\mathcal{J}h(\psi, \theta, \zeta). \tag{290}$$

Note that the coefficients before the two partial derivatives of the above equation are all independent of θ and ζ. This indicates that different Fourier harmonics in θ and ζ are decoupled. As a result of this fact, if f and the right-hand side of the above equation are Fourier expanded respectively as

$$f(\psi, \theta, \zeta) = \sum_{m,n} f_{mn}(\psi)e^{i(m\theta - n\zeta)}, \tag{291}$$

(note that, following the convention adopted in tokamak literature[7], the Fourier harmonics are chosen to be $e^{i(m\theta-n\zeta)}$, instead of $e^{i(m\theta+n\zeta)}$), and

$$-\frac{1}{\Psi'}\mathcal{J}h(\psi,\theta,\zeta) = \sum_{m,n} \gamma_{mn}(\psi)e^{i(m\theta-n\zeta)}, \tag{292}$$

then Eq. (290) can be readily solved to give

$$f_{mn} = \frac{\gamma_{mn}}{i[m-nq]}. \tag{293}$$

The usefulness of the straight line magnetic coordinates (ψ,θ,ζ) lies in that, as mentioned in the above, it makes the coefficients before the two partial derivatives both independent of θ and ζ, thus, allowing a simple solution to the magnetic differential equation.

11.6 Resonant surface of a perturbation

Equation (293) indicates that, for the differential equation (289), there is a resonant response to a perturbation $e^{i(m\theta-n\zeta)}$ on a magnetic surface with $m-nq=0$. Therefore, the magnetic surface with $q=m/n$ is called the "resonant surface" for the perturbation $e^{i(m\theta-n\zeta)}$. The phase change of the perturbation along a magnetic field is given by $m\Delta\theta - n\Delta\zeta$, which can be written as $\Delta\theta(m-nq)$. Since $m-nq=0$ on a resonant surface, the above formula indicates that there is no phase change along a magnetic field line on a resonant surface, i.e., the parallel wavenumber $k_\parallel$ is zero on a resonant surface.

11.7 Poloidal angle used in tearing mode theory

Next, we discuss a special poloidal angle, which is often used in the tearing mode theory. This poloidal angle is defined by

$$\chi = \theta - \frac{n}{m}\zeta, \tag{294}$$

where (m, n) are the mode numbers of the tearing mode. The special thing about the poloidal angle χ is that its definition is associated with a particular perturbation. It is ready to verify that the Jacobian of (ψ, χ, ζ) coordinates is equal to that of (ψ, θ, ζ) coordinates [proof: $(\mathcal{J}')^{-1} = \nabla\psi\times\nabla\chi\cdot\nabla\zeta = \nabla\psi\times\nabla(\theta-n\zeta/m)\cdot\nabla\zeta = \nabla\psi\times\nabla\theta\cdot\nabla\zeta = \mathcal{J}^{-1}$]. The component of $\mathbf{B}$ along $\nabla\chi$ direction (i.e., the covariant component) is written

$$\begin{aligned} B^{(\chi)} &\equiv \mathbf{B}\cdot\nabla\chi \\ &= -\Psi'(\nabla\zeta\times\nabla\psi + q\nabla\psi\times\nabla\theta)\cdot\nabla(\theta-n\zeta/m) \\ &= -\Psi'(\nabla\zeta\times\nabla\psi\cdot\nabla\theta) + \Psi'\frac{n}{m}(q\nabla\psi\times\nabla\theta\cdot\nabla\zeta) \\ &= -\Psi'\mathcal{J}^{-1} + \Psi'\frac{n}{m}q\mathcal{J}^{-1} \\ &= \Psi'\mathcal{J}^{-1}\Big(q\frac{n}{m}-1\Big). \end{aligned} \tag{295}$$

At the resonant surface $q=m/n$, equation (295) implies $B^{(\chi)}=0$. On the other hand, the covariant component of $\mathbf{B}$ in θ direction is written

$$\begin{aligned} B^{(\theta)} &\equiv \mathbf{B}\cdot\nabla\theta \\ &= -\Psi'(\nabla\zeta\times\nabla\psi + q\nabla\psi\times\nabla\theta)\cdot\nabla\theta \\ &= -\Psi'\nabla\zeta\times\nabla\psi\cdot\nabla\theta \\ &= -\Psi'\mathcal{J}^{-1}. \end{aligned} \tag{296}$$

Using (296), equation (295) is written

$$B^{(\chi)} = B^{(\theta)}\left(1 - \frac{n}{m}q\right). \tag{297}$$

In the cylindrical limit, $\mathcal{J}$ is a constant independent of the poloidal angle. Then Eq. (296) indicates that $B^{(\theta)}$ is also a constant on a magnetic surface.

11.8 Covariant form of magnetic field in (ψ, θ, ζ) coordinate system

In the above, we have obtained the covariant form of the magnetic field in (ψ, θ, ϕ) coordinates (i.e., Eq. (185)). Next, we derive the corresponding form in (ψ, θ, ζ) coordinate. In order to do this, we need to express the $\nabla\phi$ basis vector in terms of $\nabla\psi$, $\nabla\theta$, and $\nabla\zeta$ basis vectors. Using the definition of the generalized toroidal angle, we obtain

$$\begin{aligned}
g\nabla\phi &= g\nabla(\zeta + q\delta) \\
&= g\nabla\zeta + gq\nabla\delta + g\delta\nabla q \\
&= g\nabla\zeta + gq\left(\frac{\partial\delta}{\partial\psi}\nabla\psi + \frac{\partial\delta}{\partial\theta}\nabla\theta\right) + g\delta q'\nabla\psi \\
&= \left(gq\frac{\partial\delta}{\partial\psi} + g\delta q'\right)\nabla\psi + gq\frac{\partial\delta}{\partial\theta}\nabla\theta + g\nabla\zeta \\
&= g\frac{\partial(q\delta)}{\partial\psi}\nabla\psi + gq\frac{\partial\delta}{\partial\theta}\nabla\theta + g\nabla\zeta.
\end{aligned} \tag{298}$$

Using Eq. (298), the covariant form of the magnetic field, Eq. (185), is written as

$$\mathbf{B} = \left(\Psi'\frac{\mathcal{J}}{R^2}\nabla\psi\cdot\nabla\theta + g\frac{\partial(q\delta)}{\partial\psi}\right)\nabla\psi + \left(gq\frac{\partial\delta}{\partial\theta} - \Psi'\frac{\mathcal{J}}{R^2}|\nabla\psi|^2\right)\nabla\theta + g\nabla\zeta. \tag{299}$$

This expression can be further simplified by using equation (273) to eliminate $\partial\delta/\partial\theta$, which gives

$$\begin{aligned}
\mathbf{B} &= \left(\Psi'\frac{\mathcal{J}}{R^2}\nabla\psi\cdot\nabla\theta + g\frac{\partial(q\delta)}{\partial\psi}\right)\nabla\psi + \left(-\frac{g^2}{\Psi'} - gq\frac{R^2}{\mathcal{J}} - \Psi'|\nabla\psi|^2\right)\frac{\mathcal{J}}{R^2}\nabla\theta + g\nabla\zeta \\
&= \left(\Psi'\frac{\mathcal{J}}{R^2}\nabla\psi\cdot\nabla\theta + g\frac{\partial(q\delta)}{\partial\psi}\right)\nabla\psi + \left(-\frac{g^2 + |\nabla\Psi|^2}{\Psi'} - gq\frac{R^2}{\mathcal{J}}\right)\frac{\mathcal{J}}{R^2}\nabla\theta + g\nabla\zeta.
\end{aligned} \tag{300}$$

Using $B_0^2 = (|\nabla\Psi|^2 + g^2)/R^2$, the above equation is written as

$$\begin{aligned}
\mathbf{B} &= \left(\Psi'\frac{\mathcal{J}}{R^2}\nabla\psi\cdot\nabla\theta + g\frac{\partial(q\delta)}{\partial\psi}\right)\nabla\psi + \left(-\frac{B_0^2 R^2}{\Psi'} - gq\frac{R^2}{\mathcal{J}}\right)\frac{\mathcal{J}}{R^2}\nabla\theta + g\nabla\zeta \\
&= \left(\Psi'\frac{\mathcal{J}}{R^2}\nabla\psi\cdot\nabla\theta + g\frac{\partial(q\delta)}{\partial\psi}\right)\nabla\psi + \left(-\frac{B_0^2}{\Psi'}\mathcal{J} - gq\right)\nabla\theta + g\nabla\zeta.
\end{aligned} \tag{301}$$

Equation (301) is the covariant form of the magnetic field in (ψ, θ, ζ) coordinate system. For the particular choice of the radial coordinate $\psi = -\Psi$ and the Jacobian $\mathcal{J} = h(\psi)/B_0^2$ (i.e., Boozer's Jacobian, disscussed in Sec. 11.9), equation (301) reduces to

$$\mathbf{B} = \left(-\frac{\mathcal{J}}{R^2}\nabla\psi\cdot\nabla\theta + g\frac{\partial(q\delta)}{\partial\psi}\right)\nabla\psi + I(\psi)\nabla\theta + g\nabla\zeta, \tag{302}$$

with $I(\psi) = h(\psi) - gq$. The magnetic field expression in Eq. (302) frequently appears in tokamak literature[17]. Using $I(\psi)$, the Jabobian can also be written as

$$\mathcal{J} = \frac{gq + I}{B_0^2}. \tag{303}$$

11.9 Form of operator $(B \times \nabla\psi/B^2) \cdot \nabla$ in (ψ, θ, ζ) coordinates

In solving the MHD eigenmode equations in toroidal geometries, besides the $\mathbf{B} \cdot \nabla$ operator, we will also encounter another surface operator $(\mathbf{B} \times \nabla\psi/B^2) \cdot \nabla$. Next, we derive the form of the this operator in (ψ, θ, ζ) coordinate system. Using the covariant form of the equilibrium magnetic field [Eq. (301)], we obtain

$$\frac{\mathbf{B} \times \nabla\psi}{B^2} = \frac{1}{B^2}\left(-\frac{B^2}{\Psi'}\mathcal{J} - gq \right)\nabla\theta \times \nabla\psi + \frac{g}{B^2}\nabla\zeta \times \nabla\psi. \tag{304}$$

Using this, the $(\mathbf{B} \times \nabla\psi/B^2) \cdot \nabla$ operator is written as

$$\begin{aligned}
\frac{\mathbf{B} \times \nabla\psi}{B^2} \cdot \nabla &= \frac{1}{B^2}\left(\frac{B^2}{\Psi'}\mathcal{J} + gq \right)\mathcal{J}^{-1}\frac{\partial}{\partial\zeta} + \frac{g}{B^2}\mathcal{J}^{-1}\frac{\partial}{\partial\theta} \tag{305} \\
&= \left(\frac{1}{\Psi'} + g\frac{\mathcal{J}^{-1}}{B^2}q \right)\frac{\partial}{\partial\zeta} + g\frac{\mathcal{J}^{-1}}{B^2}\frac{\partial}{\partial\theta}, \tag{306}
\end{aligned}$$

which is the form of the operator in (ψ, θ, ζ) coordinate system.

Examining Eq. (306), we find that if the Jacobian $\mathcal{J}$ is chosen to be of the form $\mathcal{J} = h(\psi)/B^2$, where h is some magnetic surface function, then the coefficients before the two partial derivatives will be independent of θ and ζ. It is obvious that the independence of the coefficients on θ and ζ will be advantageous to some applications. The coordinate system (ψ, θ, ζ) with the particular choice of $\mathcal{J} = h(\psi)/B^2$ is called the Boozer coordinates, named after A.H. Boozer, who first proposed this choice of the Jacobian. The usefulness of the new toroidal angle ζ is highlighted in Boozer's choice of the Jacobian, which makes both $\mathbf{B} \cdot \nabla$ and $(\mathbf{B} \times \nabla\psi/B^2) \cdot \nabla$ be a constant-coefficient differential operator. For other choices of the Jacobian, only the $\mathbf{B} \cdot \nabla$ operator is a constant-coefficient differential operator.

11.10 Radial differential operator

In solving the MHD eigenmode equations in toroidal geometry, we also need the radial differential operator $\nabla\psi \cdot \nabla$. Next, we derive the form of the operator in (ψ, θ, ζ) coordinates. Using

$$\nabla f = \frac{\partial f}{\partial\psi}\nabla\psi + \frac{\partial f}{\partial\theta}\nabla\theta + \frac{\partial f}{\partial\zeta}\nabla\zeta,$$

the radial differential operator is written as

$$\begin{aligned}
\nabla\psi \cdot \nabla f &= |\nabla\psi|^2\frac{\partial f}{\partial\psi} + (\nabla\theta \cdot \nabla\psi)\frac{\partial f}{\partial\theta} + (\nabla\zeta \cdot \nabla\psi)\frac{\partial f}{\partial\zeta} \\
&= |\nabla\psi|^2\frac{\partial f}{\partial\psi} + (\nabla\theta \cdot \nabla\psi)\frac{\partial f}{\partial\theta} + \{\nabla[\phi - q\delta(\psi,\theta)] \cdot \nabla\psi\}\frac{\partial f}{\partial\zeta} \\
&= |\nabla\psi|^2\frac{\partial f}{\partial\psi} + (\nabla\theta \cdot \nabla\psi)\frac{\partial f}{\partial\theta} - \nabla[q\delta] \cdot \nabla\psi\frac{\partial f}{\partial\zeta} \\
&= |\nabla\psi|^2\frac{\partial f}{\partial\psi} + (\nabla\theta \cdot \nabla\psi)\frac{\partial f}{\partial\theta} - [q\nabla\delta + \delta\nabla q] \cdot \nabla\psi\frac{\partial f}{\partial\zeta} \\
&= |\nabla\psi|^2\frac{\partial f}{\partial\psi} + (\nabla\theta \cdot \nabla\psi)\frac{\partial f}{\partial\theta} - \left[q\left(\frac{\partial\delta}{\partial\psi}\nabla\psi + \frac{\partial\delta}{\partial\theta}\nabla\theta \right) + \delta q'\nabla\psi \right] \cdot \nabla\psi\frac{\partial f}{\partial\zeta} \\
&= |\nabla\psi|^2\frac{\partial f}{\partial\psi} + (\nabla\theta \cdot \nabla\psi)\frac{\partial f}{\partial\theta} - \left[\frac{\partial(q\delta)}{\partial\psi}|\nabla\psi|^2 + q\frac{\partial\delta}{\partial\theta}\nabla\theta \cdot \nabla\psi \right]\frac{\partial f}{\partial\zeta}, \tag{307}
\end{aligned}$$

where $\partial(q\delta)/\partial\psi$ and $q\partial\delta/\partial\theta$ are given respectively by Eqs. (280) and (273). Using the above formula, $\nabla\psi \cdot \nabla\zeta$ is written as

$$\nabla\psi \cdot \nabla\zeta = -\left[\frac{\partial(q\delta)}{\partial\psi}|\nabla\psi|^2 + q\frac{\partial\delta}{\partial\theta}\nabla\theta \cdot \nabla\psi \right]. \tag{308}$$

This formula is used in GTAW code.

12 Field-line-following coordinates

12.1 Definition of the field-line-following coordinates (ψ, θ, α)

Noting that $\nabla q \times \nabla \psi = 0$, the magnetic field in Eq. (283) can be further written

$$\mathbf{B} = -\Psi' \nabla(\zeta - q\theta) \times \nabla \psi. \tag{309}$$

This motivates us to define a new coordinate α by

$$\alpha \equiv \zeta - q\theta, \tag{310}$$

to replace ζ, then the magnetic field in Eq. (309) is written

$$\mathbf{B} = \Psi' \nabla \psi \times \nabla \alpha, \tag{311}$$

which is called the Clebsch form of the magnetic field. Equation (311) implies that

$$\mathbf{B} \cdot \nabla \alpha = 0, \tag{312}$$

and

$$\mathbf{B} \cdot \nabla \psi = 0, \tag{313}$$

which indicates that both α and ψ are constant along a magnetic field line. Taking scalar product of Eq. (311) with $\nabla \theta$, we obtain

$$\mathbf{B} \cdot \nabla \theta = -\frac{\Psi'}{\mathcal{J}}, \tag{314}$$

which is nonzero, i.e., only θ among (ψ, θ, α) is changing along a magnetic field line. (Here $\mathcal{J} = (\nabla \psi \times \nabla \theta \cdot \nabla \alpha)^{-1}$ is the Jacobian of the coordinate system (ψ, θ, α), which happens to be equal to the Jacobian of (ψ, θ, ζ) coordinates.) Due to this fact, (ψ, θ, α) coordinates are usually called "field-line-following coordinates" or "field-aligned coordinates" [1, 4].

Using Eq. (311), the magnetic differential operator $\mathbf{B} \cdot \nabla$ in the new coordinate system (ψ, θ, α) is written

$$\mathbf{B} \cdot \nabla f = -\frac{\Psi'}{\mathcal{J}} \frac{\partial}{\partial \theta} f, \tag{315}$$

which is just a partial derivative over θ and this is expected since only θ is changing along a magnetic field line.

It is widely accepted (but can still be questioned because of lacking of conclusive experiments) that turbulence in tokamak plasmas usually has $k_\parallel \ll k_\perp$, where $k_\parallel$ and $k_\perp$ are the parallel and perpendicular wavenumbers, respectively. Due to this elongated structure along the parallel direction, less grids can be used in the parallel direction than in the perpendicular direction in turbulence simulation. In this case, the field-aligned coordinates (ψ, θ, α) provide suitable coordinates to be used, where less grids can be used for θ coordinate in simulations and even some $\partial / \partial \theta$ derivatives can be neglected (high-n approximation), which simplifies the equations that need to be solved. However, this is not the most important reason why almost all gyrokinetic codes use field-aligned coordinates. The most important advantage of using field-aligned coordinates is that the stability of numerical algorthims is improved when we use coarse grids in the parallel direction because the parallel Courant condition (for explicit schemes) $\Delta t \leqslant \Delta L_\parallel / v_\parallel$ can be more easily satisfied (especially for the cases with kinetic electrons), where $\Delta L_\parallel$ is the parallel grid spacing, which is larger when coase grids are used in the parallel direction. This is also mentioned in Ref. [14] and it seems to be right from my experiences of testing several algorithm but a strict test is needed to verify this. This can also be undersood in the following way: the coarse parallel grid automatically filters out physically irrelevant but numerically problematic high-$k_\parallel$ modes, permitting much longer time steps for explicit time stepping, in both particle and fluid codes[9].

Using Eq. (277), the definition of α in Eq. (310) can be written as

$$\alpha \;=\; \phi - \int_{\theta_{\mathrm{ref}}}^{\theta} \frac{\mathbf{B} \cdot \nabla \phi}{\mathbf{B} \cdot \nabla \theta} \, d\theta \tag{316}$$

$$=\; \phi - \int_{\theta_{\mathrm{ref}}}^{\theta} \hat{q} \, d\theta, \tag{317}$$

where $\hat{q} = \mathbf{B} \cdot \nabla \phi / \mathbf{B} \cdot \nabla \theta$ is the local safety factor. For later use, define $\bar{\delta} = \int_{\theta_{\mathrm{ref}}}^{\theta} \hat{q} \, d\theta$, then $\alpha = \phi - \bar{\delta}$.

12.2 Field-aligned coordinates in GEM[5] and GENE[10] codes

In GEM[5] and GENE[10] codes, the field-aligned coordinates (x, y, z) are defined by

$$x = r - r_0, \tag{318}$$

$$y = \alpha \frac{r_0}{q_0}, \tag{319}$$

$$z = \theta q_0 R_0, \tag{320}$$

where r is an arbitrary flux surface label with length dimension, which is often chosen in GEM to be the minor radius of a magnetic surface in the midplane. Here r_0 and R_0 are constant quantities of length dimension, r_0 is the minor radius of a reference magnetic surface (usually corresponding to the center of the radial simulation box), R_0 is the major radius of the magnetic axis, q_0 is the safety factor value on the $r = r_0$ surface. The constant length $q_0 R_0$ introduced in the definition of z is to make z approximately correspond to the length along the field line in the large-aspect ratio limit. The constant length r_0 / q_0 introduced in the definition of y is to make y coresponds to the arc-length in the poloidal plane traced by a field line when its usual toroidal angle increment $\Delta \phi$ is α. This explanation makes y look like a poloidal coordinate whereas y is actually a toroidal coordinate. Assume that our simulation box is a toroidal wedge with $\Delta \alpha = 2\pi / n$, where n is an integer, then the fundamental toroidal mode number is equal to n and the fundamental wavenumber in y direction, k_y, is written as

$$k_y \equiv \frac{2\pi}{\Delta y} = \frac{2\pi}{\frac{r_0}{q_0} \Delta \alpha} = \frac{n q_0}{r_0}. \tag{321}$$

For modes with $k_\parallel \approx 0$, we have $m \approx n q_0$, where m is the usual poloidal mode number in (ψ, θ, ϕ) coordinates. In this case, the above expression is written as

$$k_y \approx \frac{m}{r_0}, \tag{322}$$

which indicates that k_y equals to the poloidal wavenumber $k_\theta = m / r_0$. Some authors call k_y or k_θ by the name "binormal wavenumber", which is not an appropriate name in my opinion. Some authors call y the binormal direction, which is also an inappropriate name since neither ∇y or $\partial \mathbf{r} / \partial y$ is along the binormal direction $\mathbf{B}_0 \times \nabla \psi$.

12.3 Visualization of grids in field aligned coordinates

I am developing a fully kinetic ions module in electromagnetic turbulence code GEM which uses field-line-following coordinates. Having an accurate understanding of the field-line-following coordinates is importan for writing the code. In this section, I try to visualize some aspects of the

coordinates relavent to the numerical implementation. The directions of the covariant basis vectors of (ψ, θ, α) coordinates are as follows:

$$\frac{\partial \mathbf{r}}{\partial \alpha}\Big|_{\psi,\theta} \longrightarrow \text{usual toroidal direction } (\hat{\boldsymbol{\phi}}), \tag{323}$$

$$\frac{\partial \mathbf{r}}{\partial \theta}\Big|_{\psi,\alpha} \longrightarrow \text{field line direction}, \mathbf{B}/B, \tag{324}$$

$$\frac{\partial \mathbf{r}}{\partial \psi}\Big|_{\theta,\alpha} \longrightarrow \text{combination of the usual radial and toroidal direction} \tag{325}$$

Here $\partial \mathbf{r}/\partial \psi|_{\theta,\alpha}$ is a combination of the usual radial and toroidal direction, which needs some clarification. Note that, for nonzero magnetic shear (i.e., $q'(\psi) \neq 0$) and $\theta \neq 0$, the usual toroidal angle ϕ is changing when changing ψ while holding θ and the generalized toroidal angle α fixed. This is given by Eq. (316), i.e.,

$$\phi = \alpha + \int_0^\theta \frac{\mathbf{B} \cdot \nabla \phi}{\mathbf{B} \cdot \nabla \theta} \, d\theta \approx \alpha + q(\psi)\theta, \tag{326}$$

where the second equality becomes exact if θ is the straight-field-line poloidal angle defined in Sec. 7.3.4. Figure 15b shows how the usual toroidal angle ϕ changes when we change ψ while holding θ and α fixed.
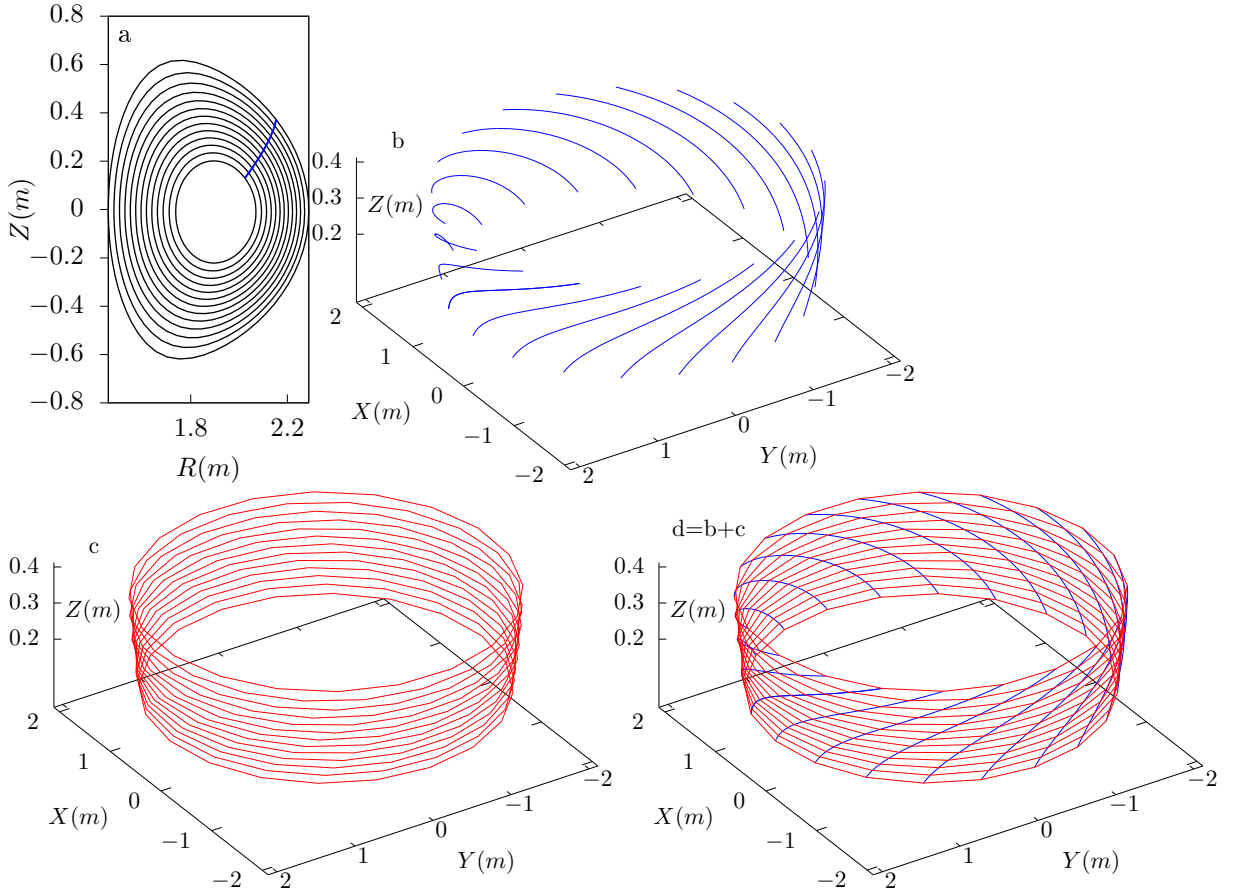
Figure 15. (a): A θ contour on $\phi = 0$ plane. Here $\theta = 9 \times 2\pi/63$. This is the direction of $\partial \mathbf{r}/\partial \psi|_{\theta,\phi}$. (b): ψ coordinate lines in (ψ, θ, α) coordinates ($\partial \mathbf{r}/\partial \psi|_{\theta,\alpha}$ is tangent to these lines) on the isosurface of $\theta = 9 \times 2\pi/63$. Here different lines correspond to different values of α. (c): α coordinate lines ($\partial \mathbf{r}/\partial \alpha|_{\psi,\theta}$ is tangent to these lines), which are along the usual toroidal direction $\hat{\boldsymbol{\phi}}$. (d): Grids on the isosurface of $\theta = 9 \times 2\pi/63$, where the red lines are α coordinate lines while the blue lines are ψ coordinate lines. Magnetic field from EAST discharge #59954@3.03s.

The relation $\phi \approx \alpha + q(\psi)\theta$ given by Eq. (326) indicates that the toroidal shift along $\partial \mathbf{r}/\partial \psi|_{\alpha,\theta}$ for a radial change form ψ_1 to ψ_2 is given by $(q(\psi_2) - q(\psi_2))\theta$, which is large for large magnetic shear or on θ isosurface with larger value of θ. An example for this is shown in Fig. 16 for $\theta = 19 \times 2\pi/63$, where $\partial \mathbf{r}/\partial \psi|_{\alpha,\theta}$ has larger toroidal shift than that in Fig. 15 for $\theta = 9 \times 2\pi/63$.
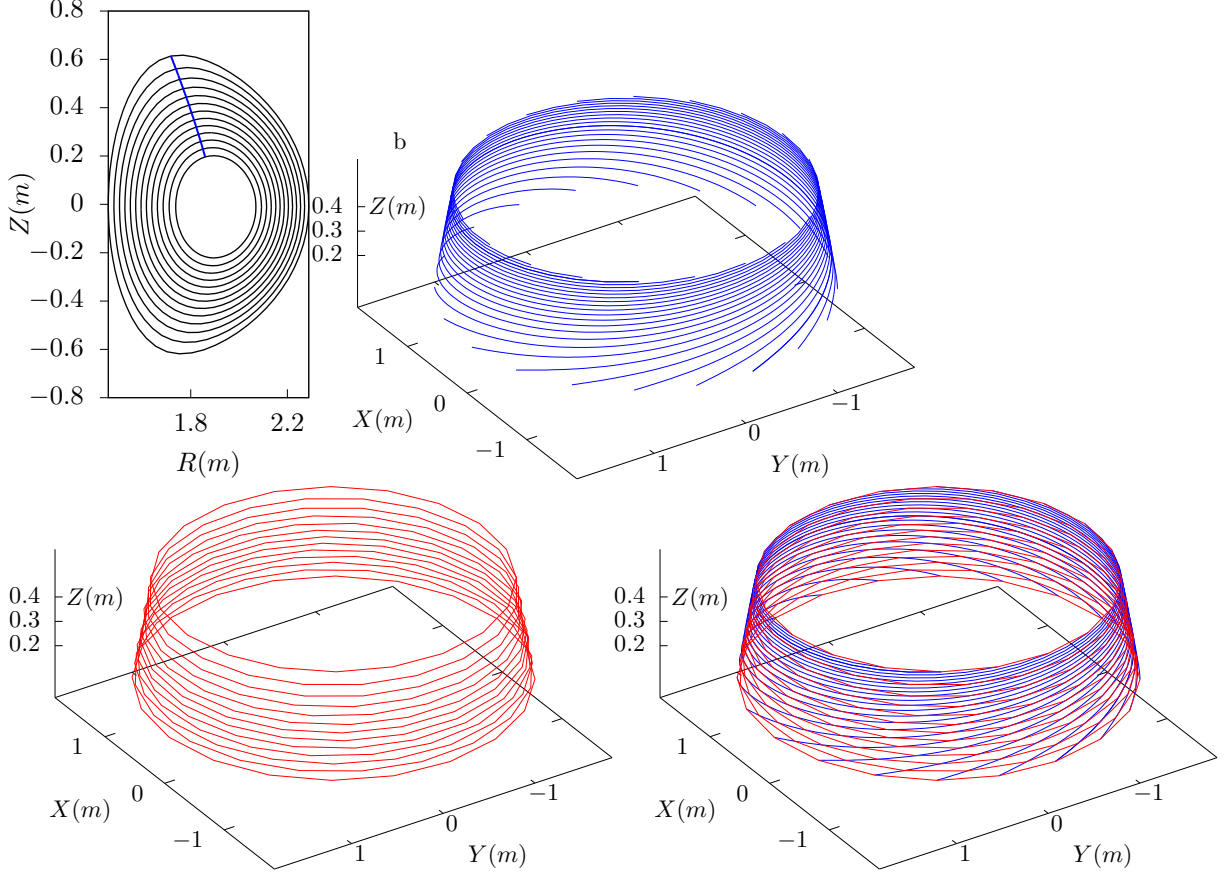
Figure 16. (a) $\theta = 19 \times 2\pi/63$ contour on $\phi = 0$ plane, $\partial \mathbf{r}/\partial \psi$ lines (upper left) and $\partial \mathbf{r}/\partial \alpha$ lines (upper right) on isosurface of $\theta = 19 \times 2\pi/63$. $\partial \mathbf{r}/\partial \alpha$ lines are identical with $\partial \mathbf{r}/\partial \phi$ lines. Lower left: Grids on the isosurface of $\theta = 19 \times 2\pi/63$, which are the combinations of $\partial \mathbf{r}/\partial \psi$ lines and $\partial \mathbf{r}/\partial \alpha$ lines.

The $\partial \mathbf{r}/\partial \psi|_{\theta,\alpha}$ lines can be understood from another perspective. Examine a family of magnetic field lines that start from the low-field-side midplane ($\theta = 0$) with the same toroidal angle $\phi = \phi_1$ but different radial coordinates. These starting points all have the same value of α, which is equal to ϕ. When following these field lines to another isosurfce of θ, the intersecting points of these field lines with the θ isosurface will trace out one $\partial \mathbf{r}/\partial \psi|_{\theta,\alpha}$ line. Examine another family of magnetic field lines similar to the above but with the starting toroidal angle $\phi = \phi_2$. They will trace out another $\partial \mathbf{r}/\partial \psi|_{\theta,\alpha}$ line on the θ isosurface. Continue the process, we finally get those lines in Fig. 15b and Fig. 16b.

12.3.1 Radial wavenumber in field-aligned coordinates (ψ, θ, α)

For a harmonic in $(\psi,\ \theta,\ \phi)$ coordinates given by $A(\psi,\ \theta,\ \phi) = \exp(i\,k_\psi\psi + im\theta + in\phi)$, the radial wave number is k_ψ. Let us calculate the corresponding radial wavenumber $k_\psi^\star$ in the new coordinates (ψ, θ, α), which is defined by

$$k_\psi^\star = \frac{\partial \text{phase}}{\partial \psi}\bigg|_{\theta,\alpha}, \tag{327}$$

where the phase is given by $\text{phase} = k_\psi\psi + m\theta + n\phi$. Then the above expression is written as

$$
\begin{aligned}
k_\psi^\star &= \frac{\partial(k_\psi\psi + m\theta + n\phi)}{\partial \psi}\bigg|_{\theta,\alpha} \\
&= k_\psi + n\frac{\partial \phi}{\partial \psi}\bigg|_{\theta,\alpha}
\end{aligned}
\tag{328}
$$

Using Using $\phi \approx \alpha + q(\psi)\theta$, the above expression is written as

$$k_\psi^\star = k_\psi + nq'\theta, \tag{329}$$

where $q' = dq/d\psi$. This result indicates that, compared with the radial wavenumber in coordinate system (ψ, θ, ϕ), the radial wavenumber in the new coordinate system (ψ, θ, α) has an increament $n\theta q'$. For nonzero magnetic shear $(q' \neq 0)$ and nonzero poloidal location $(\theta \neq 0)$, the increament $n\theta q'$ can be large for modes with toroidal mode number $n \gg 1$. Then we need to use more radial grid number (compared what is needed in (ψ, θ, ϕ) coordinates) to resolve the radial variation. This is one of disadvantage of using field-aligned coordinates. If the saving associated with using less parallel grid number outweights the cost associated with using more radial grid number, we obtain a net saving in using the field-aligned coordinates.

Let us examine how many ψ grid points are needed to resolve the ψ dependence in (ψ, θ, α) coordinates on the high-field side $(\theta = \pi)$. Assume $k_\psi \approx 0$, then $k_\psi^\star$ at $\theta = \pi$ is given by $k_\psi^\star = n\pi q'$. The corresponding wave-length is given by $\lambda_\psi^\star = 2\pi/k_\psi^\star$. The grid spacing $\Delta\psi$ should be less than half of this wave-length (sampling theorem). Then the grid number should satisfy that

$$N_\psi^\star = \frac{L_\psi}{\Delta\psi} \geqslant \frac{L_\psi}{\lambda_\psi^\star/2} = nq'L_\psi, \tag{330}$$

where L_ψ is the radial width of the computational domain.

The number of Fourier harmonics that need to be included is given by

$$N_{k_\psi^\star} = \frac{k_\psi^\star}{2\pi/L_\psi} = \frac{nq'L_\psi}{2}. \tag{331}$$

For DIII-D cyclone base case, choose the radial coordinate ψ as r. At the radial location $\psi = r_0 = 0.24m$, $q_0 = 1.4$, $\hat{s}_0 = 0.78$, then $q_0' = s_0 q_0/r_0 = 4.5 m^{-1}$. Then $N_r^\star = n \times 0.45$ for the radial width $L_r = 0.10m$.

Figure 17 plots $\partial\mathbf{r}/\partial\psi|_{\theta,\alpha}$ lines on the $\theta = 0, 2\pi$ isosurfaces, which are chosen to be on the low-field-side midplane. On $\theta = 0$ surface, $\partial\mathbf{r}/\partial\psi|_{\theta,\alpha}$ lines are idential to $\partial\mathbf{r}/\partial\psi|_{\theta,\phi}$ lines. On $\theta = 2\pi$ surface, each $\partial\mathbf{r}/\partial\psi|_{\theta,\alpha}$ line has large ϕ shift. In old version of my code, $\theta = 0, 2\pi$ surfaces are chosen as the θ cuts (in the new version $\theta = [-\pi, \pi]$). A connection condition for the perturbations

is needed between these two surfaces. This connection condition is discussed in Sec. 12.3.2.
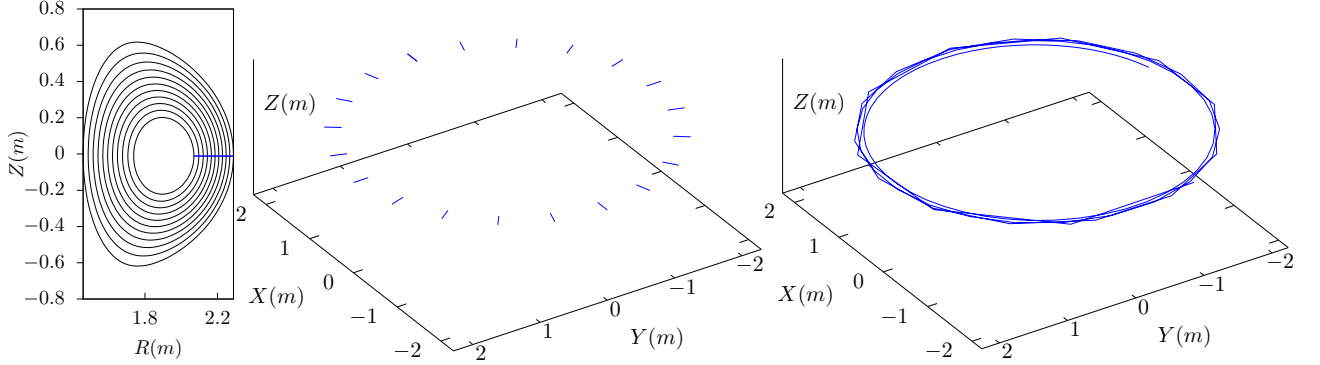

Figure 17. (a) $\theta = 0$ contour (blue line) in $\phi = 0$ plane; (b) a series of $\partial \mathbf{r} / \partial \psi |_{\theta, \alpha}$ curves (with $\alpha_j = j 2\pi / 20$, $j = 0, 1, 2, ..., 20$) on $\theta = 0$ isosurface, (c) a single $\partial \mathbf{r} / \partial \psi |_{\theta, \alpha}$ curve (with $\alpha = 0$) on $\theta = 2\pi$ isosurface. This curve finish about 4 torodial loops because $(q_{\max} - q_{\min}) 2\pi = (5.56 - 1.79) \times 2\pi \approx 4 \times 2\pi$. The radial range is $\psi = 0.2 \rightarrow 0.9$, where ψ is the normalized poloidal magnetic flux. Magnetic field from EAST discharge #59954@3.03s (gfile g059954.003030 provided by Hao BaoLong).

12.3.2 Periodic conditions of physical quantity along θ and α in field-line-following coordinates (ψ, θ, α)

Since (ψ, θ, ϕ) and $(\psi, \theta + 2\pi, \phi)$ correspond to the same spatial point, a real space continuous quantity f expressed in terms of coordinates (ψ, θ, ϕ), i.e., $f = f(\psi, \theta, \phi)$, must satisfy the following periodic condtions along θ:

$$f(\psi, \theta + 2\pi, \phi) = f(\psi, \theta, \phi). \tag{332}$$

Since (ψ, θ, ϕ) and $(\psi, \theta, \phi + 2\pi)$ correspond to the same spatial point, f must satisfy the following periodic condtions along ϕ:

$$f(\psi, \theta, \phi + 2\pi) = f(\psi, \theta, \phi). \tag{333}$$

Since (ψ, θ, α) and $(\psi, \theta, \alpha + 2\pi)$ correspond to the same spatial point, a real space continuous quantity g expressed in terms of field-line-following coordinates (ψ, θ, α), i.e., $g = g(\psi, \theta, \alpha)$, must satisty the following peroidic condition along α:

$$g(\psi, \theta, \alpha + 2\pi) = g(\psi, \theta, \alpha). \tag{334}$$

However, $P_1 = (\psi, \theta, \alpha)$ and $P_2 = (\psi, \theta + 2\pi, \alpha)$ are not usually corresponding to the same spatial point. In fact, equation (316) implies, for point P_1, its toroidal angle ϕ_1 is given by

$$\phi_1 = \alpha + \int_0^\theta \frac{\mathbf{B} \cdot \nabla \phi}{\mathbf{B} \cdot \nabla \theta} \, d\theta, \tag{335}$$

while for point P_2, its toroidal angle ϕ_2 is given by

$$\phi_2 = \alpha + \int_0^{\theta + 2\pi} \frac{\mathbf{B} \cdot \nabla \phi}{\mathbf{B} \cdot \nabla \theta} \, d\theta = \phi_1 + 2\pi q, \tag{336}$$

i.e., ϕ_1 and ϕ_2 are different by $2\pi q$. From this, we know that (ψ, θ, α) and $(\psi, \theta + 2\pi, \alpha - 2\pi q)$ correspond to the same spatial point. Therefore we have the following periodic condtion:

$$g(\psi, \theta, \alpha) = g(\psi, \theta + 2\pi, \alpha - 2\pi q), \tag{337}$$

or equivalently

$$g(\psi, \theta + 2\pi, \alpha) = g(\psi, \theta, \alpha + 2\pi q). \tag{338}$$

12.3.3 Numerical implementation of periodic condition (337)

For the fully kinetic ion module of GEM code that I am developing, θ is chosen in the range $[0 : 2\pi]$.

The condition (337) imposes the following boundary condition:

$$g(\psi, 2\pi, \alpha) = g(\psi, 0, \alpha + 2\pi q). \tag{339}$$

If α is on a grid, $\alpha + 2\pi q$ is usually not on a grid. Therefore, to get the value of $g(\psi, 0, \alpha + 2\pi q)$, an interpolation of the discrete date over the generalized toroidal angle α (or equivalently ϕ) is needed, as is shown in Fig. 18.
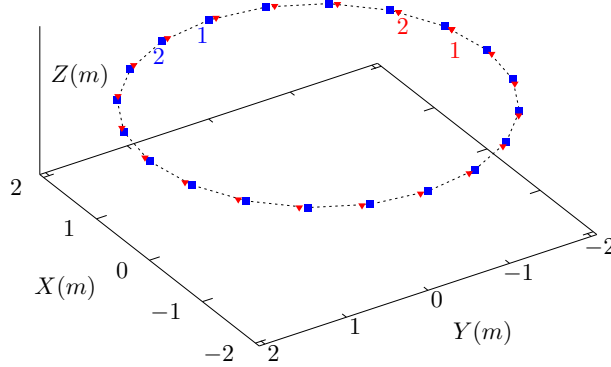

Figure 18. Twenty magnetic field lines (on $\psi = 0.2$ magnetic surface) sarting at differnt toroidal angle (blue points) on the midplane ($\theta = 0$) go a full poloidal loop (i.e., $\Delta\theta = 2\pi$), arriving at a toroidal angle (red points) which are different from their respective starting toroidal angle. The field values on the red points can be obtained by interpolating the field values on the blue points. The safety factor of the magnetic surface $q = 1.79$. Magnetic field from EAST discharge #59954@3.03s.

12.3.4 α contours on a magnetic surface

Figure 19 compares a small number of ϕ contours and α contours on a magnetic surface.
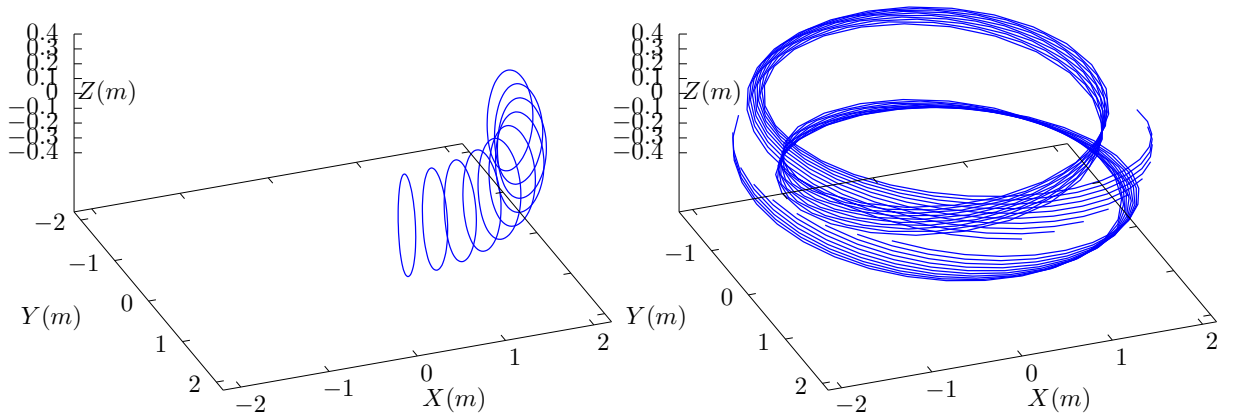
Figure 19. Comparison between a series of ϕ contours (left) and a series of α contours (right) on a magnetic surface. Here the values of ϕ are $\phi_j = \alpha_j = (j-1)2\pi/4/(10-1)$ with $j = 1, 2, ..., 10$, i.e., only $1/4$ of the full torus. The values of α contours are $\alpha_j = (j-1)2\pi/4/(10-1)$ with $j = 1, 2, ..., 10$, i.e., only $1/4$ of the full range 2π. Every ϕ and α contours start from the lower-field-side midplane and go one full poloidal loop. Magnetic field from EAST discharge #59954@3.03s.

As is shown in the left panel of Fig. 19, with ϕ fixed, an θ curve reaches its starting point when θ changes from zero to 2π. However, as shown in the right panel of Fig. 19, with α fixed, an θ curve (i.e. a magnetic field line) does not necessarily reach its starting point when θ changes from zero to 2π. There is a toroidal shift, $2\pi q$, between the starting point and ending point. Therefore there is generally no periodic condition along θ since q is not always an integer. A mixed periodic condition involves both θ and α is given in (337).

In field-line-following coordinates (ψ, θ, α), a toroidal harmonic of a physical perturbation can be written as

$$\delta A(\psi, \theta, \alpha) = \delta A_0(\psi)\cos(m'\theta + n\alpha + \alpha_0) \tag{340}$$

where n is the toroidal mode number, m', which is not necessary an integer, is introduced to describe the variation along a field line. The periodic condition given by Eq. (337) requires that

$$\cos(m'\theta + n\alpha + \alpha_0) = \cos[m'(\theta + 2\pi) + n(\alpha - 2\pi q) + \alpha_0], \tag{341}$$

To satisfy the above condition, we can choose

$$m'2\pi - n2\pi q = N2\pi, \tag{342}$$

where N is an arbitrary integer, i.e.,

$$m' = N + nq. \tag{343}$$

We are interested in perturbation with a slow variation along the field line direction (i.e., along $\partial \mathbf{r}/\partial\theta|_{\psi,\alpha}$) and thus we want the value of m' to be small. One of the possible small values given by expression (343) is to choose $N = n \times \text{NINT}((q_{\max} + q_{\min})/2)$, so that m' is given by

$$m' = nq - n \times \text{NINT}\left(\frac{q_{\max} + q_{\min}}{2}\right), \tag{344}$$

where NINT is a function that return the nearest integer of its argument, $q_{\max}$ and $q_{\min}$ is the maximal and minimal value of the safety factor in the radial region in which we are interested. [In the past, I choose $m'(\psi) = nq - \text{NINT}(nq)$. However, $m'(\psi)$ in this case is not a continuous function of ψ and thus is not physical.] This form is used to set the initial density perturbation in the fully kinetic code I am developing. Note that m' in Eq. (344) depends on the radial coordinate ψ through $q(\psi)$. Also note that m' here is differnt from the poloidal mode number m in (ψ, θ, ϕ) coordinate system. It is ready to show that the perturbation given by Eq. (340) with $m' \sim 1$ and $n \gg 1$ has large poloidal mode number m when expressed in (ψ, θ, ϕ) coordinates. [Proof: Expression (340) can be written as

$$\delta A = \delta A_0(\psi)\cos[m'\theta + n(\phi - \bar{\delta}(\psi, \theta)) + \alpha_0] \tag{345}$$

If θ is the staight-field-line poloidal angle in (ψ, θ, ϕ) coordinate system, then $\bar{\delta}(\psi, \theta) = q\theta$ and the above eqaution is written as

$$\delta A = \delta A_0(\psi)\cos[(m' - nq)\theta + n\phi + \alpha_0],$$

which indicates the poloidal mode number m in (ψ, θ, ϕ) coordinates is given by $m = m' - nq$. For the case with $m' \sim 1$ and $n \gg 1$, m is much larger than one.]

[Since α contours are magnetic field lines, they span out the 3D shape of the magnetic surface when there are enough numbe of α contours on a magnetic surface, as is shown by the right-panel of Fig. 20.
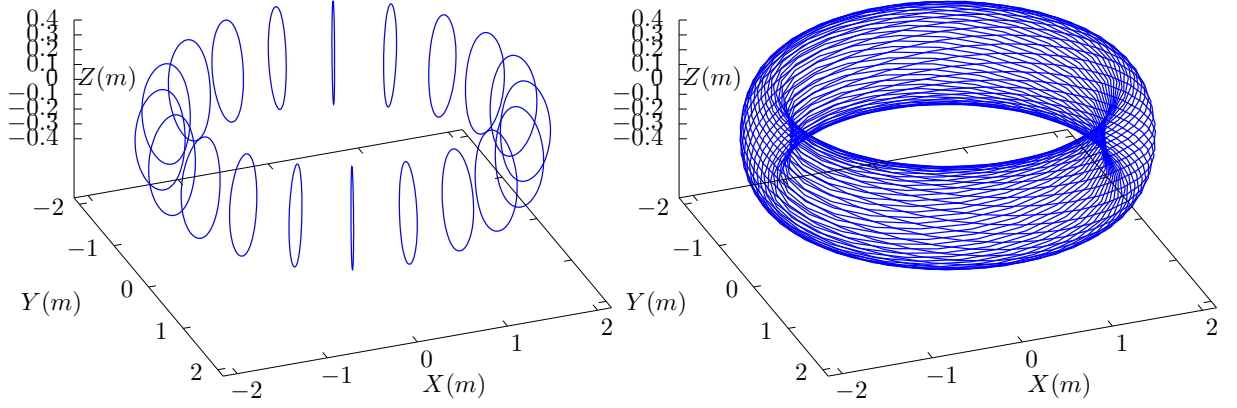
Figure 20. Comparison between a series of ϕ contours(left) and a series of α contours (left) on a magnetic surface. The α contours correspond to magnetic field lines. Here the α values of adjacent α contours differ by $d\alpha = 2\pi/20$ and each α contour goes one full poloidal loop. Magnetic field from EAST discharge #59954@3.03s.

12.3.5 α contours in a toroidal annulus

Figure 21 compares the ϕ coordinate surface of (ψ, θ, ϕ) coordinates with the α coordinate surface of (ψ, θ, α) coordinates.
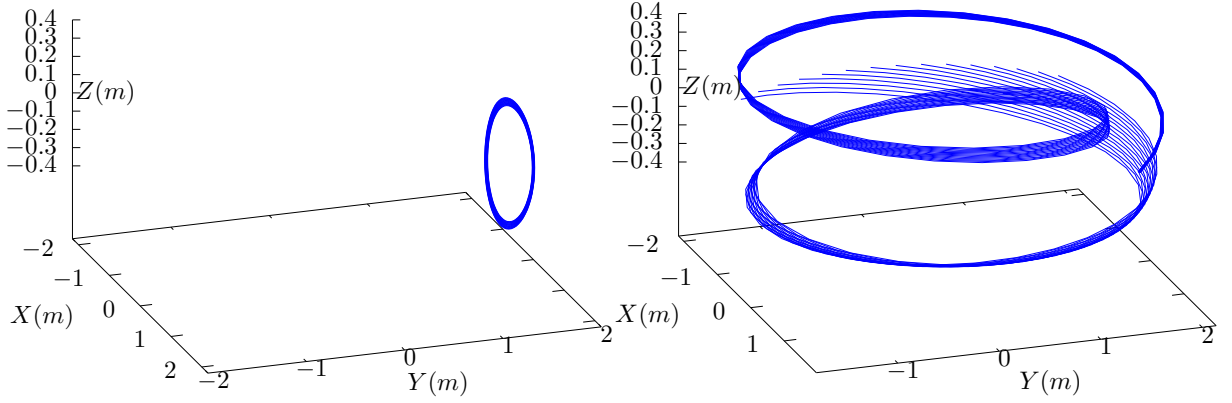
Figure 21. Comparison between isosurface of $\phi = 2\pi/8$ (projection of magnetic field lines onto $\phi = 2\pi/8$ plane) and isosurface of $\alpha = 2\pi/8$. The α isosurface is made of a family of contours of $\alpha = 2\pi/8$, which are all magnetic field lines. These field lines are traced by starting from a series of points on the low-field-side midplane ($\theta = 0$) at different radial locations and the field lines are followed by a complete poloidal loop. The radial range is given by $\psi_N \in [0.4: 0.5]$, where ψ_N is the normalized poloidal magnetic flux. Magnetic field from EAST discharge #59954@3.03s.
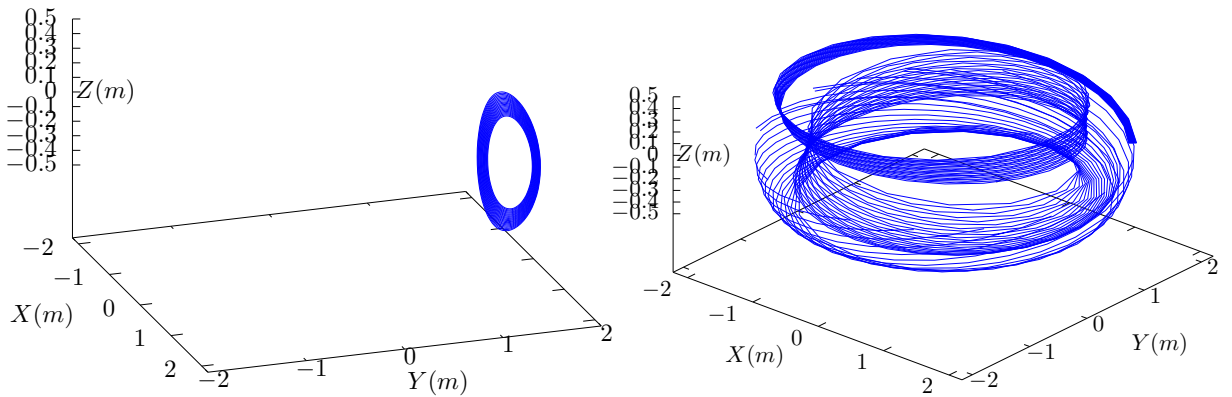
Figure 22. The same plot as in Fig. 21 but with a larger radial range. $\psi_N \in [0.4: 0.7]$, where ψ_N is the normalized poloidal magnetic flux.
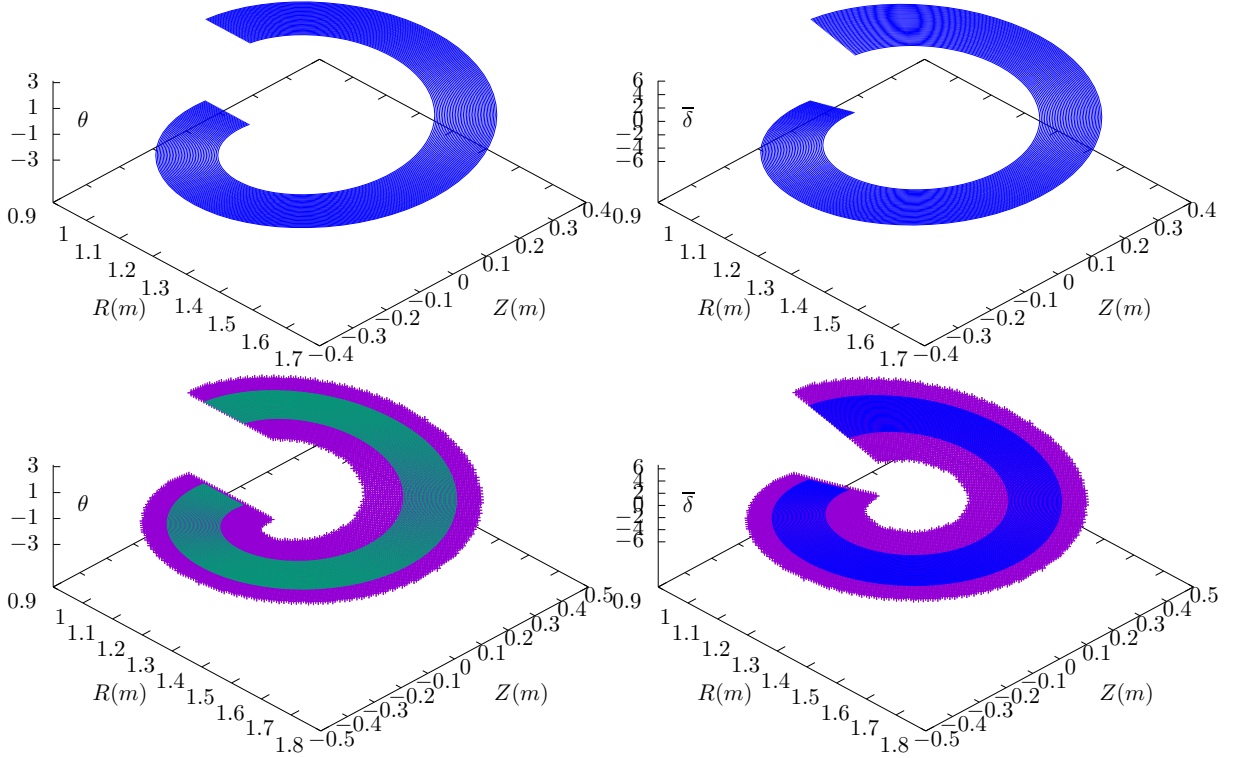
Figure 23. The value of θ and $\bar{\delta}$ on an annulus in the poloidal plane (R, Z). Upper panel: using magnetic coordinates, Lower panel: comparison with the results computed in cylindricall coordinates. $\bar{\delta} = \int_0^\theta \hat{q}\, d\theta$. Both θ and $\bar{\delta}$ are discontinuous at the θ cut, which is chosen on the high-field-side in this case.

12.4 Field-line-following mesh in gyrokinetic turbulence simulation codes

Most gyrokinetic simulation codes in magnetic fusion community use field-line-following coordinates in constructing spatial mesh. The mesh is conceptually generated by the following three steps: (1) selecting some initial points; (2) tracing out magnetic-field-lines passing through these points; (3) choose the intersecting points of these field-lines with a series of chosen surfaces as the final grid-points. The initial points and the chosen surfaces used to obtain the intersecting points differ among varisous codes and thus the resulting mesh differs. Next, let us discuss some examples.

12.4.1 Mesh in GENE, GYRO, and GEM codes

Given the definition of (ψ, θ) coordinates, choose toroidally symmetrical points (can be a toroidal wedge) in $\theta = 0$ plane (this plane is usually chosen to be the low-field-side midplane). And then trace out the magnetic-field-lines passing through these points for one poloidal circuit (usually chosen in the range $\theta \in [-\pi, \pi]$) and record the intersection points of these field-lines with various $\theta = \text{const}$ planes. These points form the 3D mesh of GENE, GYRO, and GEM codes. The 3D grids of this type are sometimes called "flux tube grids". Note that the grids in $\theta = -\pi$ plane usually do not coinside those in $\theta = +\pi$ plane due to the toroidal shift arising when the safety factor is irational. Interpolation

can be used to map physical variables defined on grids in $\theta = -\pi$ plane to those in $\theta = +\pi$ plane.

12.4.2 Mesh in GTC and GTS codes[16]

Given the definition of (ψ, θ) coordinates on the poloidal plane, 2D grid-points can be chosen on $\phi = 0$ poloidal plane based on (ψ, θ) coordinates. And then trace out the magnetic-field-lines starting from these points for one toroidal circuit and record the intersection points of these field-lines with $\phi_j = j\Delta\phi$ poloidal planes, where $j = 1, 2, ..., N_t$, $\Delta\phi = 2\pi / N_t$. It is obvious that the resulting mesh are not toroidally symmetrical. And also the grids on $\phi = 0$ plane differ from thos on $\phi = 2\pi$. Iterpolation can be used to mapping physical variables defined on $\phi = 0$ grids to those on $\phi = 2\pi$ grids. In this case, the number of "toroidal grids" N_t (i.e., the number of poloidal planes) is actually the number of grids in the parallel direction within one toroidal circuit.

12.4.3 Mesh in XGC1 code

XGC1 can handle the region outside of the LCFS. Here we only discuss the region inside the LCFS. On each radial location, select one point on $\phi = 0$ plane and trace out the magnetic field line starting form this point for one poloidal circuit and record the intersection points of this field-line with $\phi_j = j\Delta\phi$ poloidal planes, where $j = 1, 2, ..., N_t$, $\Delta\phi = 2\pi / N_t$. For the case $q > 1$, one magnetic-field-line will have more than one intersection points on some poloidal planes. Repeat tracing the field line for each radial location. Then project (toroidally) all the intersection points on different poloidal planes to a single poloidal plane and rotate (toroidally) these 2D grids to define a 3D mesh that are toroidally symmetrical.

12.5 Numerical verification of the field-aligned coordinates

The generalized toroidal angle α is numerically calculated in my code. To verify $\mathbf{B} \cdot \nabla\alpha = 0$ along a magnetic field-line, figure 24 plots the values of α along a magnetic field line, which indicates that α is constant. This indicates the numerical implementation of the field-aligned coordinates is correct.
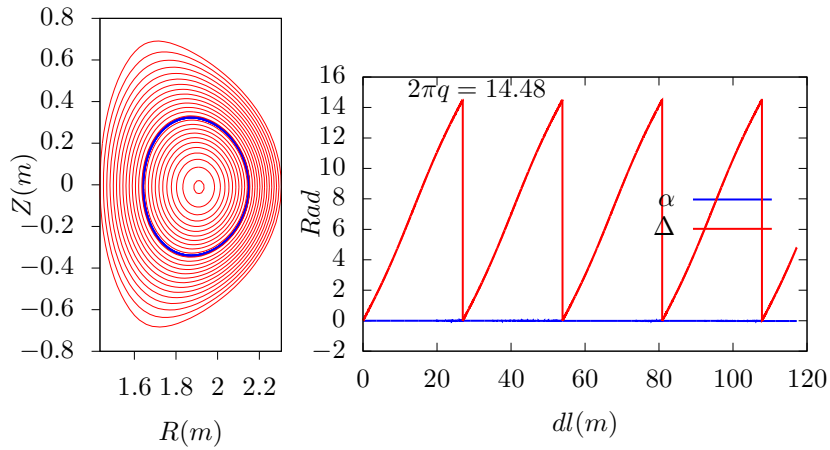

Figure 24. Left: Projection of a field line on the poloidal plane. Right: the value of Δ and α along the magnetic field line. Here α is defined by $\alpha = \phi - \Delta$, where ϕ is the usual cylindrical toroidal angle and $\Delta = \int_0^\theta \frac{\mathbf{B} \cdot \nabla\phi}{\mathbf{B} \cdot \nabla\theta} \, d\theta$,

12.6 Some discussions

The fact $\mathbf{B} \cdot \nabla\alpha = 0$ implies that α is constant along a magnetic field line. At first glance, a magnetic line on an irrational surface seems to sample all the points on the surface. This seems to indicate that α is a flux surface label for irrational surface. However, α must be a non-flux-surface-function

so that it can provide a suitable toroidal coordinate. I had once been confused by this conflict for a long time. The key point to resolve this confusion is to realize that it is wrong to say there is only one magnetic line on an irrational surface, i.e. it is wrong to say a magnetic line on an irrational surface samples all the points on the surface. There are still infinite number of magnetic field lines that can not be connected with each other on an irrational surface. Then the fact $\mathbf{B} \cdot \nabla \alpha = 0$ does not imply that α must be the same on these different magnetic field lines. In fact, although $\mathbf{B} \cdot \nabla \alpha = 0$, the gradient of α on a flux-surface along the perpendicular (to $\mathbf{B}$) direction is nonzero, i.e., $\mathbf{B} \times \nabla \Psi \cdot \nabla \alpha \neq 0$. [Proof:

$$
\begin{aligned}
\mathbf{B} \times \nabla \Psi \cdot \nabla \alpha &= \nabla \Psi \times \nabla \alpha \cdot \mathbf{B} \\
&= B^2
\end{aligned}
\tag{346}
$$

which is obviously nonzero.] This indicates that α is not constant on a flux-surface.

In (ψ, θ, ϕ) coordinates, $\nabla \phi$ is perpendicular to $\nabla \psi$. However, in field-line-following coordinates (ψ, θ, α), $\nabla \alpha$ is not perpendicular to $\nabla \psi$. Therefore $\nabla \alpha$ is not along the binormal direction $\mathbf{B} \times \nabla \psi$.

(check** may be wrong, In the practical use of the field-aligned coordinates, the θ coordinate, which is along the magnetic field line, can not be infinite, i.e., we can not follow a magnetic field for infinite distance. It must be truncated into a finite interval.

[check** may be wrong. **Next, I explain the practical use of the field-aligned coordinates in the flux-tube turbulence simulations. The flux-tube means a region that is in the vicinity of a magnetic line and follows the magnetic field line. On every magnetic surface, we follow the magnetic field line for a distance longer than the $2\pi / k_{\|\min}$, where $k_{\|\min}$ is the smallest parallel wave number included in the simulation.

may be wrong check**The perpendicular width of the flux-tube is determined by the width of α coordinate, which is chosen so that the perpendicular width of the flux tube on a magnetic surface is much larger than the perpendicular wavelength of the turbulence. Then we can use the periodic condition at $\alpha = \alpha_{\min}$ and $\alpha = \alpha_{\max}$ where $[\alpha_{\min}, \alpha_{\max}]$ is the width of α coordinate chosen by us. The radial range of the flux tube is chosen to be much larger than the largest radial wavelength of the turbulence. The radial profiles of all the equilibrium quantities are assumed to be constant and the effects of the radial gradient of the equilibrium quantities enter the model through the drive terms in the gyro-kinetic equation.**]

By the way, note that $(\mathbf{B} \cdot \nabla \alpha)/(\mathbf{B} \cdot \nabla \theta) = 0$, i.e., the magnetic field lines are straight with zero slope on (θ, α) plane.

12.6.1 Expression of $\nabla \alpha$

Next, let us calculate the gradient of the generalized toroidal angle α, which is defined by Eq. (316), i.e., $\alpha = \phi - \bar{\delta}$, where $\bar{\delta} = \int_0^\theta \hat{q} d\theta = \int_0^\theta \mathbf{B} \cdot \nabla \phi / (\mathbf{B} \cdot \nabla \theta) \, d\theta$. The gradient of α is written as

$$
\begin{aligned}
\nabla \alpha &= \nabla \phi - \nabla \bar{\delta} \\
&= \frac{\hat{\phi}}{R} - \frac{\partial \bar{\delta}}{\partial \psi} \nabla \psi - \frac{\partial \bar{\delta}}{\partial \theta} \nabla \theta.
\end{aligned}
\tag{347}
$$

Using Eqs. (227) and (228), the above expression is written as

$$
\begin{aligned}
\nabla \alpha &= \frac{\hat{\phi}}{R} + \frac{\partial \bar{\delta}}{\partial \psi} \frac{R}{\mathcal{J}} (Z_\theta \hat{\mathbf{R}} - R_\theta \hat{\mathbf{Z}}) - \frac{\partial \bar{\delta}}{\partial \theta} \frac{R}{\mathcal{J}} (Z_\psi \hat{\mathbf{R}} - R_\psi \hat{\mathbf{Z}}) \\
&= \frac{\hat{\phi}}{R} + \left(\frac{\partial \bar{\delta}}{\partial \psi} \frac{R}{\mathcal{J}} Z_\theta - \frac{\partial \bar{\delta}}{\partial \theta} \frac{R}{\mathcal{J}} Z_\psi \right) \hat{\mathbf{R}} + \left(\frac{\partial \bar{\delta}}{\partial \theta} \frac{R}{\mathcal{J}} R_\psi - \frac{\partial \bar{\delta}}{\partial \psi} \frac{R}{\mathcal{J}} R_\theta \right) \hat{\mathbf{Z}}.
\end{aligned}
\tag{348}
$$

Then

$$
\nabla \psi \cdot \nabla \alpha = \left(-\frac{R}{\mathcal{J}} Z_\theta \hat{\mathbf{R}} + \frac{R}{\mathcal{J}} R_\theta \hat{\mathbf{Z}} \right) \cdot \left[\frac{\hat{\phi}}{R} + \left(\frac{\partial \bar{\delta}}{\partial \psi} \frac{R}{\mathcal{J}} Z_\theta - \frac{\partial \bar{\delta}}{\partial \theta} \frac{R}{\mathcal{J}} Z_\psi \right) \hat{\mathbf{R}} + \left(\frac{\partial \bar{\delta}}{\partial \theta} \frac{R}{\mathcal{J}} R_\psi - \frac{\partial \bar{\delta}}{\partial \psi} \frac{R}{\mathcal{J}} R_\theta \right) \hat{\mathbf{Z}} \right]
$$

$$= -\frac{R}{\mathcal{J}}Z_\theta\left(\frac{\partial\overline{\delta}}{\partial\psi}\frac{R}{\mathcal{J}}Z_\theta - \frac{\partial\overline{\delta}}{\partial\theta}\frac{R}{\mathcal{J}}Z_\psi\right) + \frac{R}{\mathcal{J}}R_\theta\left(\frac{\partial\overline{\delta}}{\partial\theta}\frac{R}{\mathcal{J}}R_\psi - \frac{\partial\overline{\delta}}{\partial\psi}\frac{R}{\mathcal{J}}R_\theta\right). \tag{349}$$

$$\nabla\alpha\cdot\nabla\theta = \left[\frac{\hat{\phi}}{R} + \left(\frac{\partial\overline{\delta}}{\partial\psi}\frac{R}{\mathcal{J}}Z_\theta - \frac{\partial\overline{\delta}}{\partial\theta}\frac{R}{\mathcal{J}}Z_\psi\right)\hat{\mathbf{R}} + \left(\frac{\partial\overline{\delta}}{\partial\theta}\frac{R}{\mathcal{J}}R_\psi - \frac{\partial\overline{\delta}}{\partial\psi}\frac{R}{\mathcal{J}}R_\theta\right)\hat{\mathbf{Z}}.\right]\cdot\left(\frac{R}{\mathcal{J}}Z_\psi\hat{\mathbf{R}} - \frac{R}{\mathcal{J}}R_\psi\hat{\mathbf{Z}}\right)$$

$$= \left(\frac{\partial\overline{\delta}}{\partial\psi}\frac{R}{\mathcal{J}}Z_\theta - \frac{\partial\overline{\delta}}{\partial\theta}\frac{R}{\mathcal{J}}Z_\psi\right)\frac{R}{\mathcal{J}}Z_\psi - \left(\frac{\partial\overline{\delta}}{\partial\theta}\frac{R}{\mathcal{J}}R_\psi - \frac{\partial\overline{\delta}}{\partial\psi}\frac{R}{\mathcal{J}}R_\theta\right)\frac{R}{\mathcal{J}}R_\psi. \tag{350}$$

Note that $\partial\overline{\delta}/\partial\psi$ is discontinuous across the θ cut.
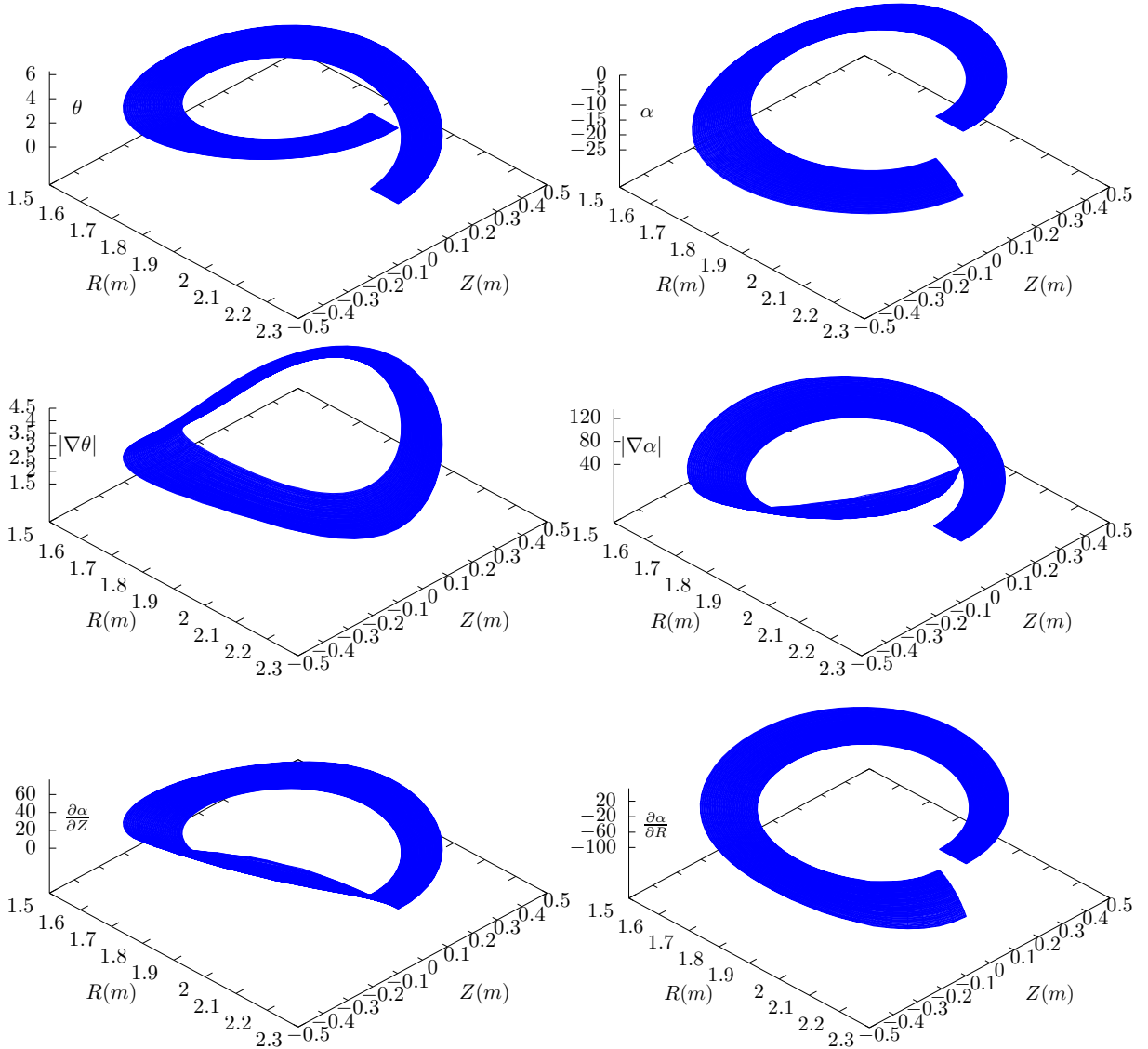
Figure 25. The value of θ, α and their gradients on an annulus on the poloidal plane (R, Z). Note that $\nabla\theta$ is single-valued while $\partial\alpha/\partial R$ and $\nabla\alpha$ are multi-valued and thus there is a jump near the branch cut when a single branch is chosen.
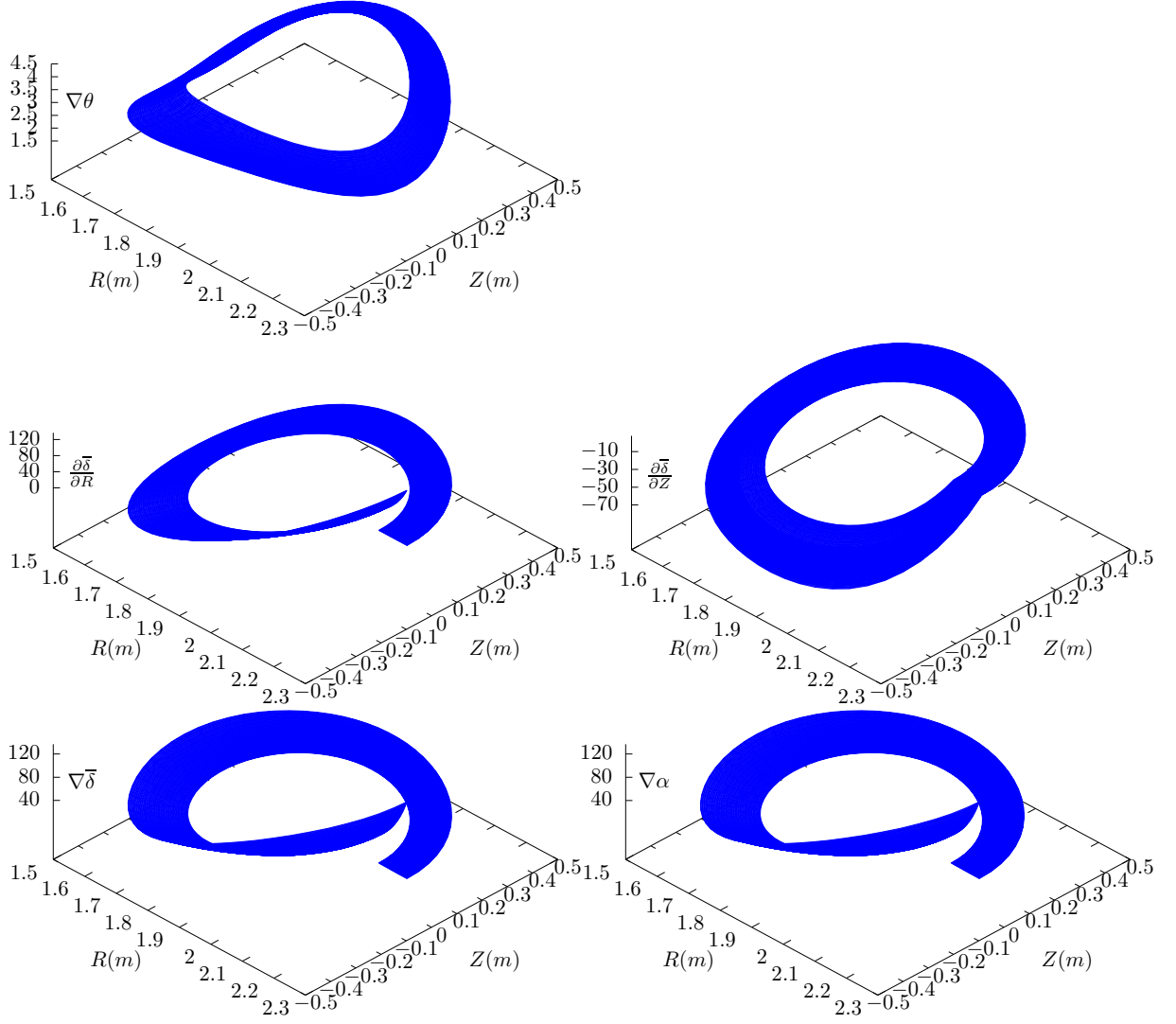
Figure 26. The same as Fig. 25, but gradients are computed in cylindrical coordinates. $\bar{\delta} = \int_0^\theta \hat{q} d\theta$, $\alpha = \phi - \bar{\delta}$. The results agrees with those of Fig. 25, which provides the confidence in the correctness of the numerical implemenation.

12.6.2 Binormal wavenumber

Let us introduce the binormal wavenumber, which is frequently used in presenting turbulence simulation results. Define the binormal direction $\mathbf{s}$ by

$$\mathbf{s} = \frac{\mathbf{B} \times \nabla \Psi}{|\mathbf{B} \times \nabla \Psi|},$$

which is a unit vector lying on a magnetic surface and perpendicular to $\mathbf{B}$. The binormal wavenumber of a mode is defined by

$$k_{bn} = \mathbf{s} \cdot \nabla p, \tag{351}$$

where p is the phase of the mode. Consider a mode given by $\exp(ik_\psi\psi + im\theta - in\zeta)$, then the phase $p = k_\psi\psi + m\theta - n\zeta$. Then k_{bn} is written as

$$
\begin{aligned}
k_{bn} &= \frac{\mathbf{B} \times \nabla\Psi}{|\mathbf{B} \times \nabla\Psi|} \cdot \nabla(k_\psi\psi + m\theta - n\zeta) \\
&= \frac{\mathbf{B} \times \nabla\Psi}{|\mathbf{B} \times \nabla\Psi|} \cdot \nabla(m\theta - n\zeta), \tag{352}
\end{aligned}
$$

where the radial phase $k_\psi\psi$ does not appear since $\mathbf{B} \times \nabla\Psi \cdot \nabla\psi = 0$. The above expression can be further written as

$$
\begin{aligned}
k_{bn} &= \frac{1}{|\mathbf{B} \times \nabla\Psi|}[m\mathbf{B} \times \nabla\Psi \cdot \nabla\theta - n\mathbf{B} \times \nabla\Psi \cdot \nabla\zeta] \\
&= \frac{1}{|\mathbf{B} \times \nabla\Psi|}[m\mathbf{B} \cdot \nabla\Psi \times \nabla\theta - n\mathbf{B} \cdot \nabla\Psi \times \nabla\zeta] \\
&= \frac{n\mathbf{B} \cdot}{|\mathbf{B} \times \nabla\Psi|}\left[\frac{m}{n}\nabla\Psi \times \nabla\theta - \nabla\Psi \times \nabla\zeta\right]. \tag{353}
\end{aligned}
$$

Equation (353) is the general expression of the binormal wavenumber. On the resonant surface of the mode, i.e., $q(\psi) = m/n$, then the above expression is written as

$$
k_{bn} = \frac{n\mathbf{B} \cdot}{|\mathbf{B} \times \nabla\Psi|}[q\nabla\Psi \times \nabla\theta - \nabla\Psi \times \nabla\zeta]. \tag{354}
$$

Using Eq. (282), i.e., $\mathbf{B} = -(\nabla\zeta \times \nabla\Psi + q\nabla\Psi \times \nabla\theta)$, the above expression is written as

$$
\begin{aligned}
k_{bn} &= \frac{-n\mathbf{B} \cdot}{|\mathbf{B} \times \nabla\Psi|}\mathbf{B} \\
&= -n\frac{B}{|\nabla\Psi|}
\end{aligned}
$$

Using $B_p = |\nabla\Psi|/R$, the above equation is written

$$
k_{bn} = -n\frac{B}{RB_p} \tag{355}
$$

which indicates the binormal wavenumber generally depends on the poloidal angle. For large aspect-ratio tokamak, we have $B_\phi \approx B$, $q \approx B_\phi r/(B_p R)$. Then Eq. (355) is written

$$
k_{bn} \approx -\frac{nq}{r}, \tag{356}
$$

which indicates the binormal wavenumber are approximately indepenent of the poloidal angle. Since $m = nq$ on a resonant surface, the above equation is written $|k_{bn}| \approx m/r$, which is the usual poloidal wave number. Due to this relation, the binormal wavenumber k_{bn} is often called the poloidal wavenumber and denoted by k_θ in papers on tokamak turbulence. In the GENE code, y coordinate is defined by $y = \alpha r_0/q_0$. Then the k_y of a mode of toroidal mode number n is given by $k_y = 2\pi/\lambda_y$ where $\lambda_y = \lambda_\alpha r_0/q_0$ and $\lambda_\alpha = 2\pi/n$. Then k_y is written as $k_y = nq_0/r_0$, which is similar to the binormal defined above. For this reason, k_y of GENE code is also called binormal wavevector, which is in fact not reasonable because neither $\partial\mathbf{r}/\partial y$ or ∇y is along the binormal direction.

12.7   Other expressions for magnetic field

The expression of the magnetic field in Eq. (283) can be rewritten in terms of the flux function Ψ_p and Ψ_t discussed in Sec. 10.2. Equation (283) is

$$
\mathbf{B} = \nabla\Psi \times \nabla\zeta + q\nabla\theta \times \nabla\Psi, \tag{357}
$$

which, by using Eq. (255), i.e., $\nabla\Psi = \nabla\Psi_p/(2\pi)$, is rewritten as

$$\mathbf{B} = \frac{1}{2\pi}(\nabla\zeta \times \nabla\Psi_p + q\nabla\Psi_p \times \nabla\theta), \tag{358}$$

which, by using Eq. (262), i.e., $q = d\Psi_t/d\Psi_p$, is further written as

$$\mathbf{B} = \frac{1}{2\pi}(\nabla\zeta \times \nabla\Psi_p + \nabla\Psi_t \times \nabla\theta). \tag{359}$$

12.8 Expression of current density

Let us derive the contravariant expression for the current density. Using

$$\mu_0\mathbf{J} = \nabla \times \mathbf{B},$$

along with magnetic field expression (185) and the curl formula (147), we obtain

$$\mu_0\mathbf{J} = -\left[\left(\Psi'\frac{\mathcal{J}}{R^2}|\nabla\psi|^2\right)_\psi + \left(\Psi'\frac{\mathcal{J}}{R^2}\nabla\psi\cdot\nabla\theta\right)_\theta\right]\nabla\psi \times \nabla\theta - g'\nabla\phi \times \nabla\psi, \tag{360}$$

which is the contravariant form of the current density vector. Next, for later use, calculate the parallel current. By using Eqs. (185) and (360), the parallel current density is written as

$$
\begin{aligned}
\mu_0\mathbf{J}\cdot\mathbf{B} &= -\left[\left(\Psi'\frac{\mathcal{J}}{R^2}|\nabla\psi|^2\right)_\psi + \left(\Psi'\frac{\mathcal{J}}{R^2}\nabla\psi\cdot\nabla\theta\right)_\theta\right]g\nabla\psi \times \nabla\theta\cdot\nabla\phi - g'\left(-\Psi'\frac{\mathcal{J}}{R^2}|\nabla\psi|^2\right)\nabla\phi \times \\
&\quad \nabla\psi\cdot\nabla\theta \\
&= -\left[\left(\Psi'\frac{\mathcal{J}}{R^2}|\nabla\psi|^2\right)_\psi + \left(\Psi'\frac{\mathcal{J}}{R^2}\nabla\psi\cdot\nabla\theta\right)_\theta\right]g\mathcal{J}^{-1} + g'\mathcal{J}^{-1}\Psi'\frac{\mathcal{J}}{R^2}|\nabla\psi|^2 \\
&= -g^2\mathcal{J}^{-1}\left\{\frac{1}{g}\left(\Psi'\frac{\mathcal{J}}{R^2}|\nabla\psi|^2\right)_\psi + \frac{1}{g}\left(\Psi'\frac{\mathcal{J}}{R^2}\nabla\psi\cdot\nabla\theta\right)_\theta - \frac{g'}{g^2}\Psi'\frac{\mathcal{J}}{R^2}|\nabla\psi|^2\right\} \\
&= -g^2\mathcal{J}^{-1}\left[\left(\frac{\Psi'}{g}\frac{\mathcal{J}}{R^2}|\nabla\psi|^2\right)_\psi + \left(\frac{\Psi'}{g}\frac{\mathcal{J}}{R^2}\nabla\psi\cdot\nabla\theta\right)_\theta\right].
\end{aligned}
\tag{361}
$$

13 Concentric-circular magnetic configuration with given safety factor profile

Assume magnetic surfaces of a magnetic configuration are known and is given by

$$R(r,\theta) = R_0 + r\cos\theta, \tag{362}$$

and

$$Z(r,\theta) = r\sin\theta, \tag{363}$$

where (r,θ) are two parameters and r is the label of magnetic surfaces (i.e., $\partial\Psi/\partial\theta|_r = 0$). The above parametric equations specify a series of concentric-circular magnetic surfaces.

Assume the toroidal field function $g(r) = RB_\phi$ is given. Then the toroidal magnetic field is determined by $B_\phi = g/R$. Futhere assume the safety factor profile $q(r)$ is given, then the magnetic field is fully determined. Next, let us derive the explicit form of the poloidal magnetic field $\mathbf{B}_p$, which is given by

$$\mathbf{B}_p = \nabla\Psi \times \nabla\phi = \frac{1}{2\pi}\nabla\Psi_p \times \nabla\phi, \tag{364}$$

which involves the poloidal magnetic flux Ψ_p. Therefore our task is to express the poloidal magnetic flux Ψ_p in terms of q and g. Using $q(r) = d\Psi_t/d\Psi_p$, we obtain

$$d\Psi_p = \frac{1}{q}d\Psi_t,$$

Integrate the above equation over r, we obtain

$$\int_0^r d\Psi_p = \int_0^r \frac{1}{q}d\Psi_t, \tag{365}$$

which an be written as

$$\Psi_p(r) - \Psi_p(0) = \int_0^r \frac{1}{q(r)}d\left(\int_0^r \int_{-\pi}^{\pi} B_\phi r\, dr\, d\theta\right), \tag{366}$$

where use has been made of $\Psi_t = \int_0^r \int_{-\pi}^{\pi} B_\phi r\, dr\, d\theta$. Using $B_\phi = g/R$ and $R = R_0 + r\cos\theta$, the above equation is written

$$\Psi_p(r) - \Psi_p(0) = \int_0^r \frac{1}{q(r)}d\left(\int_0^r \int_{-\pi}^{\pi} \frac{g}{R_0 + r\cos\theta}r\, dr\, d\theta\right) \tag{367}$$

Using `maxima` (an open-source computer algebra system), the above integration over θ can be performed analytically, giving

$$\int_{-\pi}^{\pi} \frac{1}{R_0 + r\cos\theta}d\theta = \frac{2\pi}{\sqrt{R_0^2 - r^2}}. \tag{368}$$

Using this, equation (367) is written as

$$\Psi_p(r) - \Psi_p(0) = \int_0^r \frac{1}{q(r)}d\left(\int_0^r \frac{2\pi g r}{\sqrt{R_0^2 - r^2}}dr\right), \tag{369}$$

which can be simplified as

$$\Psi_p(r) - \Psi_p(0) = \int_0^r \frac{1}{q(r)}\frac{2\pi g r}{\sqrt{R_0^2 - r^2}}dr. \tag{370}$$

This is what we want—the expression of the poloidal magnetic flux in terms of q and g. Using this, the poloidal magnetic field in Eq. (364) is written as

$$\begin{aligned}
\mathbf{B}_p &= \frac{\nabla r \times \nabla\phi}{2\pi}\frac{\partial}{\partial r}\left(\int_0^r \frac{1}{q(r)}\frac{2\pi g r}{\sqrt{R_0^2 - r^2}}dr\right) \\
&= \nabla r \times \nabla\phi\frac{1}{q(r)}\frac{g r}{\sqrt{R_0^2 - r^2}}.
\end{aligned} \tag{371}$$

[Using the formulas $\nabla r = -\frac{R}{\mathcal{J}}(Z_\theta\hat{\mathbf{R}} - R_\theta\hat{\mathbf{Z}})$ and $\mathcal{J} = R(R_\theta Z_r - R_r Z_\theta)$, where $\mathcal{J}$ is the Jacobian of the (r, θ, ϕ) coordinates, we obtain $\mathcal{J} = -Rr$ and $\nabla r = \cos\theta\hat{\mathbf{R}} + \sin\theta\hat{\mathbf{Z}}$, $\nabla\phi = \hat{\phi}/R$. Then Eq. (371) is written as

$$\mathbf{B}_p = \frac{\cos\theta\hat{\mathbf{Z}} - \sin\theta\hat{\mathbf{R}}}{R}\frac{1}{q(r)}\frac{g r}{\sqrt{R_0^2 - r^2}} \tag{372}$$

This is the explicit form of the poloidal magnetic field in terms of g and q. The magnitude of $\mathbf{B}_p$ is written as

$$B_p = \frac{1}{(R_0 + r\cos\theta)} \frac{1}{q(r)} \frac{gr}{\sqrt{R_0^2 - r^2}} \tag{373}$$

Note that both B_p and B_ϕ depend on the poloidal angle θ.]

I use Eq. (370) to compute the 2D data of Ψ ($\Psi = \Psi_p/2\pi$) on the poloidal plane when creating a numerical G-eqdsk file for the above equilibrium (Fortran code is at /home/yj/project_new/circular_configuration_with_q_given).

Assume that the poloidal plasma current is zero, then $g(r) = RB_\phi$ is a constant independent of r. This is always assumed by those authors who use concentric-circular configuration but is seldom explicitly mentioned.

13.1 Is the above B divergence-free?

Since the above field is derived from the general form given by Eq. (8), it is guaranteed that the field is divergence-free. In case of any doubt, let us directly check this. Write $\mathbf{B}$ as

$$\mathbf{B} = B^{(1)}\mathcal{J}\nabla\theta \times \nabla\phi + B^{(2)}\mathcal{J}\nabla\phi \times \nabla r + B^{(3)}\mathcal{J}\nabla r \times \nabla\theta, \tag{374}$$

where $\mathcal{J}$ is the Jacobian of (r, θ, ϕ) coordinates; $B^{(1)}$, $B^{(2)}$, and $B^{(3)}$ are given by

$$B^{(1)} = \mathbf{B} \cdot \nabla r \tag{375}$$

$$B^{(2)} = \mathbf{B} \cdot \nabla\theta \tag{376}$$

$$B^{(3)} = \mathbf{B} \cdot \nabla\phi \tag{377}$$

Use $\mathbf{B}_p$ given by (371), then $B^{(1)}$, $B^{(2)}$, and $B^{(3)}$ are written as

$$B^{(1)} = 0, \tag{378}$$

$$B^{(2)} = -\frac{1}{\mathcal{J}} \frac{1}{q(r)} \frac{g_0 r}{\sqrt{R_0^2 - r^2}}, \tag{379}$$

and

$$B^{(3)} = \frac{B_\phi}{R}, \tag{380}$$

respectively. Then, by using the divergence formula in (r, θ, ϕ) coordinates, $\nabla \cdot \mathbf{B}$ is written as

$$
\begin{aligned}
\nabla \cdot \mathbf{B} &= \frac{1}{\mathcal{J}}\left(\frac{\partial B^{(1)}\mathcal{J}}{\partial r} + \frac{\partial B^{(2)}\mathcal{J}}{\partial \theta} + \frac{\partial B^{(3)}\mathcal{J}}{\partial \phi} \right) \\
&= \frac{1}{\mathcal{J}}\left(0 + \frac{\partial B^{(2)}\mathcal{J}}{\partial \theta} + 0 \right) \\
&= \frac{1}{\mathcal{J}} \frac{\partial}{\partial \theta}\left(-\frac{1}{q(r)} \frac{g_0 r}{\sqrt{R_0^2 - r^2}} \right) \\
&= 0
\end{aligned}
\tag{381}
$$

i.e., $\mathbf{B}$ in this case is indeed divergence-free.

13.2 Is the above B a solution to the GS equation?

The answer is no. It is ready to verify that the poloidal magnetic flux function $\Psi = \Psi_p/2\pi$ given by Eq. (370) is not a solution to the GS equation (419) even if the plasma pressure in the GS equation is set to zero. The above expression is a solution to the GS equation in the limit of infinite aspect ratio and zero plasma pressure. The finite aspect ratio and plasma pressue requires the magnetic surfaces to have the Shafranov shift in order to satisfy the GS equation (see Sec. 14).

13.3 Explicit expression for the generalized toroidal angle

For the above magnetic field, the toroidal shift involved in the definition of the generalized toroidal angle can be expressed in simple analytical form. The toroidal shift is given by

$$\bar{\delta} = \int_0^\theta \hat{q}d\theta, \tag{382}$$

where the local safety factor $\hat{q}$ can be written as

$$\hat{q} = -\frac{g_0}{R^2}\frac{\mathcal{J}}{\Psi'}. \tag{383}$$

Using $\mathcal{J} = -Rr$ and

$$\Psi' = \frac{1}{q(r)}\frac{g_0 r}{\sqrt{R_0^2 - r^2}} \tag{384}$$

The local safety factor $\hat{q}$ in Eq. (383) is written as

$$\hat{q} = q\sqrt{R_0^2 - r^2}\frac{1}{R}. \tag{385}$$

Using this, expression (382) is written

$$\bar{\delta} = q\sqrt{R_0^2 - r^2}\int_0^\theta \frac{1}{R}\, d\theta \tag{386}$$

Assume $\theta \in (-\pi, \pi)$, then the integration $\int_0^\theta 1/R\, d\theta$ can be analytically performed (using maxima), yielding

$$\int_0^\theta \frac{1}{R}\, d\theta = \frac{2\arctan\left(\frac{\sin\theta(R_0 - r)}{(\cos\theta + 1)\sqrt{R_0^2 - r^2}}\right)}{\sqrt{R_0^2 - r^2}}. \tag{387}$$

Then expression (386) is written

$$\bar{\delta} = 2q\arctan\left(\frac{(R_0 - r)}{\sqrt{R_0^2 - r^2}}\tan\left(\frac{\theta}{2}\right)\right), \tag{388}$$

where use has been made of $\sin\theta/(\cos\theta + 1) = \tan(\theta/2)$. Using this, the generalized toroidal angle can be written as

$$\begin{aligned} \alpha &= \phi - \bar{\delta} \\ &= \phi - 2q\arctan\left(\frac{(R_0 - r)}{\sqrt{R_0^2 - r^2}}\tan\left(\frac{\theta}{2}\right)\right). \end{aligned} \tag{389}$$

The results given by the formula (388) are compared with the results from my code that assumes a general numerical configuration. The results from the two methods agree with each other, as is shown in Fig. 27, which provides confidence in both the analytical formula and the numerical code.
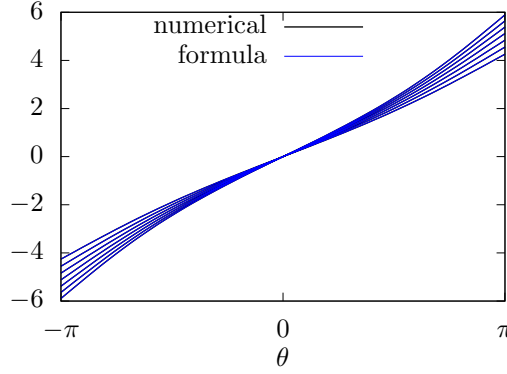
Figure 27. The results of $\bar{\delta} = \int_0^\theta \hat{q}\, d\theta$ computed by using formula (388) and the numerical code agree with each other. The different lines correspond to values of $\bar{\delta}$ on different magnetic surfaces. In the numerical code, two kinds of poloidal angles can be selected: one is the equal-volume poloidal angle, and another is the equal-arch-length angle. Make sure that the latter is selected when doing the comparison because the the poloidal angle θ appearing in the analytical formula is the equal-arc-length poloidal angle.

In passing, we note that the straight-field-line poloidal angle θ_f can also be considered to be defined by

$$\alpha = \phi - q\theta_f, \tag{390}$$

i.,e,

$$\theta_f = \frac{1}{q}(\phi - \alpha) = \frac{\bar{\delta}}{q}. \tag{391}$$

Then using Eq. (389), θ_f is written as

$$\theta_f = 2\arctan\left(\frac{(R_0 - r)}{\sqrt{R_0^2 - r^2}}\tan\left(\frac{\theta}{2}\right)\right), \tag{392}$$

which agrees with Eq. (A2) in Gorler's paper[10].

13.4 Metric elements

Let $\psi = r$ and define $h^{\psi R} = \nabla\psi \cdot \hat{\mathbf{R}}$, $h^{\alpha R} = \nabla\alpha \cdot \hat{\mathbf{R}}$, etc. Explicit expressions for these elements can be written as

$$
\begin{aligned}
h^{\psi R} &= \nabla\psi \cdot \hat{\mathbf{R}} \\
&= \nabla r \cdot \hat{\mathbf{R}} \\
&= -\frac{R}{\mathcal{J}}(Z_\theta\hat{\mathbf{R}} - R_\theta\hat{\mathbf{Z}}) \cdot \hat{\mathbf{R}} \\
&= -\frac{R}{\mathcal{J}}Z_\theta \\
&= \cos\theta
\end{aligned}
\tag{393}
$$

$$
\begin{aligned}
h^{\psi Z} &= \nabla\psi \cdot \hat{\mathbf{Z}} \\
&= \nabla r \cdot \hat{\mathbf{Z}} \\
&= -\frac{R}{\mathcal{J}}(Z_\theta\hat{\mathbf{R}} - R_\theta\hat{\mathbf{Z}}) \cdot \hat{\mathbf{Z}} \\
&= \frac{R}{\mathcal{J}}R_\theta \\
&= \sin\theta
\end{aligned}
$$

$$
\begin{aligned}
h^{\psi\phi} &= \nabla\psi \cdot \hat{\boldsymbol{\phi}} \\
&= 0
\end{aligned}
$$

$$h^{\theta R} = \nabla\theta \cdot \hat{\mathbf{R}}$$
$$= \frac{R}{\mathcal{J}}(Z_\psi\hat{\mathbf{R}} - R_\psi\hat{\mathbf{Z}}) \cdot \hat{\mathbf{R}}$$
$$= \frac{R}{\mathcal{J}}Z_\psi$$
$$= -\frac{1}{r}\sin\theta$$

$$h^{\theta Z} = \nabla\theta \cdot \hat{\mathbf{Z}}$$
$$= \frac{R}{\mathcal{J}}(Z_\psi\hat{\mathbf{R}} - R_\psi\hat{\mathbf{Z}}) \cdot \hat{\mathbf{Z}}$$
$$= -\frac{R}{\mathcal{J}}R_\psi$$
$$= \frac{1}{r}\cos\theta$$

$$h^{\theta\phi} = \nabla\theta \cdot \hat{\boldsymbol{\phi}}$$
$$= 0$$

$$h^{\alpha R} = \nabla\alpha \cdot \hat{\mathbf{R}}$$
$$= \left[\frac{\hat{\boldsymbol{\phi}}}{R} + \left(\frac{\partial\bar{\delta}}{\partial\psi}\frac{R}{\mathcal{J}}Z_\theta - \frac{\partial\bar{\delta}}{\partial\theta}\frac{R}{\mathcal{J}}Z_\psi\right)\hat{\mathbf{R}} + \left(\frac{\partial\bar{\delta}}{\partial\theta}\frac{R}{\mathcal{J}}R_\psi - \frac{\partial\bar{\delta}}{\partial\psi}\frac{R}{\mathcal{J}}R_\theta\right)\hat{\mathbf{Z}}\right] \cdot \hat{\mathbf{R}}$$
$$= \frac{\partial\bar{\delta}}{\partial\psi}\frac{R}{\mathcal{J}}Z_\theta - \frac{\partial\bar{\delta}}{\partial\theta}\frac{R}{\mathcal{J}}Z_\psi$$
$$= \frac{\partial\bar{\delta}}{\partial\psi}\frac{R}{\mathcal{J}}r\cos\theta - \frac{\partial\bar{\delta}}{\partial\theta}\frac{R}{\mathcal{J}}\sin\theta$$
$$= -\frac{\partial\bar{\delta}}{\partial\psi}\cos\theta + \frac{\partial\bar{\delta}}{\partial\theta}\frac{1}{r}\sin\theta$$
$$= -\frac{\partial\bar{\delta}}{\partial r}\cos\theta + \hat{q}\frac{1}{r}\sin\theta$$

$$h^{\alpha Z} = \nabla\alpha \cdot \hat{\mathbf{Z}}$$
$$= \left[\frac{\hat{\boldsymbol{\phi}}}{R} + \left(\frac{\partial\bar{\delta}}{\partial\psi}\frac{R}{\mathcal{J}}Z_\theta - \frac{\partial\bar{\delta}}{\partial\theta}\frac{R}{\mathcal{J}}Z_\psi\right)\hat{\mathbf{R}} + \left(\frac{\partial\bar{\delta}}{\partial\theta}\frac{R}{\mathcal{J}}R_\psi - \frac{\partial\bar{\delta}}{\partial\psi}\frac{R}{\mathcal{J}}R_\theta\right)\hat{\mathbf{Z}}\right] \cdot \hat{\mathbf{Z}}$$
$$= \frac{\partial\bar{\delta}}{\partial\theta}\frac{R}{\mathcal{J}}R_\psi - \frac{\partial\bar{\delta}}{\partial\psi}\frac{R}{\mathcal{J}}R_\theta$$
$$= -\hat{q}\frac{1}{r}\cos\theta - \frac{\partial\bar{\delta}}{\partial r}\sin\theta$$

$$h^{\alpha\phi} = \frac{1}{R}. \tag{394}$$

Using expression (388), $d\bar{\delta}/dr$ can be evaluated analytically, yielding

$$\frac{d\bar{\delta}}{dr} = 2\frac{dq}{dr}\arctan\left(\frac{(R_0-r)}{\sqrt{R_0^2-r^2}}\tan\left(\frac{\theta}{2}\right)\right) + 2q\frac{1}{1+\left(\frac{(R_0-r)}{\sqrt{R_0^2-r^2}}\tan\left(\frac{\theta}{2}\right)\right)^2}\tan\left(\frac{\theta}{2}\right)\frac{d}{dr}\left[\frac{(R_0-r)}{\sqrt{R_0^2-r^2}}\right]$$

$$= 2\frac{dq}{dr}\arctan\left(\frac{(R_0-r)}{\sqrt{R_0^2-r^2}}\tan\left(\frac{\theta}{2}\right)\right) + 2q\frac{1}{1+\left(\frac{(R_0-r)}{\sqrt{R_0^2-r^2}}\tan\left(\frac{\theta}{2}\right)\right)^2}\tan\left(\frac{\theta}{2}\right)\frac{-R_0}{(R_0+r)\sqrt{R_0^2-r^2}}$$

where use has been made of

$$\frac{d}{dx}\arctan(x) = \frac{1}{1+x^2}$$

(I did not remeber this formula and I use SymPy to obtain this.) These expressions are used to benchmark the numerical code that assume general flux surface shapes. The results show that the code gives correct result when concentric circular flux surfaces are used.

Taking the θ derivative of $\bar{\delta}$, equation (388) is written as (using Sympy)

$$\frac{\partial \bar{\delta}}{\partial \theta} = 2qA\left(\frac{\tan^2\left(\frac{\theta}{2}\right)}{2} + \frac{1}{2}\right)\frac{1}{A^2\tan^2\left(\frac{\theta}{2}\right)+1} \tag{395}$$

where

$$A = \frac{(R_0 - r)}{\sqrt{R_0^2 - r^2}} \tag{396}$$

Equation (385) should be equal to $\hat{q}$ given by Eq. (385). This was verified numerically.

Taking the r derivative of Eq. (370), we obtain

$$\frac{d\Psi_P}{dr} = \frac{1}{q(r)}\frac{2\pi g_0 r}{\sqrt{R_0^2 - r^2}} \tag{397}$$

i.e.,

$$\frac{d\Psi}{dr} = \frac{1}{q(r)}\frac{g_0 r}{\sqrt{R_0^2 - r^2}}. \tag{398}$$

$$\frac{d\psi}{dr} = \frac{1}{\Psi(a) - \Psi(0)}\frac{1}{q(r)}\frac{g_0 r}{\sqrt{R_0^2 - r^2}}. \tag{399}$$
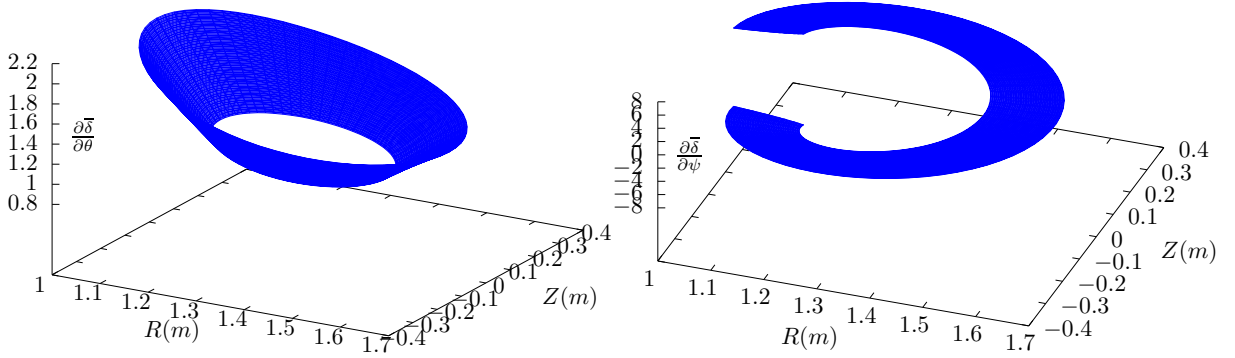
Figure 28. $\partial\bar{\delta}/\partial\theta$ and $\partial\bar{\delta}/\partial\psi$. Numerical and analytical results are plotted, which are so close to each other that they can not be distinguished by eyes. $\partial\bar{\delta}/\partial\theta$ is equal to the local safety factor $\hat{q}$. Note that $\partial\bar{\delta}/\partial\psi$ is discontinous at the θ cut, which in this case is on the high-field-side.

13.5 Safety factor profile

The magnetic shear for a concentric-circular configuration is defined by

$$\hat{s} = \frac{dq}{dr}\frac{r}{q}, \tag{400}$$

where r is the minor radius of a magnetic surface. The above expression can be re-arranged as

$$\hat{s}\frac{dr}{r} = \frac{dq}{q} \tag{401}$$

Integrating the above equation over r and assuming $\hat{s}$ is a constant, we obtain

$$\hat{s} \int_{r_0}^{r} \frac{dr}{r} = \int_{r_0}^{r} \frac{dq}{q}, \tag{402}$$

Performing the integration, the abvoe equation is written as

$$\hat{s}(\ln r - \ln r_0) = \ln q - \ln q_0, \tag{403}$$

where $q_0 = q(r_0)$. Equation (403) can be finally written as

$$q = q_0 \left(\frac{r}{r_0} \right)^{\hat{s}}. \tag{404}$$

This is a profile with a constant magnetic shear s. In Ben's toroidal ITG simulation, the following q profile is used:

$$q = q_0 + (r - r_0) q'(r_0), \tag{405}$$

with $q'(r_0) = \hat{s} q_0 / r_0$. This is a linear profile over r, with the values of q and the shear at $r = r_0$ being q_0 and $\hat{s}$, respectively.

14 Grad-Shafranov equation in (r, θ) coordinates

Consider (r, θ) coordinates, which are related to the cylindrical coordinates (R, Z) by $Z = r \sin\theta$ and $R = R_0 + r \cos\theta$, as shown in Fig. 29.
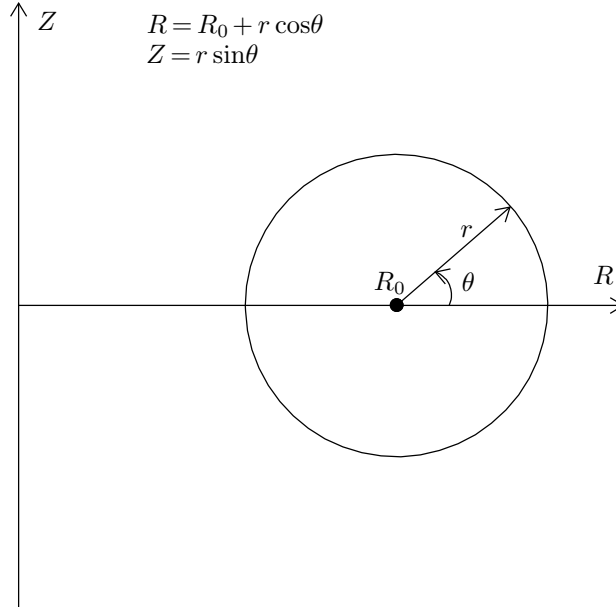
Figure 29. The relation between (r, θ) and (R, Z) coordinates.

Next, we transform the GS equation from (R, Z) coordinates to (r, θ) coordinates. Using the relations $R = R_0 + r\cos\theta$ and $Z = r\sin\theta$, we have

$$r = \sqrt{(R - R_0)^2 + Z^2} \Rightarrow \frac{\partial r}{\partial Z} = \frac{Z}{r} = \sin\theta \tag{406}$$

$$\sin\theta = \frac{Z}{\sqrt{(R - R_0)^2 + Z^2}} \Rightarrow \cos\theta\frac{\partial\theta}{\partial Z} = \frac{r - Z\frac{Z}{r}}{r^2}. \tag{407}$$

$$\Rightarrow \frac{\partial\theta}{\partial Z} = \frac{r - Z\frac{Z}{r}}{r(R - R_0)} = \frac{1 - \sin^2\theta}{R - R_0} = \frac{\cos^2\theta}{R - R_0} \tag{408}$$

$$\frac{\partial\sin\theta}{\partial Z} = \frac{r - Z\frac{Z}{r}}{r^2} = \frac{1 - \sin^2\theta}{r} = \frac{\cos^2\theta}{r} \tag{409}$$

The GS equation in (R, Z) coordinates is given by

$$\frac{\partial^2\Psi}{\partial Z^2} + R\frac{\partial}{\partial R}\left(\frac{1}{R}\frac{\partial\Psi}{\partial R}\right) = -\mu_0 R^2\frac{dP}{d\Psi} - \frac{dg}{d\Psi}g(\Psi). \tag{410}$$

The term $\partial\Psi/\partial Z$ is written as

$$\begin{aligned}
\frac{\partial\Psi}{\partial Z} &= \frac{\partial\Psi}{\partial r}\frac{\partial r}{\partial Z} + \frac{\partial\Psi}{\partial\theta}\frac{\partial\theta}{\partial Z} \\
&= \frac{\partial\Psi}{\partial r}\sin\theta + \frac{\partial\Psi}{\partial\theta}\frac{\cos^2\theta}{R - R_0}.
\end{aligned} \tag{411}$$

Using Eq. (411), $\partial^2\Psi/\partial Z^2$ is written as

$$\begin{aligned}
\frac{\partial^2\Psi}{\partial Z^2} &= \frac{\partial}{\partial Z}\left(\frac{\partial\Psi}{\partial r}\sin\theta\right) + \frac{\partial}{\partial Z}\left(\frac{\partial\Psi}{\partial\theta}\frac{\cos^2\theta}{R - R_0}\right) \\
&= \sin\theta\frac{\partial}{\partial Z}\left(\frac{\partial\Psi}{\partial r}\right) + \frac{\partial\Psi}{\partial r}\frac{\partial}{\partial Z}(\sin\theta) + \frac{\cos^2\theta}{R - R_0}\frac{\partial}{\partial Z}\left(\frac{\partial\Psi}{\partial\theta}\right) + \frac{\partial\Psi}{\partial\theta}\frac{\partial}{\partial Z}\left(\frac{\cos^2\theta}{R - R_0}\right) \\
&= \sin\theta\left(\frac{\partial^2\Psi}{\partial r^2}\sin\theta + \frac{\partial^2\Psi}{\partial r\partial\theta}\frac{\cos^2\theta}{R - R_0}\right) + \frac{\partial\Psi}{\partial r}\frac{\cos^2\theta}{r} + \frac{\cos^2\theta}{R - R_0}\left(\frac{\partial^2\Psi}{\partial\theta\partial r}\sin\theta + \frac{\partial^2\Psi}{\partial\theta^2}\frac{\cos^2\theta}{R - R_0}\right) \\
&\quad - \frac{\partial\Psi}{\partial\theta}\frac{1}{R - R_0}2\cos\theta\sin\theta\frac{\cos^2\theta}{R - R_0}
\end{aligned} \tag{412}$$

$$\frac{\partial r}{\partial R} = \frac{\partial}{\partial R}\sqrt{(R - R_0)^2 + Z^2} = \frac{R - R_0}{r} = \cos\theta \tag{413}$$

$$\sin\theta = \frac{Z}{\sqrt{(R - R_0)^2 + Z^2}}.$$

$$\cos\theta\frac{\partial\theta}{\partial R} = -Z\frac{R - R_0}{r^3}$$

$$\frac{\partial\theta}{\partial R} = -\frac{Z}{r^2}. \tag{414}$$

$$\cos\theta = \frac{R - R_0}{\sqrt{(R - R_0)^2 + Z^2}}$$

$$\frac{\partial}{\partial R}\cos\theta = \frac{r - \frac{R - R_0}{r}(R - R_0)}{r^2} = \frac{1 - \cos^2\theta}{r} = \frac{\sin^2\theta}{r} \tag{415}$$

$$
\begin{aligned}
R\frac{\partial}{\partial R}\left(\frac{1}{R}\frac{\partial \Psi}{\partial R}\right) &= R\frac{\partial}{\partial R}\left[\frac{1}{R}\left(\frac{\partial \Psi}{\partial r}\frac{\partial r}{\partial R}+\frac{\partial \Psi}{\partial \theta}\frac{\partial \theta}{\partial R}\right)\right] \\
&= R\frac{\partial}{\partial R}\left[\frac{1}{R}\left(\frac{\partial \Psi}{\partial r}\cos\theta-\frac{\partial \Psi}{\partial \theta}\frac{Z}{r^2}\right)\right] \\
&= \frac{\partial}{\partial R}\left(\frac{\partial \Psi}{\partial r}\cos\theta-\frac{\partial \Psi}{\partial \theta}\frac{Z}{r^2}\right)+R\left(\frac{\partial \Psi}{\partial r}\cos\theta-\frac{\partial \Psi}{\partial \theta}\frac{Z}{r^2}\right)\left(-\frac{1}{R^2}\right) \\
&= \left(\frac{\partial^2 \Psi}{\partial r^2}\frac{\partial r}{\partial R}+\frac{\partial^2 \Psi}{\partial r\partial \theta}\frac{\partial \theta}{\partial R}\right)\cos\theta+\frac{\partial \Psi}{\partial r}\frac{\partial}{\partial R}\cos\theta-\left(\frac{\partial^2 \Psi}{\partial \theta\partial r}\frac{\partial r}{\partial R}+\frac{\partial^2 \Psi}{\partial \theta^2}\frac{\partial \theta}{\partial R}\right)\frac{Z}{r^2}- \\
&\quad \frac{\partial \Psi}{\partial \theta}\frac{\partial}{\partial R}\left(\frac{Z}{r^2}\right)-\frac{1}{R}\left(\frac{\partial \Psi}{\partial r}\cos\theta-\frac{\partial \Psi}{\partial \theta}\frac{Z}{r^2}\right) \\
&= \left(\frac{\partial^2 \Psi}{\partial r^2}\cos\theta-\frac{\partial^2 \Psi}{\partial r\partial \theta}\frac{Z}{r^2}\right)\cos\theta+\frac{\partial \Psi}{\partial r}\frac{\sin^2\theta}{r}-\left(\frac{\partial^2 \Psi}{\partial \theta\partial r}\cos\theta-\frac{\partial^2 \Psi}{\partial \theta^2}\frac{Z}{r^2}\right)\frac{Z}{r^2}+ \\
&\quad \frac{\partial \Psi}{\partial \theta}Z\frac{1}{r^3}2\cos\theta-\frac{1}{R}\left(\frac{\partial \Psi}{\partial r}\cos\theta-\frac{\partial \Psi}{\partial \theta}\frac{Z}{r^2}\right) \\
&= \frac{\partial^2 \Psi}{\partial r^2}\cos^2\theta+\frac{\partial^2 \Psi}{\partial \theta^2}\frac{\sin^2\theta}{r^2}-2\frac{\partial^2 \Psi}{\partial r\partial \theta}\frac{Z}{r^2}\cos\theta+\frac{\partial \Psi}{\partial r}\frac{\sin^2\theta}{r}+\frac{\partial \Psi}{\partial \theta}Z\frac{1}{r^3}2\cos\theta && (416) \\
&\quad -\frac{1}{R}\left(\frac{\partial \Psi}{\partial r}\cos\theta-\frac{\partial \Psi}{\partial \theta}\frac{1}{r}\sin\theta\right) && (417)
\end{aligned}
$$

Summing the the right-hand-side of Eq. (412) and the expression on line (416) yields

$$
\frac{\partial^2 \Psi}{\partial r^2}+\frac{\partial \Psi}{\partial r}\frac{1}{r}+\frac{1}{r^2}\frac{\partial^2 \Psi}{\partial \theta^2}. \tag{418}
$$

Using these, the GS equation is written as

$$
\frac{\partial^2 \Psi}{\partial r^2}+\frac{\partial \Psi}{\partial r}\frac{1}{r}+\frac{1}{r^2}\frac{\partial^2 \Psi}{\partial \theta^2}-\frac{1}{R_0+r\cos\theta}\left(\frac{\partial \Psi}{\partial r}\cos\theta-\frac{\partial \Psi}{\partial \theta}\frac{1}{r}\sin\theta\right)=-\mu_0(R_0+r\cos\theta)^2\frac{dP}{d\Psi}-\frac{dg}{d\Psi}g(\Psi),
$$

which can be arranged in the form

$$
\left(\frac{1}{r}\frac{\partial}{\partial r}r\frac{\partial}{\partial r}+\frac{1}{r^2}\frac{\partial^2}{\partial \theta^2}\right)\Psi-\frac{1}{R_0+r\cos\theta}\left(\frac{\partial \Psi}{\partial r}\cos\theta-\frac{\partial \Psi}{\partial \theta}\frac{1}{r}\sin\theta\right)=-\mu_0(R_0+r\cos\theta)^2\frac{dP}{d\Psi}-\frac{dg}{d\Psi}g(\Psi),
$$
$$\tag{419}$$

which agrees with Eq. (3.6.2) in Wessson's book[18], where f is defined by $f=RB_\phi/\mu_0$, which is different from $g\equiv RB_\phi$ by a $1/\mu_0$ factor.

14.1 Large aspect ratio expansion

Consider the case that the boundary flux surface is circular with radius $r=a$ and the center of the cirle at $(R=R_0, Z=0)$. Consider the case $\varepsilon=a/R_0\to 0$. Expanding Ψ in the small parameter ε,

$$
\Psi=\Psi_0+\Psi_1 \tag{420}
$$

where $\Psi_0\sim O(\varepsilon^0)$, $\Psi_1\sim O(\varepsilon^1)$. Substituting Eq. (420) into Eq. (419), we obtain

$$
\frac{1}{r}\frac{\partial}{\partial r}r\frac{\partial \Psi_0}{\partial r}+\frac{1}{r}\frac{\partial}{\partial r}r\frac{\partial \Psi_1}{\partial r}+\frac{1}{r^2}\frac{\partial^2 \Psi_0}{\partial \theta^2}+\frac{1}{r^2}\frac{\partial^2 \Psi_1}{\partial \theta^2}-\frac{1}{R_0+r\cos\theta}\left(\frac{\partial \Psi_0}{\partial r}\cos\theta-\frac{\partial \Psi_0}{\partial \theta}\frac{1}{r}\sin\theta\right)-
$$
$$
\frac{1}{R_0+r\cos\theta}\left(\frac{\partial \Psi_1}{\partial r}\cos\theta-\frac{\partial \Psi_1}{\partial \theta}\frac{1}{r}\sin\theta\right)=-\mu_0(R_0+r\cos\theta)^2 P'(\Psi_0+\Psi_1)-g'(\Psi_0+\Psi_1)g(\Psi_0+\Psi_1)
$$

Multiplying the above equation by R_0^2, we obtain

$$
R_0^2\frac{1}{r}\frac{\partial}{\partial r}r\frac{\partial \Psi_0}{\partial r}+R_0^2\frac{1}{r}\frac{\partial}{\partial r}r\frac{\partial \Psi_1}{\partial r}+R_0^2\frac{1}{r^2}\frac{\partial^2 \Psi_0}{\partial \theta^2}+R_0^2\frac{1}{r^2}\frac{\partial^2 \Psi_1}{\partial \theta^2}-\frac{R_0^2}{R_0+r\cos\theta}\left(\frac{\partial \Psi_0}{\partial r}\cos\theta-\frac{\partial \Psi_0}{\partial \theta}\frac{1}{r}\sin\theta\right)-
$$
$$
\frac{R_0^2}{R_0+r\cos\theta}\left(\frac{\partial \Psi_1}{\partial r}\cos\theta-\frac{\partial \Psi_1}{\partial \theta}\frac{1}{r}\sin\theta\right)=-\mu_0 R_0^2(R_0+r\cos\theta)^2 P'(\Psi_0+\Psi_1)-R_0^2 g'(\Psi_0+\Psi_1)g(\Psi_0+
$$
$$
\Psi_1) \tag{421}
$$

Further assume the following ordering

$$R_0 \frac{\partial \Psi}{\partial r} \sim O(\varepsilon^{-1})\Psi, \tag{422}$$

and

$$\frac{\partial \Psi}{\partial \theta} \sim O(\varepsilon^0)\Psi. \tag{423}$$

Using these orderings, the order of the terms in Eq. (421) can be estimated as

$$R_0^2 \frac{1}{r} \frac{\partial}{\partial r} r \frac{\partial \Psi_0}{\partial r} \sim \frac{\Psi_0}{\varepsilon^2} \sim O(\varepsilon^{-2}) \tag{424}$$

$$R_0^2 \frac{1}{r} \frac{\partial}{\partial r} r \frac{\partial \Psi_1}{\partial r} \sim \frac{\Psi_1}{\varepsilon^2} \sim O(\varepsilon^{-1}) \tag{425}$$

$$R_0^2 \frac{1}{r^2} \frac{\partial^2 \Psi_0}{\partial \theta^2} \sim \frac{1}{\varepsilon^2} \Psi_0 \sim O(\varepsilon^{-2}) \tag{426}$$

$$R_0^2 \frac{1}{r^2} \frac{\partial^2 \Psi_1}{\partial \theta^2} \sim \frac{\Psi_1}{\varepsilon^2} \sim O(\varepsilon^{-1}) \tag{427}$$

$$\frac{R_0}{R_0 + r \cos\theta} \approx 1 - \frac{r}{R_0} \cos\theta \tag{428}$$

$$R_0 \frac{\partial \Psi_0}{\partial r} \cos\theta \sim \frac{\Psi_0}{\varepsilon} \sim O(\varepsilon^{-1}) \tag{429}$$

$$R_0 \frac{\partial \Psi_0}{\partial \theta} \frac{1}{r} \sin\theta \sim \frac{\Psi_0}{\varepsilon} \sim O(\varepsilon^{-1}) \tag{430}$$

$$R_0 \frac{\partial \Psi_1}{\partial r} \cos\theta \sim \frac{\Psi_1}{\varepsilon} = O(\varepsilon^0) \tag{431}$$

$$R_0 \frac{\partial \Psi_1}{\partial \theta} \frac{1}{r} \sin\theta \sim \frac{\Psi_1}{\varepsilon} = O(\varepsilon^0) \tag{432}$$

The leading order (ε^{-2} order) balance is given by the following equation:

$$R_0^2 \frac{1}{r} \frac{\partial}{\partial r} r \frac{\partial \Psi_0}{\partial r} + R_0^2 \frac{1}{r^2} \frac{\partial^2 \Psi_0}{\partial \theta^2} = -\mu_0 R_0^4 P'(\Psi_0) - R_0^2 g'(\Psi_0) g(\Psi_0), \tag{433}$$

It is reasonable to assume that Ψ_0 is independent of θ since Ψ_0 corresponds to the limit $a/R \to 0$. (The limit $a/R \to 0$ can have two cases, one is $r \to 0$, another is $R \to \infty$. In the former case, Ψ must be independent of θ since Ψ should be single-valued. The latter case corresponds to a cylinder, for which it is reasonable (really?) to assume that Ψ_0 is independent of θ.) Then Eq. (433) is written

$$\frac{1}{r} \frac{\partial}{\partial r} r \frac{\partial \Psi_0}{\partial r} = -\mu_0 R_0^2 P'(\Psi_0) - g'(\Psi_0) g(\Psi_0). \tag{434}$$

(My remarks: The leading order equation (434) does not correponds strictly to a cylinder equilibrium because the magnetic field $\mathbf{B} = \nabla \Psi_0 \times \nabla \phi + g \nabla \phi$ depends on θ.) The next order (ε^{-1} order) equation is

$$R_0^2 \frac{1}{r} \frac{\partial}{\partial r} r \frac{\partial \Psi_1}{\partial r} + R_0^2 \frac{1}{r^2} \frac{\partial^2 \Psi_1}{\partial \theta^2} - R_0 \frac{\partial \Psi_0}{\partial r} \cos\theta = -\mu_0 R_0^2 2 R_0 r \cos\theta P'(\Psi_0) - \mu_0 R_0^4 P''(\Psi_0) \Psi_1 - R_0^2 [g'(\Psi_0) g(\Psi_0)]' \Psi_1$$

$$R_0^2 \frac{1}{r} \frac{\partial}{\partial r} r \frac{\partial \Psi_1}{\partial r} + R_0^2 \frac{1}{r^2} \frac{\partial^2 \Psi_1}{\partial \theta^2} + \{\mu_0 R_0^4 P''(\Psi_0) + R_0^2 [g'(\Psi_0) g(\Psi_0)]'\} \Psi_1 = -\mu_0 R_0^2 2 R_0 r \cos\theta P'(\Psi_0) +$$

$$R_0 \frac{\partial \Psi_0}{\partial r} \cos\theta \tag{435}$$

$$R_0^2 \frac{1}{r} \frac{\partial}{\partial r} r \frac{\partial \Psi_1}{\partial r} + R_0^2 \frac{1}{r^2} \frac{\partial^2 \Psi_1}{\partial \theta^2} + \frac{d}{dr} \{\mu_0 R_0^4 P'(\Psi_0) + R_0^2 g'(\Psi_0) g(\Psi_0)\} \frac{dr}{d\Psi_0} \Psi_1 = -\mu_0 R_0^2 2 R_0 r \cos\theta P'(\Psi_0) +$$

$$R_0 \frac{\partial \Psi_0}{\partial r} \cos\theta \tag{436}$$

It is obvious that the simple poloidal dependence of $\cos\theta$ will satisfy the above equation. Therefore, we consider Ψ_1 of the form

$$\Psi_1 = \Delta(r)\frac{d\Psi_0(r)}{dr}\cos\theta,\tag{437}$$

where $\Delta(r)$ is a new function to be determined. Substitute this into the Eq. (), we obtain an equation for $\Delta(r)$,

$$R_0^2\frac{1}{r}\quad\frac{d}{dr}\left(r\frac{d\Psi_0}{dr}\quad\frac{d\Delta}{dr}\quad+r\,\Delta\frac{d^2\Psi_0}{dr^2}\right)\quad-\quad R_0^2\frac{1}{r^2}\quad\Delta\frac{d\Psi_0(r)}{dr}\quad+\quad\frac{d}{dr}\{\mu_0 R_0^4 P'(\Psi_0)\quad+$$

$$R_0^2 g'(\Psi_0)g(\Psi_0)\}\frac{dr}{d\Psi_0}\Delta\frac{d\Psi_0(r)}{dr} = -\mu_0 R_0^2 2R_0 r\,P'(\Psi_0) + R_0\frac{d\Psi_0}{dr}\tag{438}$$

$$R_0^2\frac{1}{r}\quad\frac{d}{dr}\left(r\frac{d\Psi_0}{dr}\quad\frac{d\Delta}{dr}\quad\right)\quad+\quad R_0^2\frac{1}{r}\quad\frac{d}{dr}\left(r\,\Delta\frac{d^2\Psi_0}{dr^2}\right)\quad-\quad R_0^2\frac{1}{r^2}\quad\Delta\frac{d\Psi_0(r)}{dr}\quad+\quad\frac{d}{dr}\{\mu_0 R_0^4 P'(\Psi_0)\quad+$$

$$R_0^2 g'(\Psi_0)g(\Psi_0)\}\Delta = -\mu_0 R_0^2 2R_0 r\,P'(\Psi_0) + R_0\frac{d\Psi_0}{dr}\tag{439}$$

$$R_0^2\frac{1}{r}\frac{d}{dr}\left(r\frac{d\Psi_0}{dr}\frac{d\Delta}{dr}\right)+\Delta R_0^2\frac{1}{r}\frac{d}{dr}\left(r\frac{d^2\Psi_0}{dr^2}\right)+R_0^2\frac{d^2\Psi_0}{dr^2}\frac{d\Delta}{dr}-R_0^2\frac{1}{r^2}\Delta\frac{d\Psi_0(r)}{dr}+\frac{d}{dr}\{\mu_0 R_0^4 P'(\Psi_0)+$$

$$R_0^2 g'(\Psi_0)g(\Psi_0)\}\Delta = -\mu_0 R_0^2 2R_0 r\,P'(\Psi_0) + R_0\frac{d\Psi_0}{dr}\tag{440}$$

$$R_0^2\frac{1}{r}\frac{d}{dr}\left(r\frac{d\Psi_0}{dr}\frac{d\Delta}{dr}\right)+\Delta R_0^2\left[\frac{1}{r}\frac{d}{dr}\left(r\frac{d^2\Psi_0}{dr^2}\right)-\frac{1}{r^2}\frac{d\Psi_0(r)}{dr}\right]+R_0^2\frac{d^2\Psi_0}{dr^2}\frac{d\Delta}{dr}+\frac{d}{dr}\{\mu_0 R_0^4 P'(\Psi_0)+$$

$$R_0^2 g'(\Psi_0)g(\Psi_0)\}\Delta = -\mu_0 R_0^2 2R_0 r\,P'(\Psi_0) + R_0\frac{d\Psi_0}{dr}\tag{441}$$

Using the identity

$$\frac{d}{dr}\left[\frac{1}{r}\frac{d}{dr}\left(r\frac{d\Psi_0}{dr}\right)\right]=\frac{1}{r}\frac{d}{dr}\left(r\frac{d^2\Psi_0}{dr^2}\right)-\frac{1}{r^2}\frac{d\Psi_0(r)}{dr},$$

equation () is written as

$$R_0^2\frac{1}{r}\quad\frac{d}{dr}\left(r\frac{d\Psi_0}{dr}\quad\frac{d\Delta}{dr}\quad\right)\quad+\quad\Delta R_0^2\frac{d}{dr}\left[\frac{1}{r}\quad\frac{d}{dr}\left(r\quad\frac{d\Psi_0}{dr}\right)\right]\quad+\quad R_0^2\frac{d^2\Psi_0}{dr^2}\quad\frac{d\Delta}{dr}\quad+\quad\frac{d}{dr}\{\mu_0 R_0^4 P'(\Psi_0)\quad+$$

$$R_0^2 g'(\Psi_0)g(\Psi_0)\}\Delta = -\mu_0 R_0^2 2R_0 r\,P'(\Psi_0) + R_0\frac{d\Psi_0}{dr}\tag{442}$$

Using the leading order equation (), we know that the second and fourth term on the l.h.s of the above equation cancel each other, giving

$$R_0^2\frac{1}{r}\frac{d}{dr}\left(r\frac{d\Psi_0}{dr}\frac{d\Delta}{dr}\right)+R_0^2\frac{d^2\Psi_0}{dr^2}\frac{d\Delta}{dr}=-\mu_0 R_0^2 2R_0 r\,P'(\Psi_0) + R_0\frac{d\Psi_0}{dr}\tag{443}$$

$$\Rightarrow\frac{1}{r}\frac{d}{dr}\left(r\frac{d\Psi_0}{dr}\frac{d\Delta}{dr}\right)+\frac{d^2\Psi_0}{dr^2}\frac{d\Delta}{dr}=-\mu_0 2R_0 r\,P'(\Psi_0)+\frac{1}{R_0}\frac{d\Psi_0}{dr}\tag{444}$$

Using the identity

$$\frac{1}{r}\frac{dr}{d\Psi_0}\frac{d}{dr}\left[r\left(\frac{d\Psi_0}{dr}\right)^2\frac{d\Delta}{dr}\right]=\frac{1}{r}\frac{d}{dr}\left(r\frac{d\Psi_0}{dr}\frac{d\Delta}{dr}\right)+\frac{d^2\Psi_0}{dr^2}\frac{d\Delta}{dr},\tag{445}$$

equation (444) is written

$$\frac{1}{r}\frac{dr}{d\Psi_0}\frac{d}{dr}\left[r\left(\frac{d\Psi_0}{dr}\right)^2\frac{d\Delta}{dr}\right]=-\mu_0 2R_0 r\,P'(\Psi_0)+\frac{1}{R_0}\frac{d\Psi_0}{dr},\tag{446}$$

$$\Rightarrow\frac{1}{r}\frac{d}{dr}\left[r\left(\frac{d\Psi_0}{dr}\right)^2\frac{d\Delta}{dr}\right]=-\mu_0 2R_0 r\frac{dP}{dr}+\frac{1}{R_0}\left(\frac{d\Psi_0}{dr}\right)^2,\tag{447}$$

Using

$$B_{\theta 0}=\frac{1}{R_0}\frac{d\Psi_0}{dr}\tag{448}$$

equation (447) is written

$$\frac{1}{r}\frac{d}{dr}\left[rB_{\theta 0}^2\frac{d\Delta}{dr}\right] = -\mu_0 2\frac{1}{R_0}r\frac{dP}{dr} + \frac{B_{\theta 0}^2}{R_0}. \tag{449}$$

$$\Rightarrow \frac{d}{dr}\left[rB_{\theta 0}^2\frac{d\Delta}{dr}\right] = \frac{r}{R_0}\left(-2\mu_0 r\frac{dP(\Psi_0)}{dr} + B_{\theta 0}^2\right), \tag{450}$$

which agrees with equation (3.6.7) in Wessson's book[18].

15 Fixed boundary tokamak equilibrium problem

The fixed boundary equilibrium problem (also called the "inverse equilibrium problem" by some authors) refers to the case where the shape of a boundary magnetic surface is given and one is asked to solve the equilibrium within this magnetic surface. To make it convenient to deal with the shape of the boundary, one usually uses a general coordinates system which has one coordinate surface coinciding with the given magnetic surface. This makes it trivial to deal with the irregular boundary. To obtain the equilibrium, one needs to solve the GS equation in the general coordinate system. Next we derive the form of the GS equation in a general coordinate system. The main task is to derive the form of the toroidal elliptic operator in the general coordinate system. The toroidal elliptic operator takes the form

$$\triangle^*\Psi \equiv R^2\nabla\cdot\left(\frac{1}{R^2}\nabla\Psi\right) \tag{451}$$

For an arbitrary general coordinate system (ψ, θ, ϕ) (the (ψ, θ, ϕ) coordinate system here is an arbitrary general coordinate system except that $\nabla\phi$ is perpendicular to both $\nabla\psi$ and $\nabla\theta$), the toroidal elliptic operator is written

$$\triangle^\star\Psi = \frac{R^2}{\mathcal{J}}\left\{\left[\Psi_\psi\frac{\mathcal{J}}{R^2}|\nabla\psi|^2\right]_\psi + \left[\Psi_\theta\frac{\mathcal{J}}{R^2}|\nabla\theta|^2\right]_\theta + \left[\Psi_\psi\frac{\mathcal{J}}{R^2}(\nabla\psi\cdot\nabla\theta)\right]_\theta + \left[\Psi_\theta\frac{\mathcal{J}}{R^2}\nabla\theta\cdot\nabla\psi\right]_\psi\right\}, \tag{452}$$

where the subscripts denotes partial derivatives, $\mathcal{J}$ is the Jacobian of the coordinate system (ψ, θ, ϕ). [Next, we provide the proof of Eq. (452). The gradient of Ψ is written as (note that Ψ is independent of ϕ)

$$\nabla\Psi = \frac{\partial\Psi}{\partial\psi}\nabla\psi + \frac{\partial\Psi}{\partial\theta}\nabla\theta \tag{453}$$

Using this expression and the divergence formula (141), the elliptic operator in Eq. (451) is written

$$
\begin{aligned}
\triangle^*\Psi &= R^2\nabla\cdot\left(\frac{1}{R^2}\frac{\partial\Psi}{\partial\psi}\nabla\psi + \frac{1}{R^2}\frac{\partial\Psi}{\partial\theta}\nabla\theta\right)\\
&= R^2\frac{1}{\mathcal{J}}\frac{\partial}{\partial\psi}\left(\mathcal{J}\frac{1}{R^2}\frac{\partial\Psi}{\partial\psi}\nabla\psi\cdot\nabla\psi + \mathcal{J}\frac{1}{R^2}\frac{\partial\Psi}{\partial\theta}\nabla\theta\cdot\nabla\psi\right) + R^2\frac{1}{\mathcal{J}}\frac{\partial}{\partial\theta}\left(\mathcal{J}\frac{1}{R^2}\frac{\partial\Psi}{\partial\psi}\nabla\psi\cdot\nabla\theta + \right.\\
&\quad \left. \mathcal{J}\frac{1}{R^2}\frac{\partial\Psi}{\partial\theta}\nabla\theta\cdot\nabla\theta\right)\\
&= \frac{R^2}{\mathcal{J}}\left[\left(\Psi_\psi\frac{\mathcal{J}}{R^2}|\nabla\psi|^2\right)_\psi + \left(\Psi_\theta\frac{\mathcal{J}}{R^2}\nabla\psi\cdot\nabla\theta\right)_\psi + \left(\Psi_\psi\frac{\mathcal{J}}{R^2}\nabla\psi\cdot\nabla\theta\right)_\theta + \left(\Psi_\theta\frac{\mathcal{J}}{R^2}|\nabla\theta|^2\right)_\theta\right],
\end{aligned}
\tag{454}
$$

which is Eq. (452).]

Using Eq. (452), the GS equation (53) is written

$$\frac{R^2}{\mathcal{J}}\left[\left(\Psi_\psi\frac{\mathcal{J}}{R^2}|\nabla\psi|^2\right)_\psi + \left(\Psi_\theta\frac{\mathcal{J}}{R^2}|\nabla\theta|^2\right)_\theta + \left(\Psi_\theta\frac{\mathcal{J}}{R^2}\nabla\psi\cdot\nabla\theta\right)_\psi + \left(\Psi_\psi\frac{\mathcal{J}}{R^2}\nabla\psi\cdot\nabla\theta\right)_\theta\right] = -\mu_0 R^2\frac{dP}{d\Psi} -$$

$$\frac{dg}{d\Psi}g, \tag{455}$$

which is the form of the GS equation in (ψ, θ, ϕ) coordinate system.

15.1 Finite difference form of toroidal elliptic operator in general coordinate system

The toroidal elliptic operator in Eq. (452) can be written

$$\triangle^* \Psi = \frac{R^2}{\mathcal{J}} [(h^{\psi\psi}\Psi_\psi)_\psi + (h^{\theta\theta}\Psi_\theta)_\theta + (h^{\psi\theta}\Psi_\theta)_\psi + (h^{\psi\theta}\Psi_\psi)_\theta], \tag{456}$$

where $h^{a\beta}$ is defined by Eq. (182), i.e.,

$$h^{\alpha\beta} = \frac{\mathcal{J}}{R^2} \nabla\alpha \cdot \nabla\beta. \tag{457}$$

Next, we derive the finite difference form of the toroidal elliptic operator. The finite difference form of the term $(h^{\psi\psi}\Psi_\psi)_\psi$ is written

$$\begin{aligned}
(h^{\psi\psi}\Psi_\psi)_\psi|_{i,j} &= \frac{1}{\delta\psi}\left[h^{\psi\psi}_{i,j+1/2}\left(\frac{\Psi_{i,j+1} - \Psi_{i,j}}{\delta\psi}\right) - h^{\psi\psi}_{i,j-1/2}\left(\frac{\Psi_{i,j} - \Psi_{i,j-1}}{\delta\psi}\right)\right] \\
&= H^{\psi\psi}_{i,j+1/2}(\Psi_{i,j+1} - \Psi_{i,j}) - H^{\psi\psi}_{i,j-1/2}(\Psi_{i,j} - \Psi_{i,j-1}),
\end{aligned} \tag{458}$$

where

$$H^{\psi\psi} = \frac{h^{\psi\psi}}{(\delta\psi)^2}. \tag{459}$$

The finite difference form of $(h^{\theta\theta}\Psi_\theta)_\theta$ is written

$$\begin{aligned}
(h^{\theta\theta}\Psi_\theta)_\theta|_{i,j} &= \frac{1}{\delta\theta}\left[h^{\theta\theta}_{i+1/2,j}\left(\frac{\Psi_{i+1,j} - \Psi_{i,j}}{\delta\theta}\right) - h^{\theta\theta}_{i-1/2,j}\left(\frac{\Psi_{i,j} - \Psi_{i-1,j}}{\delta\theta}\right)\right] \\
&= H^{\theta\theta}_{i+1/2,j}(\Psi_{i+1,j} - \Psi_{i,j}) - H^{\theta\theta}_{i-1/2,j}(\Psi_{i,j} - \Psi_{i-1,j}),
\end{aligned} \tag{460}$$

where

$$H^{\theta\theta} = \frac{h^{\theta\theta}}{(\delta\theta)^2}. \tag{461}$$

The finite difference form of $(h^{\psi\theta}\Psi_\theta)_\psi$ is written as

$$(\Psi_\theta h^{\psi\theta})_\psi|_{i,j} = \frac{1}{\delta\psi}\left[h^{\psi\theta}_{i,j+1/2}\left(\frac{\Psi_{i+1,j+1/2} - \Psi_{i-1,j+1/2}}{2\delta\theta}\right) - h^{\psi\theta}_{i,j-1/2}\left(\frac{\Psi_{i+1,j-1/2} - \Psi_{i-1,j-1/2}}{2\delta\theta}\right)\right]. \tag{462}$$

Approximating the value of Ψ at the grid centers by the average of the value of Ψ at the neighbor grid points, Eq. (462) is written as

$$(\Psi_\theta h^{\psi\theta})_\psi|_{i,j} = H^{\psi\theta}_{i,j+1/2}(\Psi_{i+1,j} + \Psi_{i+1,j+1} - \Psi_{i-1,j} - \Psi_{i-1,j+1}) - H^{\psi\theta}_{i,j-1/2}(\Psi_{i+1,j-1} + \Psi_{i+1,j} -$$
$$\Psi_{i-1,j-1} - \Psi_{i-1,j}). \tag{463}$$

where

$$H^{\psi\theta} = \frac{h^{\psi\theta}}{4\delta\psi d\theta}. \tag{464}$$

Similarly, the finite difference form of $(h^{\psi\theta}\Psi_\psi)_\theta$ is written as

$$\begin{aligned}
(\Psi_\psi h^{\psi\theta})_\theta|_{i,j} &= \frac{1}{\delta\theta}\left[h^{\psi\theta}_{i+1/2,j}\left(\frac{\Psi_{i+1/2,j+1} - \Psi_{i+1/2,j-1}}{2\delta\psi}\right) - h^{\psi\theta}_{i-1/2,j}\left(\frac{\Psi_{i-1/2,j+1} - \Psi_{i-1/2,j-1}}{2\delta\psi}\right)\right] \\
&= H^{\psi\theta}_{i+1/2,j}(\Psi_{i+1,j+1} + \Psi_{i,j+1} - \Psi_{i+1,j-1} - \Psi_{i,j-1}) - H^{\psi\theta}_{i-1/2,j}(\Psi_{i,j+1} + \Psi_{i-1,j+1} - \\
&\quad \Psi_{i,j-1} - \Psi_{i-1,j-1}).
\end{aligned} \tag{465}$$

Using the above results, the finite difference form of the operator $\mathcal{J}\triangle^*\Psi/R^2$ is written as

$$
\begin{aligned}
\left.\frac{\mathcal{J}}{R^2}\triangle^*\Psi\right|_{i,j} &= (h^{\psi\theta}\Psi_\theta)_\psi + (h^{\psi\psi}\Psi_\psi)_\psi + (h^{\theta\theta}\Psi_\theta)_\theta + (h^{\psi\theta}\Psi_\psi)_\theta \\
&= H^{\psi\psi}_{i,j+1/2}(\Psi_{i,j+1} - \Psi_{i,j}) - H^{\psi\psi}_{i,j-1/2}(\Psi_{i,j} - \Psi_{i,j-1}) \\
&+ H^{\theta\theta}_{i+1/2,j}(\Psi_{i+1,j} - \Psi_{i,j}) - H^{\theta\theta}_{i-1/2,j}(\Psi_{i,j} - \Psi_{i-1,j}) \\
&+ H^{\psi\theta}_{i,j+1/2}(\Psi_{i+1,j} + \Psi_{i+1,j+1} - \Psi_{i-1,j} - \Psi_{i-1,j+1}) - H^{\psi\theta}_{i,j-1/2}(\Psi_{i+1,j-1} + \Psi_{i+1,j} - \\
&\quad \Psi_{i-1,j-1} - \Psi_{i-1,j}) \\
&+ H^{\psi\theta}_{i+1/2,j}(\Psi_{i+1,j+1} + \Psi_{i,j+1} - \Psi_{i+1,j-1} - \Psi_{i,j-1}) - H^{\psi\theta}_{i-1/2,j}(\Psi_{i,j+1} + \Psi_{i-1,j+1} - \\
&\quad \Psi_{i-1,j-1} - \Psi_{i,j-1}) \\
&= \Psi_{i,j}(-H^{\psi\psi}_{i,j+1/2} - H^{\psi\psi}_{i,j-1/2} - H^{\theta\theta}_{i+1/2,j} - H^{\theta\theta}_{i-1/2,j}) \\
&+ \Psi_{i-1,j-1}(H^{\psi\theta}_{i,j-1/2} + H^{\psi\theta}_{i-1/2,j}) + \Psi_{i,j-1}(H^{\psi\psi}_{i,j-1/2} - H^{\psi\theta}_{i+1/2,j} + H^{\psi\theta}_{i-1/2,j}) \\
&+ \Psi_{i+1,j-1}(-H^{\psi\theta}_{i,j-1/2} - H^{\psi\theta}_{i+1/2,j}) + \Psi_{i-1,j}(H^{\theta\theta}_{i-1/2,j} - H^{\psi\theta}_{i,j+1/2} + H^{\psi\theta}_{i,j-1/2}) \\
&+ \Psi_{i+1,j}(H^{\theta\theta}_{i+1/2,j} + H^{\psi\theta}_{i,j+1/2} - H^{\psi\theta}_{i,j-1/2}) + \Psi_{i-1,j+1}(-H^{\psi\theta}_{i,j+1/2} - H^{\psi\theta}_{i-1/2,j}) \\
&+ \Psi_{i,j+1}(H^{\psi\psi}_{i,j+1/2} + H^{\psi\theta}_{i+1/2,j} - H^{\psi\theta}_{i-1/2,j}) + \Psi_{i+1,j+1}(H^{\psi\theta}_{i,j+1/2} + H^{\psi\theta}_{i+1/2,j})
\end{aligned}
$$

The coefficients are given by

$$h^{\psi\psi} = \frac{\mathcal{J}}{R^2}|\nabla\psi|^2 = \frac{1}{\mathcal{J}}(R_\theta^2 + Z_\theta^2), \tag{466}$$

$$h^{\theta\theta} = \frac{\mathcal{J}}{R^2}|\nabla\theta|^2 = \frac{1}{\mathcal{J}}(R_\psi^2 + Z_\psi^2), \tag{467}$$

and

$$h^{\psi\theta} = \frac{\mathcal{J}}{R^2}\nabla\psi\cdot\nabla\theta = -\frac{1}{\mathcal{J}}(R_\theta R_\psi + Z_\theta Z_\psi), \tag{468}$$

where the Jacobian

$$\mathcal{J} = R(R_\theta Z_\psi - R_\psi Z_\theta). \tag{469}$$

The partial derivatives, R_θ, R_ψ, Z_θ, and Z_ψ, appearing in Eqs. (466)-(469) are calculated by using the central difference scheme. The values of $h^{\psi\psi}$, $h^{\theta\theta}$, $h^{\psi\theta}$ and $\mathcal{J}$ at the middle points are approximated by the linear average of their values at the neighbor grid points.

16 Special treatment at coordinate origin, wrong! to be deleted

$$\Psi \approx a^{00} + a^{10}R + a^{01}Z + a^{11}RZ + a^{20}R^2 + a^{02}Z^2. \tag{470}$$

$$R = R_0 + b^{11}\sqrt{\psi}\cos\theta \tag{471}$$

$$Z = Z_0 + c^{11}\sqrt{\psi}\sin\theta \tag{472}$$

$$
\begin{aligned}
\Psi &\approx a^{00} + a^{10}(R_0 + b^{11}\sqrt{\psi}\cos\theta) + a^{01}c^{11}\sqrt{\psi}\sin\theta + a^{11}(R_0 + b^{11}\sqrt{\psi}\cos\theta)c^{11}\sqrt{\psi}\sin\theta + a^{20}(R_0 + \\
&\quad b^{11}\sqrt{\psi}\cos\theta)^2 + a^{02}(c^{11}\sqrt{\psi}\sin\theta)^2 \\
&= a^{00} + a^{10}R_0 + a^{10}b^{11}\sqrt{\psi}\cos\theta + a^{01}c^{11}\sqrt{\psi}\sin\theta + a^{11}R_0c^{11}\sqrt{\psi}\sin\theta + \frac{1}{2}a^{11}b^{11}\sqrt{\psi}c^{11}\sqrt{\psi}\sin2\theta + \\
&\quad 2a^{20}R_0^2 + a^{20}(b^{11})^2\psi\cos^2\theta + 2a^{20}R_0b^{11}\sqrt{\psi}\cos\theta + a^{02}(c^{11})^2\psi\sin^2\theta \\
&= d_0 + d_1\sqrt{\psi}\cos\theta + d_2\sqrt{\psi}\sin\theta + d_3\psi\sin2\theta + d_4\psi\cos^2\theta + d_5\psi\sin^2\theta
\end{aligned}
$$

$$\Psi = d_0 + d_1\sqrt{\psi}\cos\theta + d_2\sqrt{\psi}\sin\theta$$

$$R = R_0 + b^{11}\sqrt{\psi}\cos\theta + b^{12}\sqrt{\psi}\cos2\theta + b^{21}(\sqrt{\psi})^2\cos\theta + b^{22}(\sqrt{\psi})^2\cos2\theta \tag{473}$$

$$Z = Z_0 + c^{11}\sqrt{\psi}\sin\theta + c^{12}\sqrt{\psi}\sin2\theta + c^{21}(\sqrt{\psi})^2\sin\theta + c^{22}(\sqrt{\psi})^2\sin2\theta \tag{474}$$

16.1 Pressure and toroidal field function profile

The function $p(\Psi)$ and $g(\Psi)$ in the GS equation are free functions which must be specified by users before solving the GS equation. Next, we discuss one way to specify the free functions. Following Ref. [12], we take $P(\Psi)$ and $g(\Psi)$ to be of the forms

$$P(\Psi) = P_0 - (P_0 - P_b)\hat{p}(\overline{\Psi}), \tag{475}$$

$$\frac{1}{2}g^2(\Psi) = \frac{1}{2}g_0^2(1 - \gamma\hat{g}(\overline{\Psi})), \tag{476}$$

with $\hat{p}$ and $\hat{g}$ chosen to be of polynomial form:

$$\hat{p}(\overline{\Psi}) = \overline{\Psi}^\alpha, \tag{477}$$

$$\hat{g}(\overline{\Psi}) = \overline{\Psi}^\beta, \tag{478}$$

where

$$\overline{\Psi} \equiv \frac{\Psi - \Psi_a}{\Psi_b - \Psi_a}, \tag{479}$$

with Ψ_b the value of Ψ on the boundary, Ψ_a the value of Ψ on the magnetic axis, α, β, γ, P_0, P_b, and g_0 are free parameters. Using the profiles of P and g given by Eqs. (475) and (476), we obtain

$$\frac{dP(\Psi)}{d\Psi} = -\frac{1}{\Delta}(P_0 - P_b)\alpha\overline{\Psi}^{\alpha-1} \tag{480}$$

where $\Delta = \Psi_b - \Psi_a$, and

$$g\frac{dg}{d\Psi} = -\frac{1}{2}g_0^2\gamma\frac{1}{\Delta}\beta\overline{\Psi}^{\beta-1}. \tag{481}$$

Then the term on the r.h.s (nonlinear source term) of the GS equation is written

$$-\mu_0 R^2\frac{dP}{d\Psi} - \frac{dg}{d\Psi}g = \mu_0 R^2\left[\frac{1}{\Delta}(P_0 - P_b)\alpha\overline{\Psi}^{\alpha-1}\right] + \frac{1}{2}g_0^2\gamma\frac{1}{\Delta}\beta\overline{\Psi}^{\beta-1}. \tag{482}$$

The value of parameters P_0, P_b, and g_0 in Eqs. (475) and (476), and the value of α and β in Eqs. (477) and (478) can be chosen arbitrarily. The parameter γ is used to set the value of the total toroidal current. The toroidal current density is given by Eq. (63), i.e.,

$$J_\phi = R\frac{dP}{d\Psi} + \frac{1}{\mu_0}\frac{dg}{d\Psi}\frac{g}{R}, \tag{483}$$

which can be integrated over the poloidal cross section within the boundary magnetic surface to give the total toroidal current,

$$\begin{aligned}
I_\phi &= \int J_\phi dS \\
&= \int\left(R\frac{dP}{d\Psi} + \frac{1}{\mu_0}\frac{dg}{d\Psi}\frac{g}{R}\right)dRdZ \\
&= \int\left[R\left(-\frac{1}{\Delta}\right)(P_0 - P_b)\hat{p}'(\overline{\Psi}) - \frac{1}{\mu_0 R}\frac{1}{2}g_0^2\gamma\frac{1}{\Delta}\hat{g}'(\overline{\Psi})\right]dRdZ
\end{aligned} \tag{484}$$

Using

$$dRdZ = \frac{1}{R}\mathcal{J}d\psi d\theta, \tag{485}$$

Eq. (484) is written as

$$I_\phi = \int\left[\left(-\frac{1}{\Delta}\right)(P_0 - P_b)\hat{p}'(\overline{\Psi}) - \frac{1}{\mu_0 R^2}\frac{1}{2}g_0^2\gamma\frac{1}{\Delta}\hat{g}'(\overline{\Psi})\right]\mathcal{J}d\psi d\theta, \tag{486}$$

from which we solve for γ, giving

$$\gamma = \frac{-\Delta I_\phi - (P_0 - P_b)\int[\hat{p}'(\overline{\Psi})]\mathcal{J}d\psi d\theta}{\frac{1}{2\mu_0}g_0^2\int\left[\frac{1}{R^2}\hat{g}'(\overline{\Psi})\right]\mathcal{J}d\psi d\theta}. \tag{487}$$

If the total toroidal current I_ϕ is given, Eq. (487) can be used to determine the value of γ.

16.2 Boundary magnetic surface and initial coordinates

In the fixed boundary equilibrium problem, the shape of the boundary magnetic surface (it is also the boundary of the computational region) is given while the shape of the inner flux surface is to be solved. A simple analytical expression for a D-shaped magnetic surface takes the form

$$R = R_0 + a\cos(\theta + \Delta\sin\theta), \tag{488}$$

$$Z = \kappa a \sin\theta, \tag{489}$$

with θ changing from 0 to 2π. According to the definition in Eqs. (21), (22), and (24) we can readily verify that the parameters a, R_0, κ appearing in Eqs. (488) and (489) are indeed the minor radius, major radius, and ellipticity, respectively. According to the definition of triangularity Eq. (23), the triangularity δ for the magnetic surface defined by Eqs. (488) and (489) is written as

$$\delta = \sin\Delta. \tag{490}$$

Another common expression for the shape of a magnetic surface was given by Miller[6, 13], which is written as

$$R = R_0 + a\cos[\theta + \arcsin(\Delta\sin\theta)], \tag{491}$$

$$Z = \kappa a \sin\theta. \tag{492}$$

Note that Miller's formula is only slightly different from the formula (488). For Miller's formula, it is easy to prove that the triangularity δ is equal to Δ (instead of $\delta = \sin\Delta$ as given in Eq. (490)).

In the iterative metric method[8] for solving the fixed boundary equilibrium problem, we need to provide an initial guess of the shape of the inner flux surface (this initial guess is used to construct a initial generalized coordinates system). A common guess of the inner flux surfaces is given by

$$R = \psi^\alpha(R_{\text{LCFS}} - R_0) + R_0, \tag{493}$$

$$Z = \psi^\alpha Z_{\text{LCFS}}, \tag{494}$$

where α is a parameter, ψ is a label parameter of flux surface. If the shape of the LCFS is given by Eqs. (488) and (489), then Eqs. (493) and (494) are written as

$$R = R_0 + \psi^\alpha a\cos(\theta + \Delta\sin\theta), \tag{495}$$

$$Z = \psi^a \kappa a \sin\theta. \tag{496}$$

Fig. 30 plots the shape given by Eqs. (495) and (496) for $a = 0.4$, $R_0 = 1.7$, $\kappa = 1.7$, $\Delta = \arcsin(0.6)$, and $\alpha = 1$ with ψ varying from zero to one.
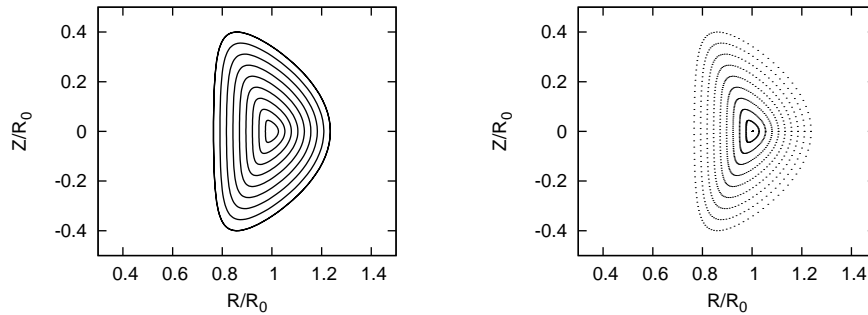

Figure 30. Shape of flux surface given by Eqs. (495) and (496). Left figure: points with the same value of ψ are connected to show ψ coordinate surface; Right figure: dot plot. Parameters are $a = 0.4$m, $R_0 = 1.7m$, $\kappa = 1.7$, $\Delta = \arcsin(0.6)$, $\alpha = 1$ with ψ varying from zero (center) to one (boundary). The shape parameters of LCFS are chosen according to the parameters of EAST tokamak.

16.3 Fixed boundary equilibrium numerical code

The tokamak equilibrium problem where the shape of the LCFS is given is called fixed boundary equilibrium problem. I wrote a numerical code that uses the iterative metric method[8] to solve this kind of equilibrium problem. Figure 31 describes the steps involved in the iterative metric method.
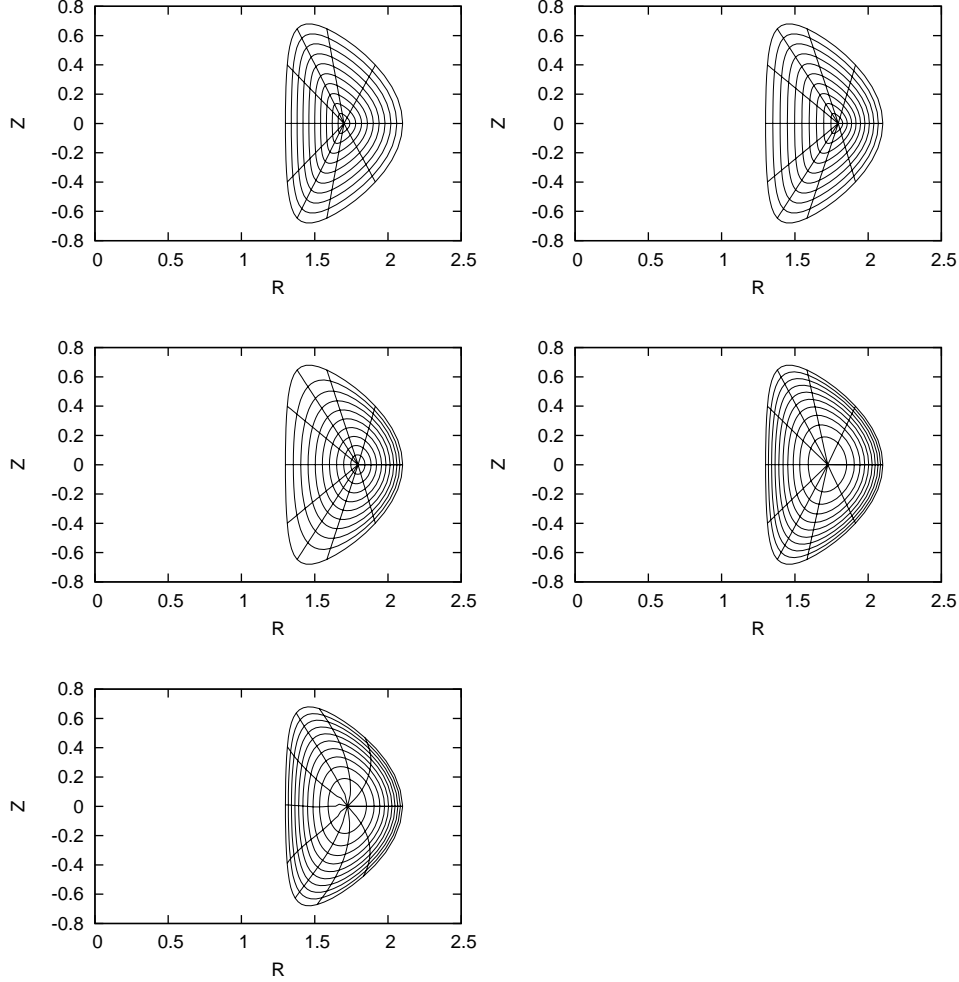

Figure 31. Upper left figure plots the initial coordinate surfaces. After solving the GS equation to obtain the location of the magnetic axis, I shift the origin point of the initial coordinate system to the location of the magnetic axis (upper right figure). Then, reshape the coordinate surface so that the coordinate surfaces $\psi = $ const lies on magnetic surfaces (middle left figure). Recalculate the radial coordinate ψ that is consistent with the Jacobian constraint and interpolate flux surface to uniform ψ coordinates (middle right figure). Recalculate the poloidal coordinate θ that is consistent with the Jacobian constraint and interpolate poloidal points on every flux surface to uniform θ coordinates (bottom left figure).

16.4 Benchmark of the code

To benchmark the numerical code, I set the profile of P and g according to Eqs. (69) and (70) with the parameters $c_2 = 0$, $c_1 = B_0(\kappa_0^2 + 1)/(R_0^2 \kappa_0 q_0)$, $\kappa_0 = 1.5$, and $q_0 = 1.5$. The comparison of the analytic and numerical results are shown in Fig. 32.
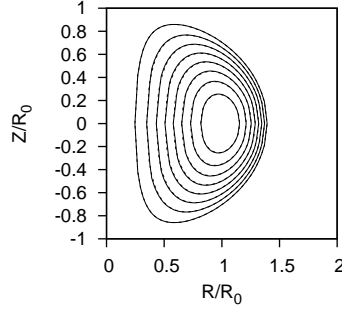
Figure 32. Agreement between the magnetic surfaces (contours of Ψ) given by the Solovev analytic formula and those calculated by the numerical code. The two sets of magnetic surfaces are indistinguishable at this scale. The boundary magnetic surface is selected by the requirement that $\overline{\Psi} = 0.11022$ in the Solovev formula (78). Parameters: $\kappa_0 = 1.5$, $q_0 = 1.5$.

Note that the parameter c_0 in the Solovev equilibrium seems to be not needed in the numerical calculation. In fact this impression is wrong: the c_0 parameter is actually needed in determining the boundary magnetic surface of the numerical equilibrium (in the case considered here c_0 is chosen as $c_0 = B_0/(R_0^2 \kappa_0 q_0)$).

16.5 Low-beta equilibrium vs. high-beta equilibrium

With the pressure increasing, the magnetic axis usually shifts to the low-field-side of the device, as is shown in Fig. 33.
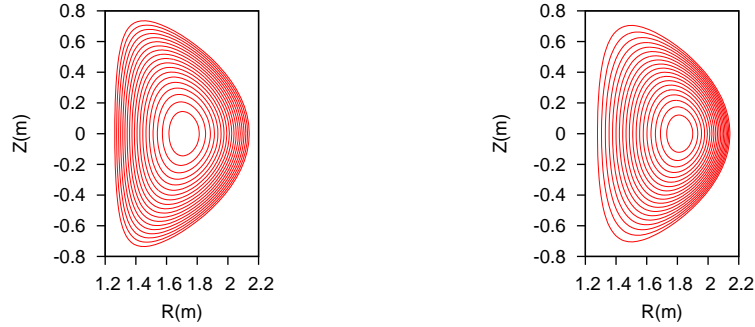

Figure 33. Comparison of two equilibria obtained with $P_0 = 10^4$Pasca (left) and $P_0 = 10^5$Pasca (right), respectively, where P_0 is the pressure at the magnetic axis. All the other parameters are the same for the two equilibria, $\alpha = 1.0$, $\beta = 1.0$, $P_b = 10^{-1}$Pasca, $g_0 = 1.0Tm$, $I_\phi = 500$kA, and the LCFS is given by miller's formulas (491) and (492) with $R_0 = 1.7$, $a = 0.45$, $\kappa = 1.7$, and $\delta = 0.6$.

16.6 Analytical form of Jacobian (need cleaning up)

Consider the Jacobian of the form

$$\mathcal{J} = \mu \left(\frac{R}{R_0} \right)^m \psi^n, \tag{497}$$

where m and n are arbitrary integers which can be appropriately chosen by users, μ_0 and R_0 are constants included for normalization. In the iterative metric method of solving fixed boundary equilibrium problem, we first construct a coordinates transformation $(\theta,\ \psi) \to (R(\theta,\ \psi), Z(\theta,\ \psi))$ (this transformation is arbitrary except for that surface $\psi = 1$ coincides with the last closed flux surface), then solve the GS equation in $(\theta,\ \psi)$ coordinate system to get the value of Ψ at

grid points, and finally adjust the value of $(R(\theta, \psi), Z(\theta, \psi))$ to make surface $\psi = \text{const}$ lies on a magnetic surface. It is obvious the Jacobian of the final transformation we obtained usually does not satisfy the constraint given by Eq. (497) since we do not use any information of Eq. (497) in the above steps. Now comes the question: how to make the transformation obtained above satisfy the constraint Eq. (497) through adjusting the values of θ? To make the constraint Eq. (497) satisfied, θ and ψ should satisfy the relation

$$\mathcal{J}(\theta, \psi) = \mu \left[\frac{R(\theta, \psi)}{R_0} \right]^m \psi^n, \tag{498}$$

which

Using Eq. (), we obtain

$$\int_0^\theta d\theta = \int_0^\theta d\theta \frac{\mathcal{J}}{\psi^n} \frac{1}{\mu} \left(\frac{R_0}{R} \right)^m$$

$$\theta = \int_0^\theta d\theta \frac{\mathcal{J}}{\psi^n} \frac{1}{\mu} \left(\frac{R_0}{R} \right)^m \tag{499}$$

normalized to 2π, the normalized θ is written as

$$\theta = 2\pi \frac{\int_0^\theta d\theta \frac{\mathcal{J}}{\psi^n} \frac{1}{\mu} \left(\frac{R_0}{R} \right)^m}{\int_0^{2\pi} d\theta \frac{\mathcal{J}}{\psi^n} \frac{1}{\mu} \left(\frac{R_0}{R} \right)^m} = 2\pi \frac{\int_0^\theta d\theta \mathcal{J} \left(\frac{1}{R} \right)^m}{\int_0^{2\pi} d\theta \mathcal{J} \left(\frac{1}{R} \right)^m} \tag{500}$$

16.7 Toroidal elliptic operator in magnetic surface coordinate system

In the magnetic surface coordinate system, by using $\partial \Psi / \partial \theta = 0$, the toroidal elliptic operator in Eq. (452) is reduced to

$$\triangle^\star \Psi = \frac{R^2}{\mathcal{J}} \left[\left(\Psi_\psi \frac{\mathcal{J}}{R^2} |\nabla \psi|^2 \right)_\psi + \left(\Psi_\psi \frac{\mathcal{J}}{R^2} \nabla \psi \cdot \nabla \theta \right)_\theta \right], \tag{501}$$

and the GS equation, Eq. (455), is reduced to

$$\frac{R^2}{\mathcal{J}} \left[\left(\Psi_\psi \frac{\mathcal{J}}{R^2} |\nabla \psi|^2 \right)_\psi + \left(\Psi_\psi \frac{\mathcal{J}}{R^2} \nabla \psi \cdot \nabla \theta \right)_\theta \right] = -\mu_0 R^2 \frac{dP}{d\Psi} - \frac{dg}{d\Psi} g(\Psi), \tag{502}$$

Equation (502) is the GS equation in magnetic surface coordinate system.

16.8 Grad-Shafranov equation with prescribed safety factor profile (to be finished)

In the GS equation, $g(\Psi)$ is one of the two free functions which can be prescribed by users. In some cases, we want to specify the safety factor profile $q(\Psi)$, instead of $g(\Psi)$, in solving the GS equation. Next, we derive the form of the GS equation that contains $q(\Psi)$, instead of $g(\Psi)$, as a free function. The safety factor defined in Eq. (191) can be written

$$q(\psi) = -\frac{1}{2\pi} \frac{g}{\Psi'} \int_0^{2\pi} \frac{\mathcal{J}}{R^2} d\theta \tag{503}$$

$$= -\frac{1}{2\pi} \frac{g}{\Psi'} \frac{\int_0^{2\pi} R^{-2} \mathcal{J} d\theta}{\int_0^{2\pi} \mathcal{J} d\theta} \int_0^{2\pi} \mathcal{J} d\theta$$

$$= -\frac{1}{2\pi} \frac{g}{\Psi'} \langle R^{-2} \rangle \int_0^{2\pi} \mathcal{J} d\theta \tag{504}$$

$$= -\text{sgn}(\mathcal{J}) \frac{V'}{(2\pi)^2} \frac{\langle R^{-2} \rangle}{\Psi'} g. \tag{505}$$

Equation (505) gives the relation between the safety factor q and the toroidal field function g. This relation can be used in the GS equation to eliminate g in favor of q, which gives

$$g = -\text{sgn}(\mathcal{J})\frac{(2\pi)^2}{V'\langle R^{-2}\rangle}\Psi' q. \tag{506}$$

$$\Rightarrow \frac{dg}{d\Psi}g = \frac{(2\pi)^2}{V'\langle R^{-2}\rangle}q\left[\frac{(2\pi)^2}{V'\langle R^{-2}\rangle}q\Psi'\right]_\psi \tag{507}$$

Multiplying Eq. (502) by R^{-2} gives

$$\frac{1}{\mathcal{J}}\left[\left(\Psi'\frac{\mathcal{J}}{R^2}|\nabla\psi|^2\right)_\psi + \left(\Psi'\frac{\mathcal{J}}{R^2}(\nabla\psi\cdot\nabla\theta)\right)_\theta\right] + \mu_0\frac{dp}{d\Psi} + R^{-2}\frac{dg}{d\Psi}\,g = 0. \tag{508}$$

Surface-averaging the above equation, we obtain

$$\frac{2\pi}{V'}\int d\theta\left[\left(\Psi'\frac{\mathcal{J}}{R^2}|\nabla\psi|^2\right)_\psi + \left(\Psi'\frac{\mathcal{J}}{R^2}(\nabla\psi\cdot\nabla\theta)\right)_\theta\right] + \mu_0\frac{dp}{d\Psi} + \langle R^{-2}\rangle\frac{dg}{d\Psi}\,g = 0, \tag{509}$$

$$\Rightarrow\frac{2\pi}{V'}\int d\theta\left(\Psi'\frac{\mathcal{J}}{R^2}|\nabla\psi|^2\right)_\psi + \mu_0\frac{dp}{d\Psi} + \langle R^{-2}\rangle\frac{dg}{d\Psi}\,g = 0, \tag{510}$$

$$\Rightarrow\frac{2\pi}{V'}\left[\Psi'\int d\theta\left(\mathcal{J}\frac{|\nabla\psi|^2}{R^2}\right)\right]_\psi + \mu_0\frac{dp}{d\Psi} + \langle R^{-2}\rangle\frac{dg}{d\Psi}\,g = 0, \tag{511}$$

$$\Rightarrow\frac{1}{V'}\left[V'\Psi'\left\langle\frac{|\nabla\psi|^2}{R^2}\right\rangle\right]_\psi + \mu_0\frac{dp}{d\Psi} + \langle R^{-2}\rangle\frac{dg}{d\Psi}\,g = 0. \tag{512}$$

$$\Rightarrow\left[V'\Psi'\left\langle\frac{|\nabla\psi|^2}{R^2}\right\rangle\right]_\psi + \mu_0 V'\frac{dp}{d\Psi} + \langle R^{-2}\rangle V'\frac{dg}{d\Psi}\,g = 0, \tag{513}$$

Substitute Eq. (507) into the above equation to eliminate $gdg/d\Psi$, we obtain

$$\Rightarrow\left[V'\Psi'\left\langle\frac{|\nabla\psi|^2}{R^2}\right\rangle\right]_\psi + \mu_0 V'\frac{dp}{d\Psi} + q(2\pi)^4\left[\frac{q\Psi'}{V'\langle R^{-2}\rangle}\right]_\psi = 0, \tag{514}$$

Eq. (514) agrees with Eq. (5.55) in Ref. [12].

$$\Rightarrow V'\left\langle\frac{|\nabla\psi|^2}{R^2}\right\rangle\Psi'' \quad + \quad \left[V'\left\langle\frac{|\nabla\psi|^2}{R^2}\right\rangle\right]_\psi\Psi' \quad + \quad \mu_0 V'\frac{dp}{d\Psi} \quad + \quad q(2\pi)^4\left[\frac{q}{V'\langle R^{-2}\rangle}\right]\Psi'' \quad +$$

$$q(2\pi)^4\left[\frac{q}{V'\langle R^{-2}\rangle}\right]_\psi\Psi' = 0 \tag{515}$$

$$\Rightarrow\Psi'' = -\frac{1}{V'D}\left\{\left[V'\left\langle\frac{|\nabla\psi|^2}{R^2}\right\rangle\right]_\psi\Psi' + q(2\pi)^4\left[\frac{q}{V'\langle R^{-2}\rangle}\right]_\psi\Psi' + \mu_0 V'\frac{dp}{d\Psi}\right\} \tag{516}$$

where

$$D = \left\langle\frac{|\nabla\psi|^2}{R^2}\right\rangle + \frac{(2\pi)^4}{\langle R^{-2}\rangle}\left(\frac{q}{V'}\right)^2 \tag{517}$$

The GS equation is

$$\triangle^\star\Psi = -\mu_0 R^2\frac{dp}{d\Psi} - g\frac{dg}{d\Psi} \tag{518}$$

$$\Rightarrow\triangle^\star\Psi = -\mu_0 R^2\frac{dp}{d\Psi} - \frac{q(2\pi)^4}{V'\langle R^{-2}\rangle}\left[\frac{q\Psi'}{V'\langle R^{-2}\rangle}\right]_\psi \tag{519}$$

$$\Rightarrow\triangle^\star\Psi = -\mu_0 R^2\frac{dp}{d\Psi} - \frac{q(2\pi)^4}{V'\langle R^{-2}\rangle}\left\{\left[\frac{q}{V'\langle R^{-2}\rangle}\right]_\psi\Psi' + \left[\frac{q}{V'\langle R^{-2}\rangle}\right]\Psi''\right\} \tag{520}$$

Using Eq. (516) to eliminate Ψ'' in the above equation, the coefficients before $(-\mu_0 dp / d\Psi)$ is written as

$$
\begin{aligned}
B &= R^2 - \frac{q(2\pi)^4}{V'\langle R^{-2}\rangle}\left\{\left[\frac{q}{V'\langle R^{-2}\rangle}\right]\frac{1}{V'D}V'\right\} \\
&= \frac{1}{D}\left\{R^2 D - \left(\frac{q}{V'}\right)^2\frac{(2\pi)^4}{\langle R^{-2}\rangle^2}\right\}.
\end{aligned}
\tag{521}
$$

Substituting the expression of D into the above equation, we obtain

$$
\begin{aligned}
B &= \frac{1}{D}\left\{R^2\left\langle\frac{|\nabla\psi|^2}{R^2}\right\rangle + R^2\frac{(2\pi)^4}{\langle R^{-2}\rangle}\left(\frac{q}{V'}\right)^2 - \left(\frac{q}{V'}\right)^2\frac{(2\pi)^4}{\langle R^{-2}\rangle^2}\right\} \\
&= \frac{1}{D}\left\{R^2\left\langle\frac{|\nabla\psi|^2}{R^2}\right\rangle + \left(\frac{q}{V'}\right)^2\frac{(2\pi)^4}{\langle R^{-2}\rangle}\left(R^2 - \frac{1}{\langle R^{-2}\rangle}\right)\right\},
\end{aligned}
\tag{522}
$$

which is equal to the expression (5.58) in Ref. [12]. The coefficient before Ψ' is written as

$$
A = -\frac{q(2\pi)^4}{V'\langle R^{-2}\rangle}\left\{\left[\frac{q}{V'\langle R^{-2}\rangle}\right]_\psi - \left[\frac{q}{V'\langle R^{-2}\rangle}\right]\frac{1}{V'D}\left[\left(V'\left\langle\frac{|\nabla\psi|^2}{R^2}\right\rangle\right)_\psi + q(2\pi)^4\left[\frac{q}{V'\langle R^{-2}\rangle}\right]_\psi\right]\right\}
$$

Define

$$
\alpha = \left\langle\frac{|\nabla\psi|^2}{R^2}\right\rangle,
$$

$$
\beta = \frac{q}{V'\langle R^{-2}\rangle}.
$$

$$
A = -(2\pi)^4\beta\left\{\beta_\psi - \beta\frac{1}{V'D}[(V'\alpha)_\psi + q(2\pi)^4\beta_\psi]\right\}
$$

$$
\Longrightarrow \frac{D}{-(2\pi)^4\beta}A = D\beta_\psi - \beta\frac{1}{V'}[(V'\alpha)_\psi + q(2\pi)^4\beta_\psi]
\tag{523}
$$

$$
\Longrightarrow \frac{D}{-\beta(2\pi)^4}A = D\beta_\psi - \beta\frac{1}{V'}[V''\alpha + V'\alpha_\psi + q(2\pi)^4\beta_\psi]
\tag{524}
$$

Using

$$
D = \alpha + (2\pi)^4\langle R^{-2}\rangle\beta^2
\tag{525}
$$

Eq. () is written as

$$
\Longrightarrow \frac{D}{-\beta(2\pi)^4}A = \alpha\beta_\psi + (2\pi)^4\langle R^{-2}\rangle\beta^2\beta_\psi - \beta\frac{1}{V'}V''\alpha - \beta\frac{1}{V'}V'\alpha_\psi - \beta\frac{1}{V'}q(2\pi)^4\beta_\psi\Big]
\tag{526}
$$

$$
\Longrightarrow \frac{D}{-\beta(2\pi)^4}A = \alpha\beta_\psi + (2\pi)^4\langle R^{-2}\rangle\beta^2\beta_\psi - \beta\frac{1}{V'}V''\alpha - \beta\alpha_\psi - \beta\frac{1}{V'}q(2\pi)^4\beta_\psi\Big]
\tag{527}
$$

$$
\frac{A}{-\beta(2\pi)^4}D = \alpha\beta_\psi + (2\pi)^4\langle R^{-2}\rangle\beta^2\beta_\psi - \beta\frac{1}{V'}V''\alpha - \beta\alpha_\psi - \beta^2\langle R^{-2}\rangle(2\pi)^4\beta_\psi
\tag{528}
$$

$$
\Longrightarrow \frac{A}{-\beta(2\pi)^4}D = \alpha\beta_\psi - \beta\frac{1}{V'}V''\alpha - \beta\alpha_\psi
\tag{529}
$$

$$
\Longrightarrow \frac{A}{-\beta(2\pi)^4}D = -\beta^2\left(\frac{\alpha}{\beta}\right)_\psi - \beta\frac{1}{V'}V''\alpha
\tag{530}
$$

$$
\Longrightarrow \frac{A}{-\beta(2\pi)^4}D = -\beta^2\left(\frac{\alpha}{\beta}\right)_\psi - \beta^2\frac{1}{V'}V''\frac{\alpha}{\beta}
\tag{531}
$$

$$
\Longrightarrow \frac{A}{-\beta(2\pi)^4}D = -\beta^2\left[\left(\frac{\alpha}{\beta}\right)_\psi + \frac{1}{V'}V''\frac{\alpha}{\beta}\right]
\tag{532}
$$

$$\Longrightarrow \frac{A}{-\beta(2\pi)^4}D = -\beta^2 \frac{1}{V'}\left[\left(\frac{\alpha}{\beta}\right)_\psi V' + V''\frac{\alpha}{\beta}\right] \tag{533}$$

$$\Longrightarrow \frac{A}{-\beta(2\pi)^4}D = -\beta^2 \frac{1}{V'}\left(\frac{\alpha}{\beta}V'\right)_\psi \tag{534}$$

$$\Longrightarrow A = \frac{(2\pi)^4}{D}\left(\frac{q}{V'\langle R^{-2}\rangle}\right)^3 \frac{1}{V'}\left[\left\langle\frac{|\nabla\psi|^2}{R^2}\right\rangle\frac{\langle R^{-2}\rangle}{q}V'^2\right]_\psi \tag{535}$$

But the expression of A is slightly different from that given in Ref. [12] [Eq. (5.57)]. Using the above coefficients, the GS equation with the q-profile held fixed is written as

$$\left(\Delta^\star - A\frac{\partial}{\partial\psi}\right)\Psi = -B\mu_0\frac{dp}{d\Psi}. \tag{536}$$

17 Misc contents

17.1 Cylindrical tokamak

For a large aspect-ratio, circular cross section tokamak, the R on a magnetic surface is nearly constant, $R \approx R_0$. The poloidal angle dependence of the magnetic field can be neglected, i.e., $B_\phi(r, \theta) \approx B_\phi(r)$, and $B_p(r,\theta) \approx B_p(r)$. Using these, the safety factor in Eq. (29) is approximated to

$$q = \frac{1}{2\pi}\oint\frac{1}{R}\frac{B_\phi}{B_p}d\ell_p \approx \frac{1}{2\pi}\frac{B_\phi(r)}{B_p(r)}\frac{1}{R_0}\oint d\ell_p = \frac{1}{2\pi}\frac{B_\phi(r)}{B_p(r)}\frac{1}{R_0}2\pi r = \frac{r}{R_0}\frac{B_\phi(r)}{B_p(r)}, \tag{537}$$

where r is the minor radius of the magnetic surface.

17.2 (s, α) parameters

The normalized pressure gradient, α, which appears frequently in tokamak literature, is defined by[2]

$$\alpha = -R_0 q^2 \frac{1}{B_0^2/2\mu_0}\frac{dp}{dr}, \tag{538}$$

which can be further written

$$\alpha = -R_0 q^2 \frac{d\bar{p}}{dr}, \tag{539}$$

where $\bar{p} = p/(B_0^2/2\mu_0)$. Equation (539) can be further written as

$$\alpha = -\frac{1}{\varepsilon_a}q^2\frac{d\bar{p}}{d\bar{r}}, \tag{540}$$

where $\varepsilon_a = a/R_0$, $\bar{r} = r/a$, and a is the minor radius of the boundary flux surface. (Why is there a q^2 factor in the definition of α?)

The global magnetic shear s is defined by

$$s = \frac{r}{q}\frac{dq}{dr}, \tag{541}$$

which can be written

$$s = \frac{\bar{r}}{q} \frac{dq}{d\bar{r}}. \tag{542}$$

In the case of large aspect ratio and circular flux surface, the leading order equation of the Grad-Shafranov equation in (r, θ) coordinates is written

$$\frac{1}{r} \frac{d}{dr} r \frac{d\Psi}{dr} = -\mu_0 R_0 J_\phi(r), \tag{543}$$

which gives concentric circular flux surfaces centered at $(R = R_0, Z = 0)$. Assume that J_ϕ is uniform distributed, i.e., $|J_\phi| = I / (\pi a^2)$, where I is the total current within the flux surface $r = a$. Further assume the current is in the opposite direction of $\nabla\phi$, then $J_\phi = -I / (\pi a^2)$. Using this, Eq. (543) can be solved to give

$$\Psi = \frac{\mu_0 I}{4\pi a^2} R_0 r^2. \tag{544}$$

Then it follows that the normalized radial coordinate $\rho \equiv (\Psi - \Psi_0) / (\Psi_b - \Psi_0)$ relates to $\bar{r}$ by $\bar{r} = \sqrt{\rho}$ (I check this numerically for the case of EAST discharge #38300). Sine in my code, the radial coordinate is Ψ, I need to transform the derivative with respect to $\bar{r}$ to one with respect to Ψ, which gives

$$\alpha = -\frac{1}{\varepsilon} q^2 \frac{d\bar{p}}{d\bar{r}} = -\frac{1}{\varepsilon} q^2 \frac{d\bar{p}}{d\sqrt{\rho}} = -\frac{1}{\varepsilon} q^2 \frac{d\bar{p}}{d\rho} \frac{1}{2\sqrt{\rho}} = -\frac{1}{\varepsilon} q^2 \frac{d\bar{p}}{d\Psi} \frac{1}{2\sqrt{\rho}} (\Psi_b - \Psi_0). \tag{545}$$

$$s = \frac{\bar{r}}{q} \frac{dq}{d\bar{r}} = \frac{\sqrt{\rho}}{q} \frac{dq}{d\Psi} \frac{1}{2\sqrt{\rho}} (\Psi_b - \Psi_0) = \frac{1}{2q} \frac{dq}{d\Psi} (\Psi_b - \Psi_0). \tag{546}$$

The necessary condition for the existence of TAEs with frequency near the upper tip of the gap is given by[2]

$$\alpha < -s^2 + \varepsilon, \tag{547}$$

which is used in my paper on Alfvén eigenmodes on EAST tokamak[11]. Equations (545) and (546) are used in the GTAW code to calculate s and α.

17.3 Toroidal magnetic field of EAST tokamak

Using Ampere's circuital law

$$\oint \mathbf{B} \cdot d\mathbf{l} = \mu_0 I, \tag{548}$$

along the toroidal direction and assuming perfect toroidal symmetry, Eq. (548) is written

$$2\pi R B_\phi = \mu_0 I, \tag{549}$$

which gives

$$B_\phi = \frac{\mu_0 I}{2\pi R}. \tag{550}$$

Neglecting the poloidal current contributed by the plasma, the poloidal current is determined solely by the current in the TF (Toroidal Field) coils. The EAST tokamak has 16 groups of TF coils, with each coils having 130 turns of wire (I got to know the number of turns from Dr. Sun Youwen). Denote the current in a single turn by I_s, then Eq. (550) is written

$$B_\phi = \frac{\mu_0 \times 16 \times 130 \times I_s}{2\pi R} = 4.160 \times 10^{-4} \frac{I_s}{R} \tag{551}$$

Using this formula, the strength of the toroidal magnetic field at $R = 1.7m$ for $I_s = 10^4 A$ is calculated to be $B_\phi = 2.447T$. This field ($I_s = 10^4 A$, and thus $B_t = 2.447$ at $R = 1.7m$) was chosen as one of the two scenarios of EAST experiments during 2014/6-2014/9 (another scenario is $I_s = 8 \times 10^3 A$). (The limit of the current in a single turn of the TF coils is 14.5kA (from B. J. Xiao's paper [19]).

Note that the exact equilibrium toroidal magnetic field B_ϕ is given by $B_\phi = g(\Psi)/R$. Compare this with Eq. (550), we know that the approximation made to obtain Eq. (551) is equivalent to $g(\Psi) \approx \mu_0 I_{\text{TF}}/2\pi$, i.e. assuming g is a constant function of Ψ. The poloidal plasma current density is related to g by $g'(\Psi)B_p/\mu_0$. The constant g corresponds to zero plasma poloidal current, which is consistent to the assumption used to obtain Eq. (551).

17.4 Comparison of EAST with DIII-D tokamak

The size of EAST tokamak is similar to that of DIII-D tokamak. The comparison of the main parameters are summarized in Table. 1. The significant difference between EAST and DIII-D is that DIII-D has a larger minor radius (0.67m for DIII-D and 0.45m for EAST), which makes DIII-D able to operate with a larger toroidal current than that EAST can do (3.0MA for DIII-D and 1.0MA for EAST) for the same current density. Another significant difference between EAST and DIII-D is that the coils of EAST are supper-conductive while the coils of DIII-D are not. The supper-conductive coils make EAST be able to generate much larger magnetic field (maximum $3.5T$ for EAST and maximum $2.2T$ for DIII-D) and operate at longer pulse.

	EAST	DIII-D
Major radius R_0	1.85m	1.67m
minor radius a	0.45m	0.67m
Maximum plasma current	1.0MA	3.0MA
Maximum toroidal field B_t	3.5T	2.2T
Available Ohm magnetic flux	12Vs	≈10.5Vs

Table 1. Comparison of main parameters of EAST and DIII-D tokamak.

17.5 Miller's formula for shaped flux surfaces

According to Refs. [6, 13], Miller's formula for a series of shaped flux surfaces is given by

$$R = R_0(r) + r\cos\{\theta + \arcsin[\delta(r)\sin\theta]\}, \tag{552}$$

$$Z = \kappa(r)r\sin\theta, \tag{553}$$

where $\kappa(r)$ and $\delta(r)$ are elongation and triangularity profile, $R_0(r)$ is the Shafranov shift profile, which is given by

$$R_0(r) = R_0(a) - \frac{aR_0'}{2}\Big[1 - \Big(\frac{r}{a}\Big)^2\Big], \tag{554}$$

where R_0' is a constant, $R_0(a)$ is the major radius of the center of the boundary flux surface. The triangularity profile is

$$\delta(r) = \delta_0\Big(\frac{r}{a}\Big)^2, \tag{555}$$

and the elongation profile is

$$\kappa(r) = \kappa_0 - 0.3 + 0.3\Big(\frac{r}{a}\Big)^4. \tag{556}$$

The nominal ITER parameters are $\kappa_0 = 1.8$, $\delta_0 = 0.5$ and $R_0' = -0.16$. I wrote a code to plot the shapes of the flux surface (/home/yj/project/miller_flux_surface). An example of the results is given in Fig. 34.
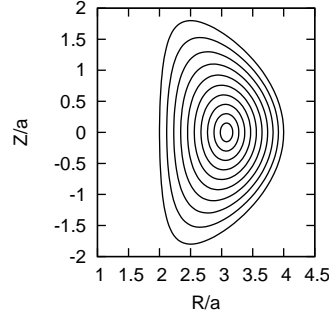
Figure 34. Flux-surfaces given by Eqs. (552) and (553) with r/a varying from 0.1 to 1.0 (corresponding boundary surface). Other parameters are $R_0(a)/a = 3$, $\kappa_0 = 1.8$, $\delta_0 = 0.5$, $R_0' = -0.16$.

17.6 Double transport barriers pressure profile

An analytic expression for the pressure profile of double (inner and external) transport barriers is given by

$$P(\psi) = a_i\left(1 + \tanh\left(\frac{-(\psi - \psi_i)}{w_i}\right)\right) + a_e\left(1 + \tanh\left(\frac{-(\psi - \psi_e)}{w_e}\right)\right) - c \tag{557}$$

where ψ is the normalized poloidal flux, w_i and w_e are the width of the inner and external barriers, ψ_i and ψ_e are the locations of the barriers, a_i and a_e is the height of the barriers, c is a constant to ensure $P(\psi) = 0$ at $\psi = 1$.
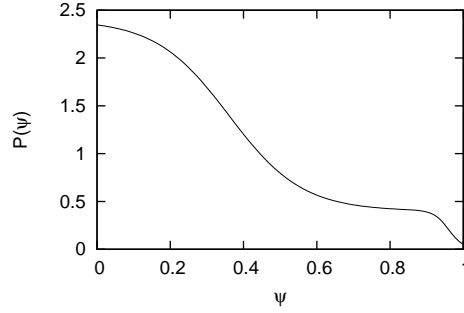

Figure 35. Pressure profile of double (inner and external) transport barriers given by Eq. (557) with $a_i = 1$, $b_i = 0.2$, $\psi_i = 0.36$, $\psi_e = 0.96$, $w_i = 0.2$, $w_e = 0.04$, $c = 0$.
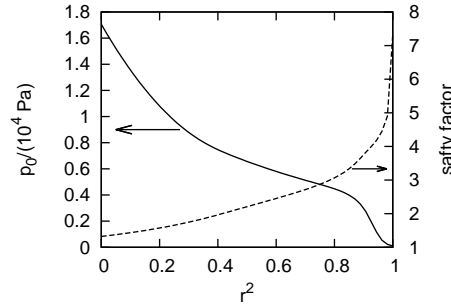

Figure 36. Equilibrium pressure profile for EAST discharge #38300 at 3.9s (reconstructed by EFIT code, gfile name: g038300.03900), which shows a boundary transport barrier.

17.7 Ballooning transformation

To construct a periodic function about θ, we introduces a function $\bar{z}(\theta)$ which is defined over $-\infty < \theta < \infty$ and vanishes sufficiently fast as $|\theta| \to \infty$ so that the following infinite summation converge:

$$\sum_{l=-\infty}^{\infty} \bar{z}(\theta + 2\pi l). \tag{558}$$

If we use the above sum to define a function

$$z(\theta) = \sum_{l=-\infty}^{\infty} \bar{z}(\theta + 2\pi l), \tag{559}$$

then it is obvious that

$$z(\theta + 2\pi) = z(\theta), \tag{560}$$

i.e., $z(\theta)$ is a periodic function about θ with period of 2π.

If we use the right-hand-side of Eq. (559) to represent $z(\theta)$, then we do not need to worry about the periodic property of $z(\theta)$ (the periodic property is guaranteed by the representation)

17.8 Discussion about the poloidal current function, check!

Note that, on both an irrational surface and a rational surface, there are infinite number of magnetic field lines that are not connected with each other (it is wrong to say there is only one magnetic field line on a irrational surface). Sine $\mathbf{B} \cdot \nabla \Psi = 0$, the value Ψ is a constant along any one of the magnetic field lines. Now comes the question: whether the values of Ψ on different field lines are equal to each other? To answer this question, we can choose a direction different from $\mathbf{B}$ on the magnetic surface and examine whether Ψ is constant or not along this direction, i.e, whether $\mathbf{k} \cdot \nabla \Psi$ equals zero or not, where $\mathbf{k}$ is the chosen direction. For axsiymmetric magnetic surfaces, it is ready to see that $\mathbf{k} = \hat{\phi}$ is a direction on the magnetic surface and it is usually not identical with $\mathbf{B}/B$. Then we obtain

$$\mathbf{k} \cdot \nabla \Psi = \hat{\phi} \cdot \nabla \Psi = \frac{1}{R} \frac{\partial \Psi}{\partial \phi} = 0. \tag{561}$$

Then, since $\mathbf{B} \cdot \nabla \Psi = 0$ and $\mathbf{k} \cdot \nabla \Psi = 0$, where $\mathbf{B}$ and $\mathbf{k}$ are two different directions on the magnetic surfaces, we know that Ψ is constant on the surface, i.e., the values of Ψ on different field lines are equal to each other. This reasoning is for the case of axsiymmetric magnetic surfaces. It is ready to do the same reasoning for non-axisymmetrica magnetic surface after we find a convient direction $\mathbf{k}$ on the magnetic surface.

[check***As discussed in Sec. 3.2, the force balance equation of axisymmetric plasma requires that $\mathbf{B} \cdot \nabla g = 0$. From this and the fact $\mathbf{B} \cdot \nabla \Psi = 0$, we conclude that g is a function of Ψ, i.e., $g = g(\Psi)$. However, this reasoning is not rigorous. Note the concept of a function requires that a function can not be a one-to-more map. This means that $g = g(\Psi)$ indicates that the values of g must be equal on two different magnetic field lines that have the same value of Ψ. However, the two equations $\mathbf{B} \cdot \nabla g = 0$ and $\mathbf{B} \cdot \nabla \Psi = 0$ do not require this constraint. To examine whether this constraint removes some equilibria from all the possible ones, we consider a system with an X point. Inside one of the magnetic islands, we use

$$g = \Psi^2 / (B_0 R_0^3), \tag{562}$$

and inside the another, we use

$$g = \Psi^3 / (B_0^2 R_0^5), \tag{563}$$

Then solve the two GS equations respectively within the boundary of the two islands. It is easy to obtain two magnetic surfaces that have the same value of Ψ respectively inside the two islands. Equations (562) and (563) indicate that the values of g on the two magnetic surfaces are different from each other. It is obvious the resulting equilibrium that contain the two islands can not be recovered by directly solving a single GS equation with a given function $g(\Psi)$.**check]

17.9 tmp check!

(In practice, I choose the positive direction of θ and ϕ along the direction of toroidal and poloidal magnetic field (i.e., $\mathbf{B} \cdot \nabla \phi$ and $\mathbf{B} \cdot \nabla \theta$ are always positive in (ψ, θ, ϕ) coordinates system). Then, the q_{local} defined by Eq. (186) is always positive. It follows that q_{global} should be also positive. Next, let us examine whether this property is correctly preserved by Eq. (192). Case 1: The radial coordinate ψ is chosen as $\Psi' \equiv d\Psi / d\psi > 0$. Then the factor before the integration in Eq. (192) is negative. We can further verify that $\mathcal{J}$ is always negative for either the case that $\nabla \Psi$ is pointing inward or outward. Therefore the .r.h.s. of Eq. (192) is always positive for this case. Case 2: The radial coordinate ψ is chosen as $\Psi' \equiv d\Psi / d\psi < 0$. Then the factor before the integration in Eq. (192) is positive. We can further verify that $\mathcal{J}$ is always positive for either the case that $\nabla \Psi$ is pointing inward or outward. The above two cases include all possibilities. Therefore, the positivity of q_{global} is always guaranteed)

a magnetic surface forms a central hole around Z axis. Using Gauss's theorem in the volume within the central hole, and noting that no magnetic field line point-intersects a magnetic surface, we know that the magnetic flux through any cross section of the hole is equal to each other. Next we calculate this magnetic flux. To make the calculation easy, we select a plane cross section perpendicular to the Z axis, as is shown by the dash line in Fig. 1. In this case, only B_Z contribute to the magnetic flux, which is written (the positive direction of the cross section is chosen in the direction of $\hat{\mathbf{e}}_Z$)

$$
\begin{aligned}
\Psi_{p1} &= \int_0^{R_c} B_z(R, Z_c) 2\pi R dR \\
&= \int_0^{R_c} \frac{1}{R} \frac{\partial \Psi}{\partial R} 2\pi R dR \\
&= 2\pi \int_0^{R_c} \frac{\partial \Psi}{\partial R} dR \\
&= 2\pi [\Psi(R_c, Z_c) - \Psi(0, Z_c)].
\end{aligned}
$$

Note that the axisymmetry requires that the axis of symmetry, Z axis, must be a magnetic field line. Since $\mathbf{B} \cdot \nabla \Psi = 0$, it follows that the value of Ψ on the Z axis is a constant (denoted by Ψ_a below). Further note that the value of Ψ is constant on a magnetic surface. Thus, Ψ_{p1} in Eq. (18) is written

$$
\Psi_{p1} = 2\pi (\Psi - \Psi_a). \tag{564}
$$

be generalized to any revolution surface that is generated by rotating a curve segment on the poloidal plane around Z axis. For instance, a curve on the poloidal plane that connects the magnetic axis and a point on a flux surface can form a toroidal surface (e.g., surface S_2 in Fig. 53). The magnetic flux through the toroidal surface S_2 is given by

i.e.

$$
\Psi - \Psi_a = \frac{\Psi_{p1}}{2\pi}, \tag{565}
$$

which indicates that the difference of Ψ between the Z axis and a magnetic surface is the poloidal magnetic flux per radian through the central hole, $\Psi_{p1} / 2\pi$.

The magnetic surface forms a central hole around Z axis. The magnetic flux through any cross section of the central hole is equal to each other and is given by $\Psi_p = 2\pi(\Psi_b - \Psi_a)$, where Ψ_a and Ψ_b are the value of Ψ at the Z axis and the magnetic surface, respectively.

The conclusion in Eq. (564) can be generalized to any revolution surface that is generated by rotating a curve on the poloidal plane about Z axis. For instance, a curve on the poloidal plane that connects the magnetic axis and a point on a flux surface can form a toroidal surface (e.g., surface S_2 in Fig. 53).

Also note the difference between Ψ_p and Ψ_{p1} defined in Sec. 1.4: Ψ_{p1} is the magnetic flux through the central hole of a torus and thus includes the flux in the center transformer, and Ψ_p is the magnetic flux through the ribbon between the magnetic axis and the magnetic surface.

17.10 Radial coordinate to be deleted

We know that the toroidal flux ψ_t, safety factor q, and the Ψ in the GS equation are related by the following equations:

$$d\psi_t = 2\pi q \, d\Psi \tag{566}$$

$$\Longrightarrow \psi_t = 2\pi \int_0^\Psi q \, d\Psi \tag{567}$$

Define:

$$\rho \equiv \sqrt{\frac{\psi_t}{\pi}} \tag{568}$$

(In the Toray_ga code, the radial coordinate ρ is defined as

$$\rho \equiv \sqrt{\frac{\psi_t}{\pi B_{t0}}}, \tag{569}$$

where B_{t0} is a constant factor. ρ defined this way is of length dimension, which is an effective geometry radius obtained by approximating the flux surface as circular.)

I use Eq. (568) to define ρ. Then we have

$$\psi_t = \pi \rho^2 \tag{570}$$

$$\Longrightarrow \frac{d\psi_t}{d\rho} = 2\pi \rho \tag{571}$$

$$\Longrightarrow \frac{d\psi_t}{d\psi} \frac{d\psi}{d\rho} = 2\pi \rho \tag{572}$$

$$\Longrightarrow 2\pi q \frac{d\psi}{d\rho} = 2\pi \rho \tag{573}$$

$$\Longrightarrow \frac{d\psi}{d\rho} = \frac{\rho}{q} \tag{574}$$

Eq. (574) is used to transform between ψ and ρ.

$$d\rho = \frac{1}{\sqrt{\Phi/\pi R_0^2 B_0}} \frac{1}{2} \frac{1}{\pi B_0 R_0^2} d\Phi = \frac{1}{\rho} \frac{1}{2} \frac{1}{\pi B_0 R_0^2} 2\pi q \, d\psi = \frac{1}{\rho} \frac{1}{B_0 R_0^2} q \, d\psi$$

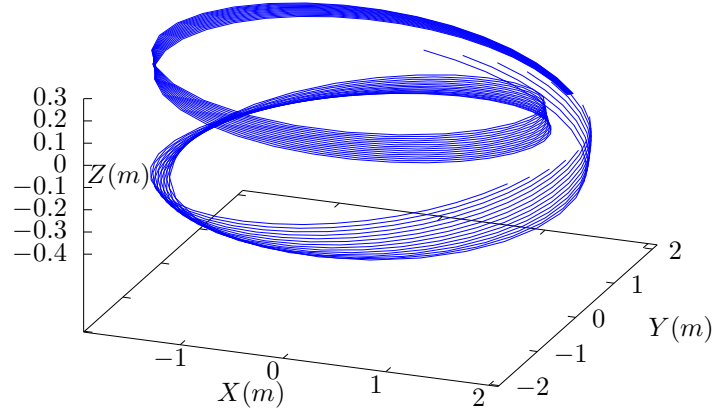$$\Rightarrow d\psi = \frac{\rho B_0 R_0^2}{q} d\rho$$

Figure 37. to be delted, Isosurface of $\alpha = 2\pi/8$. The surface is made of a family of contours of $\alpha = 2\pi/8$, which are all magnetic field lines. These field lines are traced by starting from a series of points on the low-field-side midplane ($\theta = 0$) at different radial locations and the field lines are followed by a complete poloidal loop. Magnetic field from EAST discharge #59954@3.03s.

Bibliography

[1] M. A. Beer, S. C. Cowley, and G. W. Hammett. Field-aligned coordinates for nonlinear simulations of tokamak turbulence. *Phys. Plasmas (1994-present)*, 2(7):2687–2700, 1995.

[2] H. L. Berk, J. W. Van Dam, D. Borba, J. Candy, G. T. A. Huysmans, and S. Sharapov. More on core localized toroidal alfvén eigenmodes. *Phys. Plasmas*, 2(9):3401–3406, 1995.

[3] Allen H. Boozer. Physics of magnetically confined plasmas. *Rev. Mod. Phys.*, 76:1071–1141, Jan 2005.

[4] Yang Chen and Scott E. Parker. A delta-f particle method for gyrokinetic simulations with kinetic electrons and electromagnetic perturbations. *Journal of Computational Physics*, 189(2):463–475, 2003.

[5] Yang Chen and Scott E. Parker. Electromagnetic gyrokinetic δf particle-in-cell turbulence simulation with realistic equilibrium profiles and geometry. *Journal of Computational Physics*, 220(2):839–855, 2007.

[6] Yang Chen, Scott E. Parker, J. Lang, and G.-Y. Fu. Linear gyrokinetic simulation of high-n toroidal alfvén eigenmodes in a burning plasma. *Phys. Plasmas*, 17(10):102504, 2010.

[7] C.Z Cheng and M.S Chance. Nova: a nonvariational code for solving the mhd stability of axisymmetric toroidal plasmas. *J. of Comput. Phys.*, 71(1):124–146, 1987.

[8] J DeLucia, S.C Jardin, and A.M.M Todd. An iterative metric method for solving the inverse tokamak equilibrium problem. *Journal of Computational Physics*, 37(2):183–204, 1980.

[9] A. M. Dimits. Fluid simulations of tokamak turbulence in quasiballooning coordinates. *Phys. Rev. E*, 48:4070–4079, Nov 1993.

[10] T. Görler, N. Tronko, W. A. Hornsby, A. Bottino, R. Kleiber, C. Norscini, V. Grandgirard, F. Jenko, and E. Sonnendrücker. Intercode comparison of gyrokinetic global electromagnetic modes. *Physics of Plasmas*, 23(7):72503, 2016.

[11] Youjun Hu, Guoqiang Li, N. N. Gorelenkov, Huishan Cai, Wenjun Yang, Deng Zhou, and Qilong Ren. Numerical study of alfvén eigenmodes in the experimental advanced superconducting tokamak. *Phys. Plasmas*, 21(5):0, 2014.

[12] Stephen C. Jardin. *Computational methods in plasma physics*. CRC Press, 2010.

[13] R. L. Miller, M. S. Chu, J. M. Greene, Y. R. Lin-Liu, and R. E. Waltz. Noncircular, finite aspect ratio, local equilibrium model. *Phys. Plasmas*, 5(4):973–978, 1998.

[14] M. Ottaviani. An alternative approach to field-aligned coordinates for plasma turbulence simulations. *Physics Letters A*, 375(15):1677–1685, 2011.

[15] S.A. Sabbagh, A.C. Sontag, J.M. Bialek, D.A. Gates, A.H. Glasser, J.E. Menard, W. Zhu, M.G. Bell, R.E. Bell, A. Bondeson, C.E. Bush, J.D. Callen, M.S. Chu, C.C. Hegna, S.M. Kaye, L.L. Lao, B.P. LeBlanc, Y.Q. Liu, R. Maingi, D. Mueller, K.C. Shaing, D. Stutman, K. Tritz, and C. Zhang. Resistive wall stabilized operation in rotating high beta nstx plasmas. *Nucl. Fusion*, 46(5):635, 2006.

[16] W. X. Wang, Z. Lin, W. M. Tang, W. W. Lee, S. Ethier, J. L. V. Lewandowski, G. Rewoldt, T. S. Hahm, and J. Manickam. Gyro-kinetic simulation of global turbulent transport properties in tokamak experiments.

Physics of Plasmas, 13(9):92505, 2006.

[17] R. B. White and M. S. Chance. Hamiltonian guiding center drift orbit calculation for plasmas of arbitrary cross section. *The Physics of Fluids*, 27(10):2455–2467, 1984.

[18] John Wesson. *Tokamaks*. Oxford University Press, 2004.

[19] B J Xiao, D A Humphreys, and M L Walker. East plasma control system. *Fusion Engineering and Design*, 83:181, 2008.